THE OXIDATION OF O-XYLENE IN A FIXED BED CATALYTIC REACTOR

by

Lloyd Caldwell B.Sc.

Thesis submitted for the degree of Ph.D.

February 1971

UNIVERSITY OF EDINBURGH

EDINBURGEN EX BIBL UNIV.

"What you need to make phthalic anhydride is a nice big hot spot"

I.C.I. folk-lore.

ACKNOWLEDGEMENTS

The author is much indebted to his supervisor, Professor P.H. Calderbank, for encouragement, advice and helpful discussion, to Mr. Stewart Ellis for assistance with some of the experimental work, and to the workshop staff - particularly Mr. D. Ketchin, Mr. W. Young and Mr. G. Campbell - for all their work in building the apparatus.

TABLE OF CONTENTS

SUMMARY

A survey is presented of the literature relating to the manufacture of phthalic anhydride by air oxidation of o-xylene in fixed bed catalytic reactors. The reaction mechanism is discussed and it is concluded that the simplified reaction scheme of Froment gives an adequate picture of the course of the reaction as carried out industrially. A theoretical model of the reactor is developed and this is used to demonstrate that (in accordance with Froment's suggestion) on the basis of this simplified scheme the phthalic anhydride yeild from a reactor of reasonable dimensions (3 metres length) may be substantially improved by a policy of non-uniform catalyst dilution. The dilution required is greatest at the point where the reactor "hot spot" would normally occur (in the absence of dilution) and tails off towards the reactor exit. An improvement of up to ten percentage points in the yield can be obtained.

Results are given from an experimental study using a single one incha diameter jacketed reactor. Catalyst dilution had no appreciable influence on the yield of phthalic anhydride under the conditions employed. The behaviour of the reactor was not at all in accordance with the results of calculations on the model. Reactor ignition and extinction phenomena were observed, with peak temperature (in the ignited condition) as much as 150°C above the jacket temperature. The ignited state appeared to be necessary to obtain good yields, and no harmful effects of high temperature were discovered - in contrast to many statements in the literature. Signs of variable catalyst activity were noted.

The reactor behaviour is explained qualitatively by taking account of the heat and mass transfer resistance between the surface of a catalyst pellet and the bulk gas. It is shown that

a reasonable choice of parameters for the reaction system leads to the possibility of an 'unignited' and an 'ignited' steady state for a catalyst pellet under identical bulk gas conditions, corresponding to the observed phenomena in the fixed bed reactor. In order to account for certain other features of the experimental results, however, it is necessary to modify the theory to take account of the oxidation-reduction cycle on the catalyst surface.

CHAPTER 1 THE FIXED BED CATALYTIC OXIDATION OF O-XYLENE TO PHTHALIC ANHYDRIDE

1.1 History of commercial processes for phthalic anhydride manufacture

Since the end of the nineteenth century phthalic anhydride has been an important intermediate product of the chemical industry. At that time it was produced by the oxidation of naphthalene with sulphuric acid and was principally used in the manufacture of synthetic dyes - a market which still exists in 1970, although it now accounts for a small fraction of total production[1].

During the First World War processes for the fixed-bed catalytic air oxidation of naphthalene in the gas phase were developed independently in Germany and the U.S.A.[1,2]. Since then the annual production of phthalic anhydride has multiplied but the manufacturing process is basically unchanged. World production capacity increased from 200,000 t.p.a. in 1945 to 1,400,000 t.p.a. in 1968[3]; this increase has been largely due to the demand for phthalic anhydride in plasticisers for polyvinyl chloride, in alkyd resins and polyester resins. It is anticipated that this demand will continue to increase at the rate of about 10% per annum in the next few years[1,4].

In 1945 the Sherwin-Williams Co. of Chicago built the first fluidized bed plant for phthalic anhydride. This process suffered from rapid attrition of the catalyst: an improved catalyst was introduced by the United Coke & Chemicals Co. Ltd. in 1959, and this is now used in nearly all fluidized bed plants. 20.3% of world production capacity for phthalic anhydride was accounted for by fluidized bed plants in 1967[5].

Early phthalic anhydride plants all made use of naphthalene obtained from coal tar distillation. In the period between the first and second world wars the coal gas industry declined

and naphthalene became available from petrochemical sources. However petrochemical naphthalene was neither cheap nor freely available and accordingly catalysts were sought which would convert ortho-xylene to phthalic anhydride by processes essentially similar to naphthalene oxidation. Today it appears that o-xylene has largely superseded naphthalene as a raw material for new installations[2,4], although the greater part of existing phthalic anhydride capacity (55-60%) still uses naphthalene as feedstock. The exceptions to this trend are, for the most part, plants associated with steel companies, where napthalene is produced as a byproduct of the coking of coal[4]. Until very recently no fluid bed process operated with o-xylene as feedstock - it appears that no attrition resistant catalyst giving good yields of phthalic anhydride could be found - but one such plant has now been commissioned[3]. The estimated capacities for o-xylene and phthalic anhydride production in the early 1970's indicate that there will be a considerable surplus of o-xylene in the foreseeable future[6], which reinforces the view that it will become the dominant raw material for phthalic anhydride. However, market predictions are notoriously unreliable, and the development of catalysts which can operate on both naphthalene and o-xylene feedstocks[1,2] suggests that manufacturers are not prepared to commit themselves in either direction at the present time.

In recent years a liquid phase process for o-xylene oxidation has been developed and a plant to produce 15,000 t.p.a. of phthalic anhydride is in operation[1,3]. The o-xylene is dissolved in acetic acid and oxidised by air in the presence of a cobalt acetate catalyst at temperatures between 100°C and 275°C and pressure up to 1,500 p.s.i.

1.2 Fixed-bed processes

A generalised flowsheet for the fixed bed process based

on o-xylene is shown in Figure 1. Liquid o-xylene is evaporated into a filtered and heated air stream and the combined stream enters the reactor which consists of a large number of catalyst packed tubes immersed in a suitable heat transfer medium. Older plants used mercury or mercury amalgams; molten salt mixtures (e.g. sodium nitrate/potassium nitrate) are preferred in modern installations. The heat transfer medium absorbs the large heat of reaction and is itself cooled by raising steam under pressure. In some cases the steam raising tubes are contained in the reactor shell and the salt mixture is circulated by an agitator: other plants use an external heat exchanger with a pump to circulate the salt between reactor and exchanger. It is claimed that the latter alternative provides more uniform cooling of the reactor tubes[7]. Reactors were formerly limited to an output of about 5,000 t.p.a., but of late this figure has been increased to 15,000 t.p.a.[4,7] with plant capacities of the order of 50,000 t.p.a.

In addition to phthalic anhydride a number of by-products are formed in the reactor. These include o-tolualdehyde, benzoic acid, o-toluic acid, maleic anhydride, phthalide, tricarbonic acids, and carbon oxides[1,2]. The heat of reaction, including the side reactions, is said to be about 445,000 cals/gm.mol o-xylene[1,2].

The reaction gases are cooled to about 170°C in a waste heat boiler and then pass to one of two (or more) switch condensers, where the phthalic anhydride condenses as a "hay" of needle crystals on oil-cooled tubes. The exhaust gas from the condenser is usually scrubbed with water or alkali before discharge to the atmosphere. While one condenser is collecting the other is discharging: hot oil is passed through the tube side to melt the crystals and the liquid phthalic anhydride runs down into a crude storage tank. Purification involves a heat treatment stage to decompose any phthalic acid to

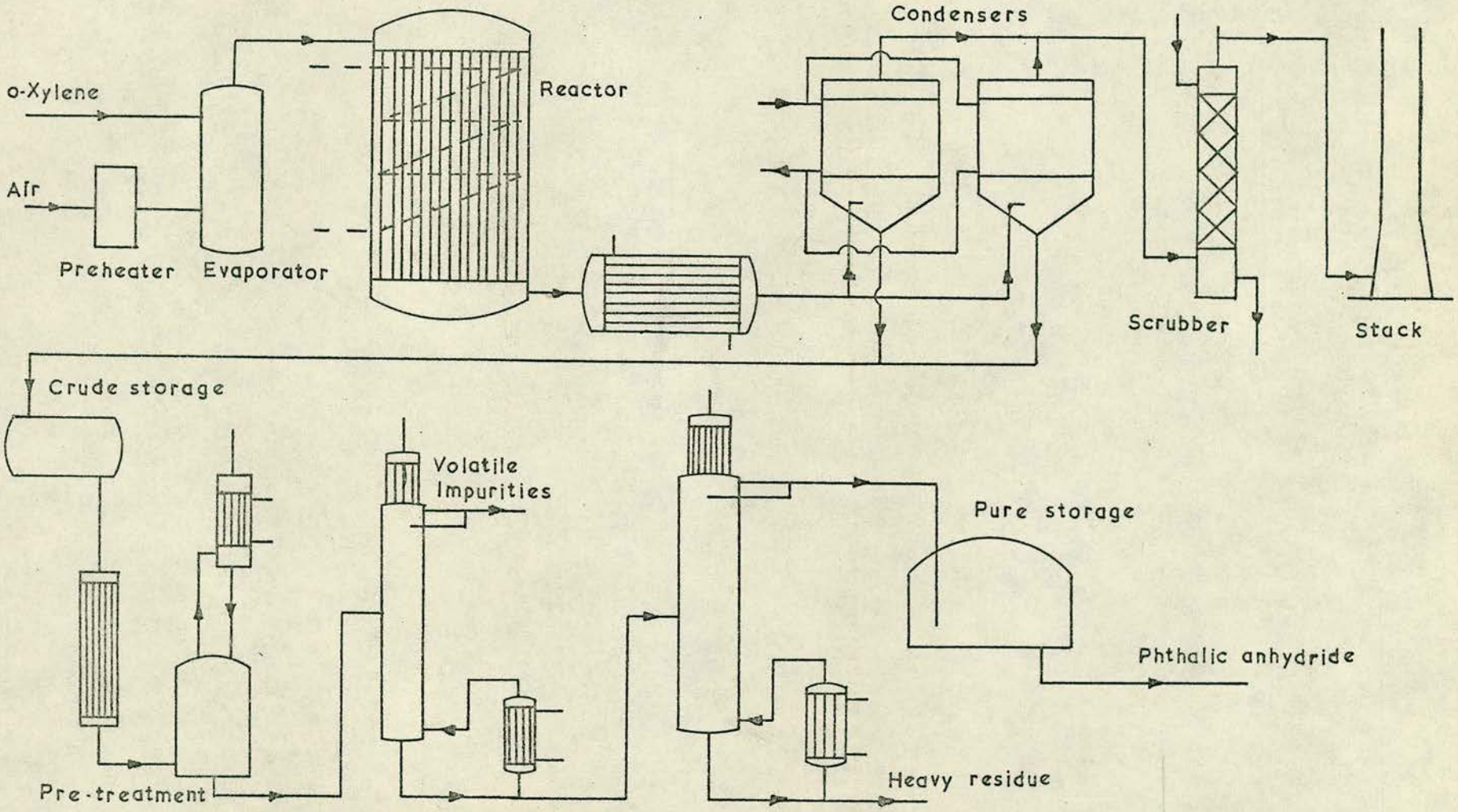

FIGURE 1 FIXED BED PROCESS FOR o-XYLENE OXIDATION

phthalic anhydride and drive off volatile impurities (principally water) followed by vacuum distillations to "top" and "tail" the product.

There are a number of licensed processes which operate according to the general scheme just outlined. A full list is given in the article by Leach[3]. The principal difference between these processes, for present purposes, lies in the nature of the catalyst employed and the mode of operation of the reactor. As noted in Section 1.1, the vapour phase oxidation of naphthalene was discovered and developed independently in Germany and the U.S.A., and catalysts are still described today as being of "German" or "American" type. The German type is employed in low space velocity processes, notably the Von Heyden and BASF (Badische Anilin & Soda Fabrik) processes. It is a relatively mild catalyst and functions at temperatures in the range 350-400°C: the catalyst support is usually silica and a potassium promoter may be added[8]. An o-xylene feed concentration of about 0.78% by volume is used and yields up to about 73-75% (moles of phthalic anhydride per mole of o-xylene) are obtained[1,2,3]. The American type of catalyst is more active (possibly by a factor of twenty or thirty[9]); it functions at temperatures of 450-600°C and is employed in high space velocity processes. The catalyst support may be alundum or carborundum[8]. The feed contains about 1.4% by volume o-xylene and yields up to about 68-70% are achieved[3]. Some high space velocity processes would therefore appear to operate inside the explosive limits for o-xylene in air. The range is variously quoted as 1.0-5.3 mole %[15] and 1.1-7.0 mole %[16]. (It may be noted here that the particular advantage of the fluid bed process is that higher hydrocarbon:air ratios can safely be employed than with fixed bed processes[5]. By injecting the hydrocarbon directly into the fluidized bed the danger of explosions is eliminated: apparently the catalyst suppresses the chain branching reactions. Hence a greater throughput

can be achieved for a given size of plant and product collection is made easier.) The low space velocity processes generally show a better yield but the high space velocity processes give a higher output from a given reactor size. Since the cost of raw material represents a major part of phthalic anhydride production costs - in some cases as much as 60%[2,3] - the low space velocity processes appear to be more attractive, and this is confirmed by the literature. It is stated that of the 1.3 million tons of anhydride produced in 1969 about 0.5 million tons were produced by the Von Heyden process alone[2] - and the 1.3 million tons includes fluid bed process production (which was 20.3% of the total in 1967[5]). Leach claims that the Von Heyden and BASF process together "account for most of the new phthalic anhydride capacity currently being installed"[3], and this is supported by Allen[4]. However, the superiority of the low space velocity process may not be solely due to yield considerations; this point will be taken up later.

As one might expect, details of reactor design and operation for the various processes are not readily available. Froment gives data[10] which he believes to be fairly representative of industrial practice with the German type catalyst[11]. The reactor tube diameter is 2.5 cms, the packed length 2.5-3.0 metres, the mass velocity 4,684 Kg/m^2, and the reactor has 2,500 tubes. This gives a space velocity of about 1,200 per hour. The feed concentration is given as 0.924% by volume o-xylene, and if we assume 70% yield the reactor has a capacity of about 1,500 t.p.a. - fairly small by today's standards.

The latest versions of the Von Heyden and BASF processes are said to operate with space velocities which are respectively two and three times greater than in the traditional process[2,3,7]. This would put them in the range 2,400-3,600 per hour if we accept Froment's

figures as representing the traditional process.

On the other hand reference 12 quotes contact times of 4-5 secs. for the low space velocity processes (and 0.4-0.6 secs. for the high space velocity processes). These figures do not agree with Froment's value, giving space velocities of at most 720-900 per hour and probably rather lower (depending on the bed voidage and the definition of 'contact time'). Reference 12, however, is probably based on rather out-of-date information which may account for the discrepancy.

One of the chief difficulties of reactor design - probably the major difficulty - is how to deal with the large heat release. This question is intimately bound up with considerations of reaction mechanism and kinetics and discussion will therefore be postponed until these topics have been covered. However, we may note here that the traditional reactor design involves a large number of small diameter tubes so as to achieve a high heat transfer area per unit volume of catalyst. An article written in 1965 mentions tube diameters of 0.5 ins.[13]. Froment gives one inch as a typical tube diameter, and there are strong indications that the latest BASF and Von Heyden processes also use one inch tubes. The BASF reactor at Ludwigshafen is said to be 13.8 ft. in diameter and contain 8,900 tubes[14]. This works out to be 60 tubes per square foot: one inch tubes with half inch spacing would give 64 tubes per square foot. (Moreover, making the assumption of one inch tubes and taking reasonable values for the yield and feed concentration leads to a space velocity of about 4,000 per hour - in good agreement with the figure quoted earlier). The latest Von Heyden reactors contain 12,000 tubes in a shell of greater diameter than the BASF reactor[14], which again suggests one inch diameter tubes.

An interesting feature of some phthalic anhydride processes is the addition of small quantities of sulphur dioxide to the gases prior to entry into the reactor. It is plain from the original patent[17] that the idea was originally applied to a high space velocity process: the catalyst bed depth in the commercial reactor referred to in the patent was only nineteen inches, and the salt bath temperature was of the order of 460°C. It was found that whereas in the absence of sulphur dioxide addition the temperature profile in the reactor showed an abrupt rise from 444°C to 550°C in a four inch segment of the bed, the addition of sulphur dioxide under otherwise comparable conditions gave a smoother profile with the peak temperature reduced to about 525°C but with a much greater proportion of the bed at temperatures above 510°C. This reduction in the peak temperature was claimed to be beneficial since "excessive hot spot temperatures may result in fusion of the catalyst, total oxidation and destruction of the product, and corrosive and structural damage to equipment as a result of excessive heat release associated with total oxidation." The maximum tolerable reactor temperature was put at 650°C and it was estimated that the throughput of a reactor could be substantially increased before reaching this maximum when sulphur dioxide addition was made. In addition it was claimed that sulphur dioxide was particularly beneficial during the break-in period (about three months) for a fresh charge of catalyst.

More recently we find that sulphur dioxide addition is also a feature of the Von Heyden process[1,2]. The purpose of this addition, however, is to maintain catalyst activity rather than to smooth the temperature profile or increase throughput. The quantity added is given as 0.1-0.2% of the feed mixture[2]. The BASF process does not employ sulphur dioxide addition[7].

1.3 Reaction products and kinetics

It is not the intention in this section to give a comprehensive account of the published work in this field but rather to summarize the most important and well-established features of the o-xylene partial oxidation reaction. In view of the existence of two more or less distinct industrial processes for this reaction we shall be interested to observe how far the distinction is made in laboratory studies.

Table 1 gives a list of experimental laboratory studies of o-xylene oxidation. It will be seen that both types of catalyst are well represented. With the exception of the work of Juusola, Mann and Downie (who do not report phthalic anhydride formation), Mann and Downie, and Simard et al (where the conversion was kept below 25%) the maximum yields of phthalic anhydride were in the 50-70% range, comparable with industrial yields.

A number of reaction schemes have been proposed and some of these are shown in Figure 2. Those of Bernardini and Ramacci [28], Levine [29] and Vrbaski and Matthews [30] have been simplified considerably. Froment's scheme [10] was only intended to give a reasonable picture of the industrial process rather than a detailed guide to the mechanism. There is a considerable measure of agreement between the various proposals. It seems clear that phthalic anhydride is formed by the reaction sequence

$$X \longrightarrow TA \longrightarrow PA$$

as indicated in five of the schemes. Three of the schemes show an alternative mode of formation for phthalic anhydride in which phthalide is the intermediate, and three also indicate that phthalic anhydride may be formed directly from o-xylene.

Table 1 Laboratory Studies of the Oxidation of O-xylene over V_2O_5 catalyst

Investigators	Catalyst	Working temperatures °C	Products	Maximum PA yield %	Contact time secs	Date
Novella & Benlloch (fluidized bed) (18,19,20)	K_2SO_4 promoted on silica, 0.123 mms. dia.	310-370	PA,MA,TA, CO,CO_2	Approx. 53	20	1962
Herten & Froment (21)	"Doped V_2O_5" (Synoxy)[5]	325-402	PA,PI,TA, CO,CO_2	Approx. 70	1	1968
Mann & Downie (22)	K_2SO_4 promoted on silica. Surface area 52 m^2/gm	300-325	PA,TA,PI, CO,CO_2,p-benzoquinone, phthalaldehyde	?	0.1	1968
Juusola, Mann & Downie (23)	" "	290-310	TA (80%) p-benzoquinone (12%) CO_2 (8%),CO(trace)	0	?	1970
Simard et al.(24)	V_2O_5 on 6-8 mesh SiC	460	PA,MA,CO,CO_2	Approx. 50	0.26	1955
Simard (unpublished) (25)	V_2O_5 on SiC	400-450	PA,PI,TA,CO,CO_2	25	0.01-0.06	
Bhattacharyya & Gulati (26)	Fused V_2O_5	450-480	PA,MA,CO_2, quinone	60	0.6	1958
Bhattacharyya & Krishnamurthy (27) (fluidized bed)	Fused V_2O_5	490	PA,TA,CO_2, quinone	67.8	0.36	1959
Bernardini & Ramacci (28)	V_2O_5 on 8-10 mesh corundum. Surface area 2-4 m^2/gm	450-500	PA,MA,TA,PI, benzoic & toluic acids	52-65	0.07	1966

Note: The contact times given are subject to uncertainty in some cases.

FIGURE 2

Reaction schemes for o-xylene oxidation

Novella and Benlloch

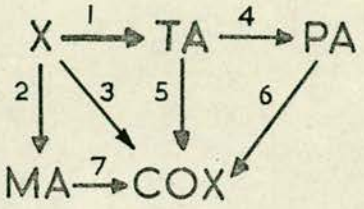

Levine (simplified)

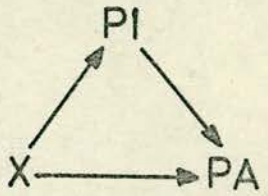

Herten and Froment

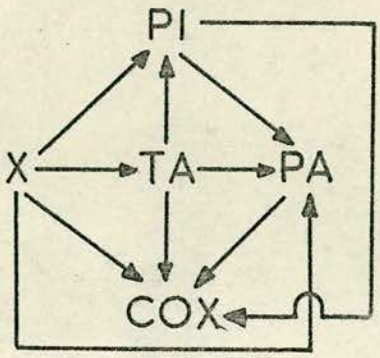

Simard

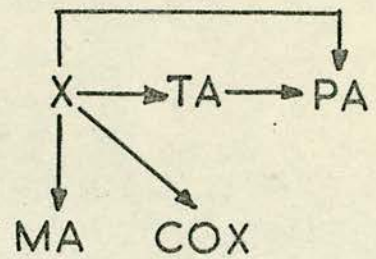

Bernardini and Ramacci
(simplified)

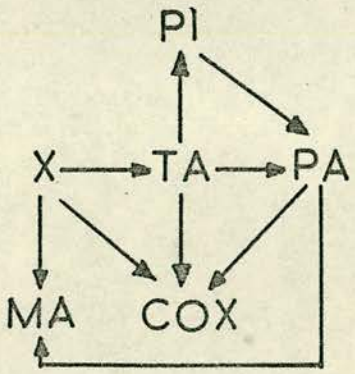

Froment

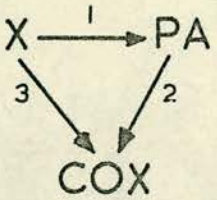

Vrbaski and Matthews (simplified)

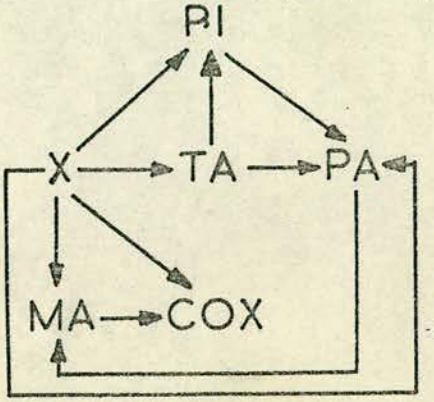

Maleic anhydride appears as a by-product in most of the reaction schemes and is always shown as being formed (in part at least) directly from o-xylene. Novella and Benlloch found that (under the same conditions as in their experiments with o-xylene oxidation) phthalic anhydride could not be oxidized to maleic anhydride; they therefore concluded that maleic anhydride was formed only from o-xylene. Bernardini and Ramacci performed similar experiments and found that at low temperatures (360°C, which is in the range of Novella and Benlloch's work) no maleic anhydride resulted. At higher temperatures, however, (400-500°C, as used in their own experiments on o-xylene oxidation) appreciable quantities of maleic anhydride were formed. There is therefore no real conflict on this point but one difference between the two types of catalyst emerges: because of the low temperature phthalic anhydride does not react to maleic on the German catalyst, but will do so at the higher temperatures used with the American catalyst. The work of Vrbaski and Matthews[30] on the oxidation of o-methyl benzyl alcohol supports this view. They found that the formation of maleic anhydride passed through a minimum at 425°C at which temperature the formation of phthalic anhydride was a maximum. This suggests the scheme

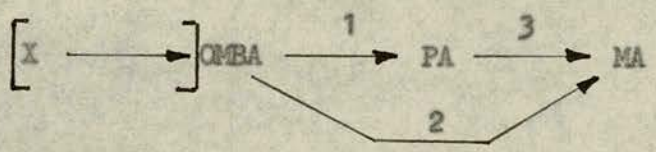

where the activation energy for step 1 exceeds that for step 2, and step 3 is slow at low temperatures.

The formation of carbon oxides is of interest to the engineer, not only because these products limit the yield of phthalic anhydride, but also because of the large heat release associated with the complete combustion reactions. The reaction schemes of Table 1, which for the most part indicate that all the organic species may be

oxidized to carbon oxides, are no doubt formally correct but are not very enlightening in the absence of information about the magnitudes of the rate constants and activation energies for the various reaction steps. We should also require kinetic data in order to establish how far a simplified reaction scheme such as that of Froment is justified.

Unfortunately, but not unexpectedly in view of the complexity of the reaction system, there is very little published kinetic data. The most extensive contribution is that of Novella and Benlloch who determined the rate constants and activation energies for each step in their proposed reaction scheme. They concluded that each step was first order in organic reactant and independent of oxygen concentration under the conditions studied: their results for the reaction scheme of Figure 2 are given in Table 2. Herten and Froment give data for the rate of disappearance of o-xylene, as do Mann and Downie and Juusola, Mann and Downie; Vrbaski and Matthews give similar data for the oxidation of o-methyl benzyl alcohol and toluedehyde. Froment provides data for his simplified reaction scheme.

The figures in Table 2 indicate that the oxidation of phthalic anhydride to carbon oxides is the slowest of all the steps in the scheme of Novella and Benlloch. Herten and Froment state that "with excessive residence times the decomposition of PA into CO and CO_2 is beyond doubt and was easily proved"; nevertheless, their plots of phthalic anhydride yield against total xylene conversion reveal no sign of a maximum in the yield at total conversion of xylene, and one may conclude that the rate of decomposition of phthalic anhydride is negligibly small under "normal" operating conditions. Bernardini and Ramacci consider that the oxidation of phthalic anhydride is inhibited by the presence of xylene and intermediates since pure phthalic anhydride is very readily oxidised under the conditions used for its production from xylene. (Hughes and Adams also found that pure phthalic anhydride could be readily oxidized). Vrbaski and Matthews in their reaction scheme only show indirect

Table 2 Kinetic Data of Novella & Benlloch[18,19,20]

Temperature (°C)	K_1	K_2	K_3	K_4	K_5	K_6	K_7
			(gm.moles/Kg.hr.atm.)				
310	19.8	8.3	2.0	40	5	0.6	7.5
330	24.6	9.6	5.0	57	9	1.25	12.5
350	33.4	11.3	7.0	74	14	2.46	20.7
370	41.3	12.8	12.9	100	23	4.50	32.0
Activation Energy (cals/gm.mole)	9200	5400	22900	11350	18600	25000	18000

Note: The rate constants refer to the reaction scheme of Figure 2

formation of carbon oxides from phthalic anhydride (via maleic anhydride), although they do state that small quantities may be formed directly. Taken together these results seem to indicate that phthalic anhydride is fairly stable towards further oxidation. Landau and Simon remark in this content "It is possible indeed to obtain excellent yields of phthalic (anhydride) over a wide range of temperature (320-550°C), depending on the catalyst, because phthalic anhydride is a very stable molecule." Furthermore there appears to be no fundamental distinction between the two catalyst types in this respect.

Apart from the results of Novella and Benlloch the available kinetic data is mostly confined to expressions for the rate of disappearance of o-xylene. This is presented graphically in Figure 3 which shows the rate of reaction of o-xylene as a function of temperature for a number of different catalysts at the same reactant concentrations. Froment's fictitious data and data for o-methyl benzyl alcohol and tolualdehyde oxidation are also shown. It will be seen that there is only a moderate (roughly tenfold) variation in catalyst activity. The temperature range covered by the graph is 300-400°C and one would therefore expect that the catalysts represented would all be of the less active (German) type. This is largely the case, but it is interesting to note that the catalyst used by Vrbaski and Matthews was an unpromoted fused V_2O_5, and this shows a lower activity than any of the others. The activation energies found for o-xylene disappearance are mostly in the 25-30 Kcal/gm.mole range; Novella and Benlloch report the exceptionally low value of 15.4 Kcal/gm.mole.

It must be admitted that no very clear picture of the reaction scheme or the relative ease of the various steps emerges from the published literature. In view of the undoubted fact that industrial reactors operate with 60-70% yields of phthalic anhydride and only traces of other products (apart from carbon oxides) we can

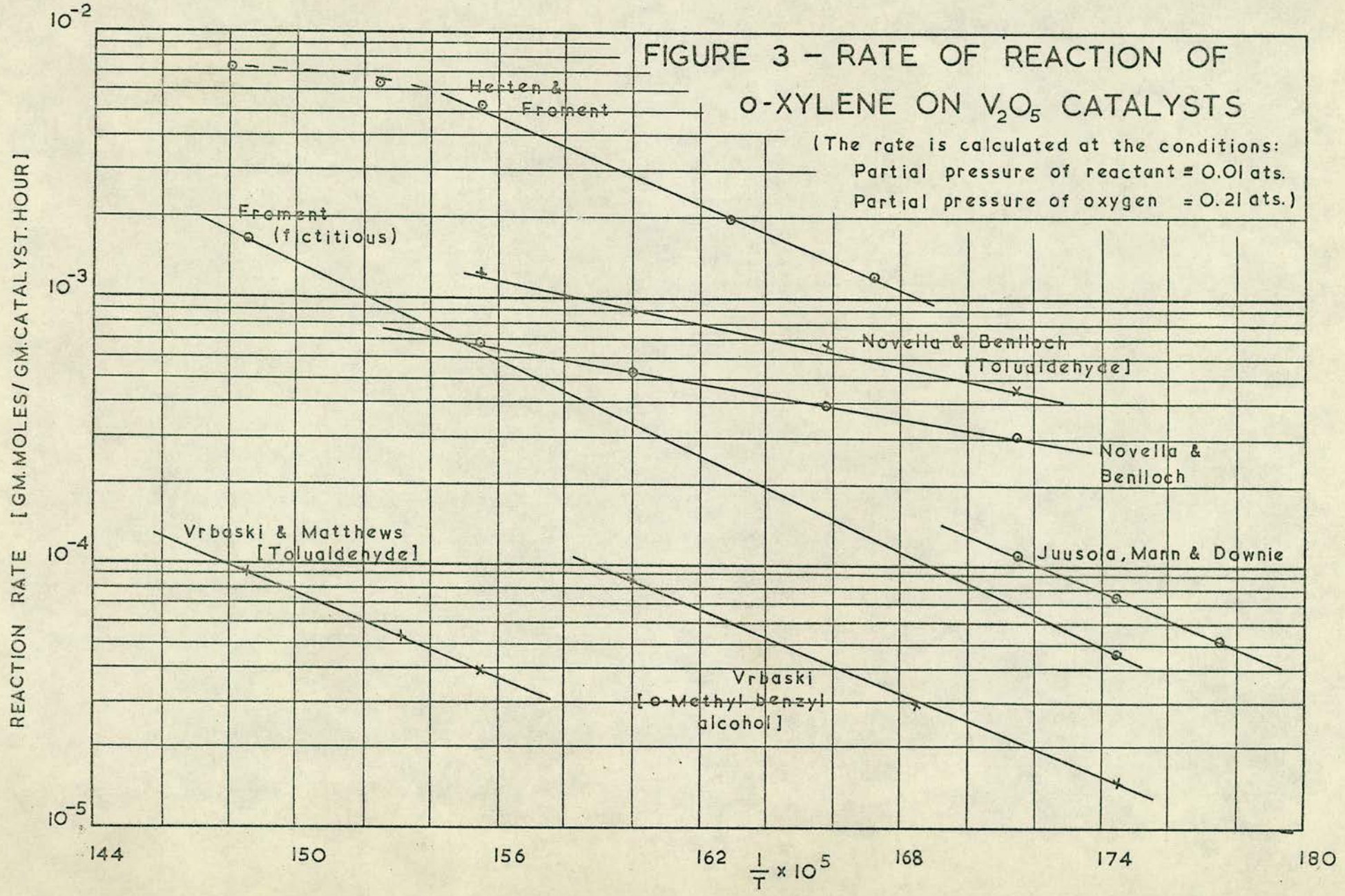
FIGURE 3 – RATE OF REACTION OF o-XYLENE ON V_2O_5 CATALYSTS
(The rate is calculated at the conditions:
Partial pressure of reactant = 0.01 ats.
Partial pressure of oxygen = 0.21 ats.)
REACTION RATE [GM.MOLES/GM.CATALYST.HOUR]
10^{-2}
10^{-3}
10^{-4}
10^{-5}
Herten & Froment
Froment (fictitious)
Novella & Benlloch [Tolualdehyde]
Novella & Benlloch
Vrbaski & Matthews [Tolualdehyde]
Juusola, Mann & Downie
Vrbaski [o-Methyl benzyl alcohol]
144
150
156
162
168
174
180
$\frac{1}{T} \times 10^5$

only conjecture that all reaction intermediates are fairly readily oxidized: we are then left with the simplified reaction scheme of Froment:

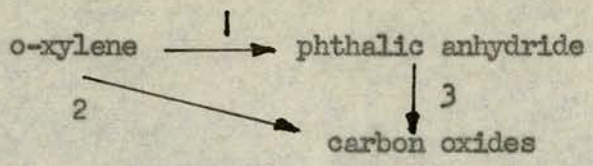

We may still argue about the relative rates for the three steps but the scheme itself adequately represents the overall reaction. No significant difference between the two catalysts can be seen, though rate data for the American type is lacking.

A number of workers mention the occurrence of homogeneous oxidation and oxidation catalyzed by the reactor walls. For example, Bernardini and Ramacci found that a stainless steel reactor oxidized 8-13% of the feed phthalic anhydride at 500°C and 0.14 secs. contact time; the catalyst packed reactor oxidized 70-80% at 500°C and 0.067 secs. contact time. A glass reactor without catalyst only oxidized 1% of the phthalic anhydride under the same conditions as the metallic reactor. Similarly Hughes and Adams report 2% combustion of phthalic anhydride in an empty Pyrex reactor at 575°C compared with 15% combustion in a steel reactor. Vrbaski and Matthews found that only 2% of their feed o-methyl benzyl alcohol reacted in a blank run at 450°C and 0.6 secs. contact time. Most of the studies of o-xylene oxidation make no mention of homogeneous or blank reaction with the exception of Mann and Downie and Juusola, Mann and Downie. The latter found that the blank reaction was greater with glass than stainless steel (in contrast with the observed results for phthalic anhydride quoted above), and that even with stainless steel the blank reaction was significant compared with the catalytic reaction at temperatures above 315°C. It would be interesting to know whether other workers did not find or did not look for the presence

of a blank reaction.

There have been a number of studies specifically directed to the homogeneous oxidation of o-xylene in the gas phase[33-37]. Wright found thirty eight different reaction products: the principal products were carbon oxides, methane, hydrogen, water, toluene and 1 methyl 2 vinyl benzene[35]. Wright[34] and Burgoyne[33] both report an activation energy of 38 Kcal/mole for the overall disappearance of o-xylene; Denisova and Denisov[37] give 31 Kcal/mole and Satterfield and Loftus[36] give 20 Kcal/mole. Actual values for the rate constants given by these authors do not agree but they all show that the rate is very much slower than that of the catalytic oxidation. Satterfield and Loftus calculate that (in the absence of any interaction between the catalyst and the homogeneous reaction) at 550°C and 0.15 seconds contact time about 2% of the feed o-xylene to a catalyst packed reactor would disappear by homogeneous reaction.

1.4 Reaction models and mechanism

The theory of hydrocarbon oxidation reactions on vanadium pentoxide catalysts has its foundations in the observations that during the oxidation process the catalyst exists partly in a reduced form[38] and that the oxidation may be carried out by the catalyst without the presence of oxygen in the gas phase[39]. These two facts suggest a cyclic process in which the hydrocarbon is first oxidized by the catalyst; the reduced catalyst is subsequently re-oxidized by gas phase oxygen. This view is supported by the observations of Maxted[40], who found that a number of aromatic hydrocarbons of varying character could be oxidized at about the same rate at a given temperature on V_2O_5 catalysts - a fact which can be explained by the hypothesis that the rate of reaction is largely determined (for all the substances considered) by the rate of re-oxidation of the catalyst.

Mars and van Krevelen developed this theory to obtain an expression for the overall rate of reaction and tested this against the experimental results for the oxidation of naphthalene, toluene, benzene and anthracene[41]. They pictured the chemical reaction as occurring between an organic molecule in the gas phase and an oxygen atom (ion) on the surface of the catalyst lattice. This reaction leads to a deficiency of oxygen in the surface layer of the catalyst which is made up by the uptake of oxygen from the gas phase. The two processes establish a dynamic equilibrium according to the ideas of Langmuir and Hinshelwood.

Let

K_1, K_2 = rate constants

p_1, p_2 = partial pressures of hydrocarbon and oxygen respectively in the bulk gas

S = fraction of the potentially active catalyst surface in the oxidized state

N = number of oxygen molecules required to oxidize one hydrocarbon molecule

r_1, r_2 = rates of reaction

The rate of hydrocarbon reaction is given by

$$r_1 = K_1 . p_1 . S$$

if the reaction is assumed first order in hydrocarbon and directly proportional to the fraction of the catalyst in the oxidized state.

The rate of re-oxidization is given by

$$r_2 = K_2 . p_2 . (1 - S)$$

making similar assumptions to the above. At the steady state we have

$$r_1 = \frac{1}{N} r_2$$

therefore

$$K_1 \cdot p_1 \cdot S = K_2 \cdot p_2 \cdot (1 - S)/N$$

therefore

$$S = \frac{K_2 \cdot p_2}{N \cdot K_1 \cdot p_1 + K_2 \cdot p_2}$$

therefore

$$r_1 = \frac{1}{\frac{1}{K_1 \cdot p_1} + \frac{N}{K_2 \cdot p_2}}$$

According to the theory the constant K_2 should have identical values for the oxidation of different hydrocarbons over the same catalyst at the same temperature. Mars and van Krevelen confirmed this for three of the four hydrocarbons which they studied, but found a deviation in the case of toluene.

A useful paper by Simard et al. shows that o-xylene oxidation on V_2O_5 presents the same general features. Experiments were carried out in which the composition of a V_2O_5 on silicon carbide catalyst was determined by X-ray and chemical analysis after operation under various conditions. It was found that during "normal" operation with a 1.1 mole % xylene feed the catalyst contained V_2O_5, V_2O_4 and the intermediate oxide $V_2O_{4.34}$ (or $V_{12}O_{26}$). Moreover it was not merely the surface layer of the catalyst which was reduced but the entire depth, and electron diffraction measurements indicated that the less reduced $V_2O_{4.34}$ overlay the more reduced V_2O_4. When using a feed containing 3.3 mole % o-xylene the catalyst was rapidly reduced to the point where it consisted almost entirely of V_2O_4 with some V_2O_3: in this condition it was no longer active for the production of phthalic anhydride. A sample of catalyst was also found to oxidize (for a brief period of 2-5 minutes) a 1 mole % xylene in nitrogen feed, thus confirming the role of lattice oxygen in the

oxidation process.

In the same paper experiments on the uptake of oxygen by vanadium oxides are reported. A vanadium pentoxide sample showed no measurable gain or loss of oxygen when heated cyclically between 25°C and 400°C at 170 mm.Hg oxygen pressure. The introduction of a small quantity of V^{+4} ions to vanadium pentoxide caused a marked change in behaviour: the sample adsorbed oxygen on cooling and desorbed it on heating provided a temperature of about 390°C was not exceeded. Above this limit an irreversible adsorption of oxygen occurred. The uptake of oxygen by $V_2O_{4.34}$, V_2O_4 and V_2O_3 was also studied in the 400-500°C range. These processes followed a parabolic rate law and had activation energies of 30, 30 and 17 Kcal/gm.mole respectively.

The reaction of o-xylene was visualized by these authors as preceeding in the following manner:

1. Chemisorption of the hydrocarbon on the catalyst surface
2. Reaction with oxygen ions of the catalyst
3. Desorption of intermediate or final products
4. Replenishment of oxygen to the catalyst from the feed air

The second step may take place via the diffusion of vanadium or oxygen ions in the lattice. This is shown by

(a) the fact that the catalyst is reduced in depth during normal operation

(b) the catalyst continues to function for some time when oxidizing xylene in nitrogen.

Clark and Berets investigated the electrical properties of vanadium pentoxide catalysts[42]. They found that the Tamman temperature for the bulk catalyst was of the order of 350°C, compared with 115-180°C for the surface layer. Above these limits the anionic vacancies would therefore be mobile.

Kasatkina, Boreskov et al[43] reported an activation energy of 39-53 Kcal/gm.mole for the exchange of ^{18}O with V_2O_5 catalysts (the variation being due to different modes of catalyst preparation) and Reiter[44] used an ^{18}O tracer to demonstrate that lattice oxygen appears in the products of hydrocarbon oxidation on V_2O_5 catalysts.

A series of papers by Downie, Graydon et al have appeared describing the oxidation of a variety of organic substances (including o-xylene and naphthalene) over samples of the same batch of catalyst[22,23,45-48]. In the original paper[45] on naphthalene oxidation a model was proposed which is referred to as the steady state adsorption model. This model assumes that oxygen is adsorbed on the surface of the catalyst and that reaction occurs when an organic molecule in the gas phase strikes this adsorbed oxygen. The developed rate equation from this model turns out to be identical with thatfrom the oxidation-reduction model: the rate constant K_2 must now be called the rate constant for oxygen adsorption rather than the rate constant for catalyst re-oxidation. Kinetic data is therefore unable to distinguish between the models. The facts reported above, however, on the reduction "in depth" of the catalyst and the transfer of ^{18}O from the lattice to the oxidation products, provide powerful support for the oxidation-reduction model. Probably the most sensible view is to regard the steady state adsorption model as a special case of the oxidation-reduction model, since it is doubtful whether the bond between chemisorbed oxygen and the surface can be distinguished from any other V-O bond in the surface region.

Hughes and Adams[32] studied the oxidation of phthalic anhydride on a fused V_2O_5/SiC catalyst and found that the results could be correlated by an expression of the form

$$\text{Rate of PA reaction} = \frac{Ap}{1 + Bp}$$

where p is the partial pressure of phthalic anhydride, and A and B are temperature dependent constants. They proposed the reaction model shown below,

$$PA + (VO) \underset{K_{-1}}{\overset{K_1}{\rightleftharpoons}} (VOPA) \qquad (1)$$

$$(VOPA) \xrightarrow{K_2} (V) + (O - PA) \qquad (2)$$

$$(V) + O_2 \xrightarrow{\text{fast}} (V) \qquad (3)$$

i.e. a reversible chemisorption, desorption of products and a rapid re-oxidation of the catalyst. They showed that this mechanism led to a rate expression of the above type where

$$A = \frac{K_1 K_2 K'}{K_{-1} + K_2}$$

$$B = \frac{K_1}{K_{-1} + K_2}$$

$$A/B = K_2 K'$$

(K' is a conversion factor to convert from the fraction of surface covered to the true surface concentration.) Values of A and B are recorded for temperatures from 497°C to 575°C and activation energies for the various steps are given. One interesting experimental observation was an increase in the rate of phthalic anhydride oxidation with <u>decreasing</u> oxygen partial pressure below 0.1 atmospheres - a phenomenon attributed to catalyst reduction by the authors. Above this value the rate was independent of oxygen pressure.

We note that the rate expression of Hughes and Adams may readily be derived from the Mars and van Krevelen expression if the oxygen partial pressure is assumed constant (as may well be the case if an excess of air is used)

$$r = \frac{1}{\frac{1}{K_1 p_1} + \frac{1}{K_2 p_2}}$$

$$= \frac{K_1 p_1}{1 + \frac{N K_1 p_1}{K_2 p_2}}$$

$$= \frac{A p_1}{1 + B p_1}$$

where

$$A = K_1$$

$$B = \frac{N.K_1}{K_2.p_2}$$

$$A/B = \frac{K_2.p_2}{N}$$

Hence the value of 44 Kcal/gm.mole which Hughes and Adams report as the "heat of activation for the desorption of oxidized PA" could also be interpreted as the activation energy for catalyst re-oxidation. The fact that different models lead to the same rate expression necessitates caution in claiming support for any one model.

A paper by Allen[49] discusses the mechanism of o-xylene (and naphthalene) oxidation with particular reference to the lattice and organic molecule dimensions. It is estimated that the surface area of a V_2O_5 - $V_2O_{4.34}$ catalyst is approximately 12.2 $\mathring{A}^2$ per available oxygen atom, whereas the average area of an adsorbed organic molecule such as o-xylene or phthalic anhydride is about 33 $\mathring{A}^2$. Hence the oxidation of xylene to tolualdehyde (requiring two oxygen atoms per molecule of xylene) would be possible - either by collision of the

organic molecule with the surface or adsorption on the surface - but higher oxidation products could not be directly formed. Allen rejects various mechanisms such as repeated adsorption and desorption of intermediate products (on the grounds that appreciable quantities of intermediate products are not found in the reaction mixture), mobile free radicals on the catalyst surface and collisinn of gaseous oxygen with an adsorbed organic molecule, and he concludes that the important stages in the process are

1. Chemisorption of the hydrocarbon on the catalyst
2. Further oxidation at the adsorbed site followed by desorption
3. Replenishment of oxygen to the surface.

The second step involves mobility of oxygen in the lattice and Allen cites some of the references given above in support of this. He concludes that the rate determining step is the diffusion of oxygen through the surface layers of the catalyst.

It seems fairly certain that Allen's mechanism (which is more or less the same as that of Simard et al) must be involved in the direct transformation of o-xylene to phthalic anhydride (as shown in the reaction schemes of Herten and Froment, Vrbaski and Matthews, etc.). However the investigations of Bernardini and Ramacci (among others) which were published after Allen's paper appeared show that o-xylene can react to phthalic anhydride via a number of intermediates.

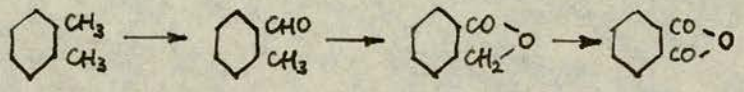

Each stage in this sequence could be accomplished without the need for oxygen diffusion through the catalyst.

Vrbaski and Vrbaski and Matthews[30,50,51] studied the

oxidation of o-methyl benzyl alcohol and tolualdehyde over a V_2O_5 catalyst. They also conclude that two basic mechanisms can contribute to the reaction: at milder conditions (lower temperatures) there is a stepwise oxidation between a series of organic intermediates (o-toluic acid, phthalide, etc.) and oxygen ions adsorbed on the surface. At higher temperatures there can occur a direct oxidation to phthalic anhydride by reaction with lattice oxygen. They also found that the partly reduced catalyst favoured complete combustion before becoming totally inactive.

The effect of promoters such as potassium sulphate on the action of a V_2O_5 catalyst is very much a matter for speculation. It is known[41] that the potassium sulphate is partly converted to pyrosulphate in the presence of SO_3 (and, of course, SO_2 is added to the feed in von Heyden process), and that pyrosulphate forms a melt in which V^{5+} and V^{4+} ions can dissolve. Hence an oxidation-reduction cycle may be set up in the superficial liquid phase on the catalyst surface. Alkaline sulphate promoters give increased activity when added to vanadium pentoxide catalysts for the oxidation of sulphur dioxide and carbon monoxide: one might therefore reasonably expect to find increased activity in the case of hydrocarbon oxidation (as indeed is shown by the results of Figure 3) in contrast with the statement that unpromoted American catalysts are more active than the promoted German catalysts. The effect of the promoter is to lengthen (and hence weaken) some of the V - O bonds in the lattice, as may be shown by infrared analysis[52].

1.5 Fixed bed reactor design

The primary objective here, as with all reactor design problems where raw material costs are relatively high, is to achieve the maximum possible yield of product. Secondary objectives are that

the reactor should operate in a smooth and stable manner, and be easy to control. The reaction schemes for o-xylene oxidation discussed in Section 1.3 show clearly that reactions can occur which consume both the feed material and the desired product unprofitably: the designer must seek to minimise the occurrence of these undesirable reactions. Theoretical aspects of optimization problems such as this have been much discussed in the literature. For example, Bilous and Amundson have examined the case of two consecutive reactions

$$A \xrightarrow{E_1} B \xrightarrow{E_2} C$$

where the intermediate product, B, is the desired one[53]. As one would intuitively expect a declining temperature sequence along the tubular reactor favours the production of B if $E_2 > E_1$, but the temperature should be held at the maximum permitted value if $E_1 > E_2$.

In practice there are two reasons why it is rarely possible to make much use of optimization techniques in reactor design. The first of these is that the reaction parameters are rarely known with any accuracy (as is the case with o-xylene oxidation) and hence only a qualitative assessment is possible. Secondly, and of more fundamental importance, it is usually assumed in optimization studies that the optimization is effected by controlling either the temperature or the concentration of one of the reactants. This may be possible to some extent with a batch reactor when the heat effect of reaction is small, but with a tubular reactor it is only possible to vary concentration by making reactant additions at a number of points along the reactor which would greatly add to the cost and complexity of the system, and the temperature profile of the reactor is perhaps even less amenable to control. Nevertheless some attempt at temperature control must be made in the case of xylene oxidation - not only with a view to obtaining a high yield, but also to avoid damage

to the reactor and catalyst charge. The adiabatic temperature rise for the desired reaction (to phthalic anhydride) is of the order of 300-400°C for the conditions employed industrially. Clearly, anything approaching adiabatic operation would lead to the occurrence of such high temperatures that both feed and product material would readily combust. For the complete combustion of o-xylene to carbon dioxide the adiabatic temperature rise is of the order of 1000°C, so that there is a very real danger to the reactor system if the combustion reaction takes hold.

It was recounted in an earlier section that new phthalic anhydride installations were mostly based on the low space velocity process. The reason for this is unquestionably in part due to the higher yields obtainable from this process, but it also seems that high space velocity processes have a poor safety record. A recent article[14] describing the replacement of an existing plant by a fixed-bed low space velocity plant makes the following comment in connection with the large number of available processes "However the multiplicity of choice doesn't necessarily ensure trouble-free operation. Up to now, a number of phthalic anhydride plants have been temporarily or permanently shut down by mishaps such as fires, explosions, catalyst deactivation, etc." An unpublished N.R.D.C. report has this to say: "There are two types of o-xylene catalyst, both having vanadium pentoxide as the active ingredient, but one having siliceous support whilst the other has a carborundum support. The first may be regarded as a mild catalyst whilst the other is much more active, producing the same amount of anhydride in a tube of about one-third the length. Naturally the (temperature) peak is more intense and shorter with the more active catalyst and the selectivity is somewhat lower. However, mechanical design considerations make it very expensive to produce a large reactor taking advantage of the shorter

tube length possible with the active catalyst and attempts to exploit its use have been disastrous to the extent that plants designed for this catalyst are now being scrapped and replaced by those using the mild catalyst." It seems that the larger temperature peak associated with the high space velocity process (superimposed on a base temperature which is already higher than for the low space velocity process) means that the tendency for the combustion reactions to take hold is very much increased.

Faced with the problem of a reaction having a very large heat release and a tendency to produce unwanted carbon oxides as the temperature increases designers have produced the multi-tube reactor. As the tube diameter is decreased so the surface to volume ratio increases and hence heat dissipation is improved relative to heat production. Moreover the difference between axial and wall temperatures in the reactor tube is decreased as tube size decreases and this also leads to improved temperature control and stability. The bundle of reactor tubes is immersed in a circulating heat transfer medium which provides a more or less uniform jacket temperature. Such is the traditional and present day reactor design for highly exothermic reactions requiring temperature control. It will be shown in the following chapter that this design had disadvantages and may readily be improved by the technique of catalyst dilution.

CHAPTER 2 TEMPERATURE CONTROL BY CATALYST DILUTION

2.1 Deficiency of the multi-tube reactor

We consider, for simplicity, the case of a single irreversible first order reaction which takes place in a tubular reactor. This gives a reasonable first approximation to xylene oxidation under normal operating conditions. We also neglect radial gradients of concentration and temperature, an assumption which is valid for tubes of small diameter. Heat and mass balances on a differential length of reactor give

$$F.\pi R^2.Cp.dT = F.\pi R^2.N_A.dX.(-\Delta H) - 2\pi R.dZ.U.(T - T_j) \qquad (1)$$

$$F.\pi R^2.N_A.dX = r.dW = K.N_A.P.(1 - X)\rho_B.\pi R^2.dZ \qquad (2)$$

Combining (1) and (2) we obtain

$$\frac{dT}{dZ} = \frac{\Delta T_{ad}.K.P.\rho_B(1 - X)}{F} - \frac{2U(T - T_j)}{F.R.Cp} \qquad (3)$$

a differential equation describing the variation of temperature along the reactor.

In industrial reactors of the type under consideration the feed enters with zero conversion and at the temperature of the jacket fluid. This will be assumed to be the case here and in subsequent discussion unless otherwise stated. Equation (3) then shows that the temperature gradient is initially positive having a value

$$\frac{dT}{dZ} = \frac{\Delta T_{ad}.K.P.\rho_B}{F} \qquad (4)$$

(where K is evaluated at T_j) and that a maximum occurs in the temperature profile when

$$\frac{\Delta T_{ad}.K.P.\rho_B(1 - X)}{F} = \frac{2U(T - T_j)}{F.R.Cp} \qquad (5)$$

The location of this peak temperature is often referred to as the reactor "hot spot". All reactors of sufficient length must exhibit such a peak inasmuch as the conversion X must ultimately approach unity. Subject to this restriction, however, the form of the temperature profile can show considerable variation. Some typical curves are drawn in Figure 4. Although firm pronouncements can only be made in respect of a particular system, we can say roughly that curves A and D represent unsatisfactory operating conditions whereas curves B and C are reasonable. Curve A is unsatisfactory because reaction is so slow that an appreciable portion of the reactant will be left unconsumed at the end of the reactor. Curve D, on the other hand, is unsatisfactory because it shows an excessively high temperature at the hot spot; let us suppose that the difference between the peak temperature and the coolant is almost equal to the adiabatic temperature rise. If this were a permissible situation then there would be no need to employ an expensive multi-tube cooled reactor for the reaction: a large diameter adiabatic reactor could be used. Excessive temperatures are undesirable with cooled tubular reactors because of the onset of undesirable side reactions or because the catalyst is affected above some critical temperature: both of these possibilities apply in the case of oxylene oxidation.

It may even turn out in a particular case that reactor operation with a temperature profile of the form of curve C is unsatisfactory if the phenomenon known as parametric sensitivity is encountered. The occurrence of parametric sensitivity implies that a very small change in some operating parameter (e.g. jacket temperature or feed concentration) causes a marked change in the

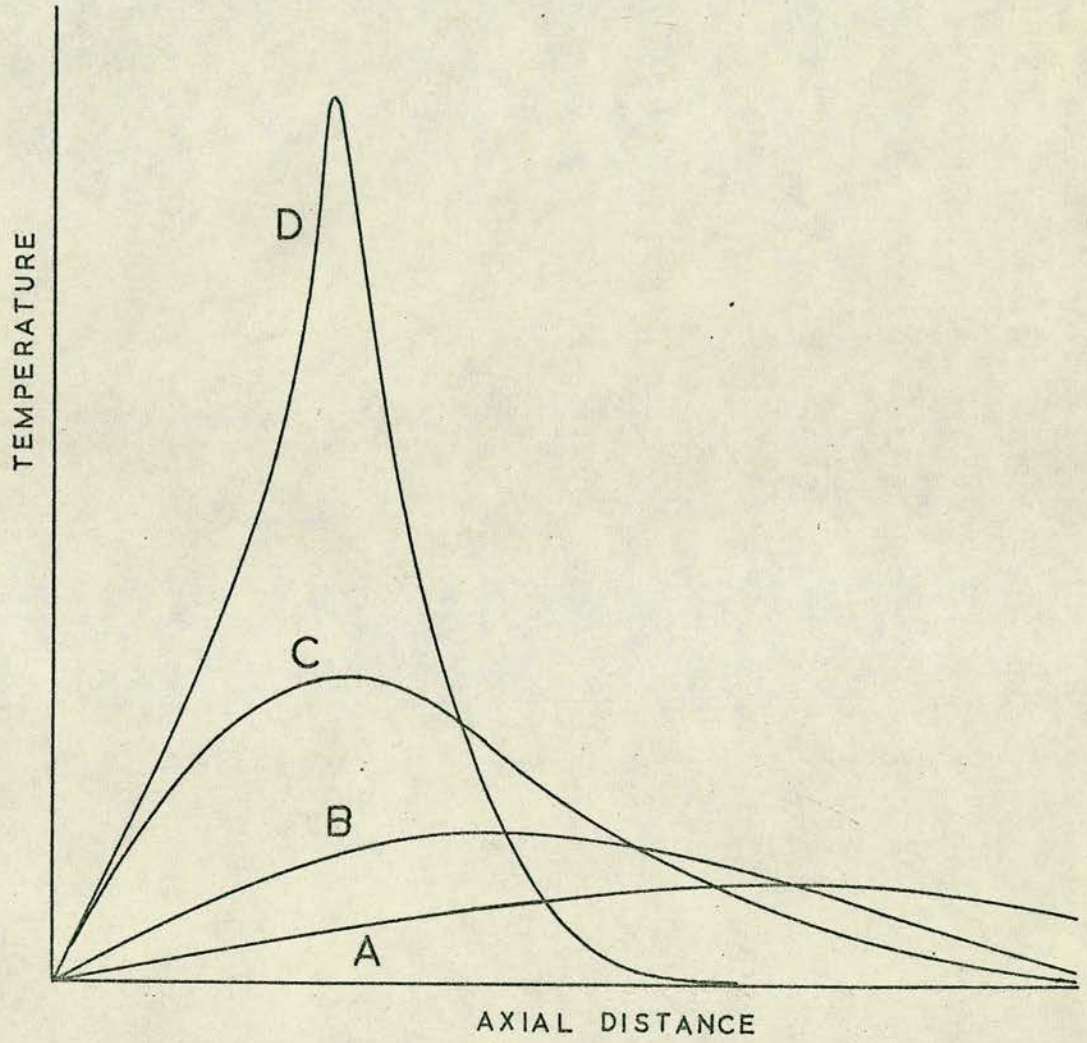

FIGURE 4 – TYPICAL TEMPERATURE PROFILES FOR EXOTHERMIC REACTIONS IN COOLED TUBULAR REACTORS

temperature profile in general and the size of the peak in particular. Thus a curve of the form of C might very readily transform into curve D following a small increase in jacket temperature. This has been demonstrated by Bilous and Amundson[54] who used an analogue computer to examine the dependence of the temperature profile of a first order exothermic reaction on various parameters. A criterion for the onset of parametric sensitivity has been developed by Barkelew, who integrated the appropriate differential equations on a digital computer for a large number of parameter combinations, and examined the dependence of the peak temperature on those parameters[55]. He expressed his results in the form of a correlation between the dimensionless groups:

$$S = \Delta T_{ad}.E/R_G T_j^2$$

$$N = 2U/R.Cp.K.\rho_B.P$$

We shall use these groups to develop a criterion for the onset of temperature runaway - a condition which we may define by

$$\frac{dT}{dZ} > 0$$

$$\frac{d^2T}{dZ^2} > 0$$

- and which is therefore exemplified by curve D of Figure 4.

If we differentiate equation (3) we obtain

$$\frac{d^2T}{dZ^2} = \frac{\Delta T_{ad}.P.\rho_B}{F}\left[\frac{dK}{dZ}(1 - X) - K\frac{dX}{dZ}\right] - \frac{2U}{F.R.Cp}.\frac{dT}{dZ}$$

$$= \frac{\Delta T_{ad}.K.P.\rho_B(1 - X)}{F}\left[\frac{E}{R_G T^2}.\frac{dT}{dZ} - \frac{K.P.\rho_B}{F}\right] - \frac{2U}{F.R.Cp}.\frac{dT}{dZ}$$

$$= \frac{\Delta T_{ad}.K.P.\rho_B(1 - X)}{F^2}\left[\frac{E}{R_G T^2}\left[\Delta T_{ad}.K.P.\rho_B(1 - X) - \frac{2U(T - T_j)}{RCp}\right]\right.$$

$$\left. - KP\rho_B\right] - \frac{2U}{F^2 RCp}\left[\Delta T_{ad}.K.P.\rho_B(1 - X) - \frac{2U(T - T_j)}{RCp}\right]$$

Hence $\frac{d^2T}{dZ^2} \leq 0$ if

$$\Delta T_{ad}.K.P.\rho_B(1 - X)\left[\frac{E}{R_G T^2}\left[\Delta T_{ad}.K.P.\rho_B(1 - X) - \frac{2U(T - T_j)}{RCp}\right] - K.P.\rho_B\right]$$

$$\leq \frac{2U}{RCp}\left[\Delta T_{ad}.K.P.\rho_B(1 - X) - \frac{2U(T - T_j)}{RCp}\right]$$

$$\text{i.e. } A(1 - X)\left[\frac{E}{R_G T^2}\left[A(1 - X) - B(T - T_j)\right] - C\right] \leq B\left[A(1 - X) - B(T - T_j)\right]$$

where $A = \Delta T_{ad}.K.P.\rho_B$

$B = \frac{2U}{RCp}$

$C = K.P.\rho_B$

This condition may be put in the form:

$$\left[A(1 - X) - B(T - T_j)\right]\left[A(1 - X)\frac{E}{R_G T^2} - (B + C)\right] \leq C.B.(T - T_j) \quad (6)$$

From this we may deduce that the condition for temperature runaway not to occur at the entrance to the reactor is

$$A\left[A.\frac{E}{R_G T_j^2} - (B + C)\right] \leq 0$$

Note Added, 22.4.1971.

This conclusion is incorrect. The second bracketed term on the left hand side of inequality (6) contains the rate constant K as a component of the factor A. Hence as T and X increase this second term may become positive even if it were negative initially. Therefore the criterion given here does not define the onset of temperature runaway but merely gives the conditions which would lead to runaway conditions at the entrance of the reactor. The distinction between these two situations (in terms of the operating parameters required to produce them) is likely to be small.

or $$A.\frac{E}{R_G T_j^2} \leq B + C \qquad (7)$$

We will now show that (for a single first order reaction) if temperature runaway does not occur at the entrance to the reactor it will not occur at all.

If we consider inequality (6) the first bracketed term, $\left[A(1 - X) - B(T - T_j)\right]$, is proportional to the temperature gradient $\frac{dT}{dZ}$, and hence is always positive in the region of interest to us. We have just shown that the second term on the left hand side is either zero or negative at the entrance to the reactor if temperature runaway does not occur there. Clearly this term will become more negative as X and T increase. The term $C.B(T - T_j)$ is positive and increasing in the region of interest. Hence inequality (6) is satisfied at all points if it is satisfied at the reactor entrance. (The diagrams in Barkelew's paper do not support this conclusion, which is presumably attributable to the modified form of the Arrhenius expression used by Barkelew.)

Following from this proof the condition for temperature runaway in the reactor is given by the reverse of inequality (7):

$$A \frac{E}{R_G T_j^2} \geq B + C$$

or $$\Delta T_{ad}.K.P.\rho_B.E/R_G T_j^2 \geq \frac{2U}{RC_p} + K.P.\rho_B$$

In Barkelew's terminology this becomes

$$S \geq N + 1$$

or $$\frac{S - 1}{S} \geq \frac{N}{S} \qquad (8)$$

This condition is shown in Figure 5, together with

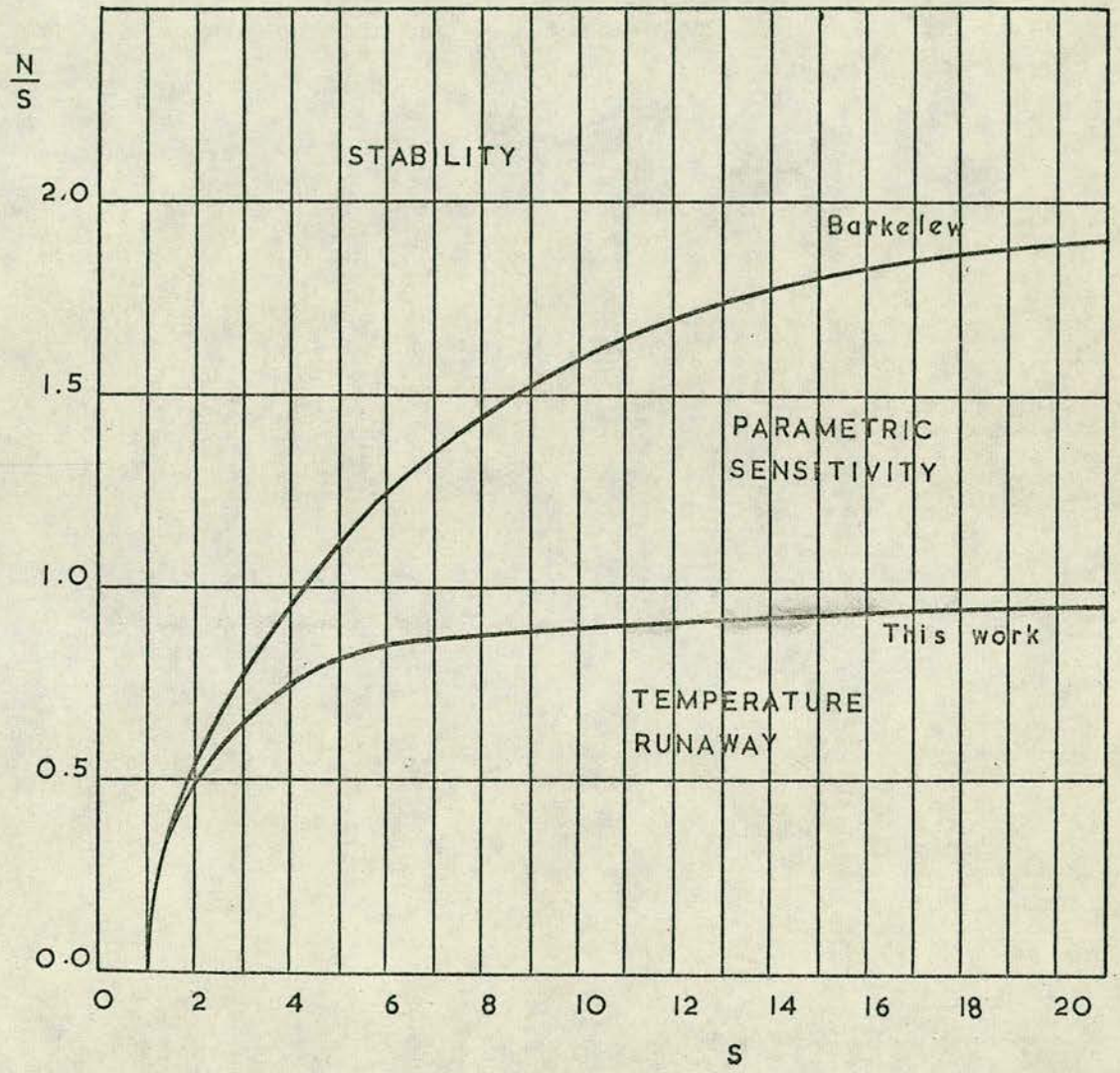

FIGURE 5 – STABILITY CRITERIA FOR A SINGLE FIRST ORDER REACTION IN A TUBULAR REACTOR

Barkelew's criterion for the onset of parametric sensitivity. As expected, Barkelew's criterion is more conservative.

We have seen in a qualitative fashion that for every cooled reactor there exists a region of satisfactory operation intermediate between the extremes of incomplete reaction in a reasonable reactor length and excessive temperature peaks. It is conceivable that this region will be uncomfortably small so that an industrial operation subject to normal fluctuations will be unable to keep within its boundaries. A paper by Froment has shown that this is the case for o-xylene oxidation under conditions said to be typical of the industrial reaction[10]. These conditions are summarised in Table 3, and include the kinetic data for his simplified reaction scheme which was referred to in Chapter 1. There appears to be no strict justification for the values given to the kinetic parameters, but the activation energies are certainly of the right order and the overall appropriateness of the figures can be judged from Table 4, which shows the maximum yield of phthalic anhydride attainable in an isothermal reactor (and the required reactor length). (Appendix I describes the derivation of the results of Table 4.) It may be seen that the maximum yield from a reasonably short reactor is about 70% which is in line with industrial yields. Froment took into account radial gradients of temperature and concentration and solved the resulting conservation equations numerically. He found that a jacket temperature variation of only $3^{\circ}C$ was sufficient to displace the reactor performance from the region of insufficient reaction (in a length of 2.5 - 3.0 metres) to the region of temperature runaway. This is clearly an unsatisfactory position and the obvious remedies such as decreasing the tube diameter (already only 1.0 inch) or decreasing the concentration of o-xylene in the feed have equally obvious disadvantages. There remains the possibility, suggested by

Table 3 Parameters of the Froment O-xylene Oxidation Model

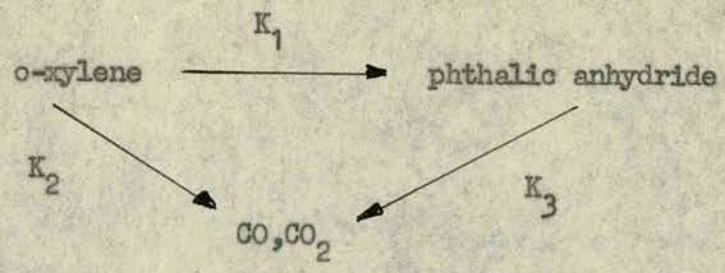

All reactions are first order with respect to the organic component and also with respect to oxygen.

$$K_1 = \exp\left(\frac{-27,000}{RT} + 11.648\right) \text{ gm.mols/gm.sec.atm}^2$$

$$K_2 = \exp\left(\frac{-31,400}{RT} + 12.67\right) \text{ gm.mols/gm.sec.atm}^2$$

$$K_3 = \exp\left(\frac{-28,600}{RT} + 10.78\right) \text{ gm.mols/gm.sec.atm}^2$$

Heat of reaction 1	= + 307 K.cal/gm.mol.
Heat of reaction 3	= -1090 K.cal/gm.mol
Reactor tube diameter	= 1 inch
Catalyst particle diameter	= 0.3 cms.
Catalyst bulk density	= 1.3 gms/cm^3
Mole fraction o-xylene in feed	= 0.00924
Mole fraction oxygen in feed	= 0.208 (assumed constant)
Mass velocity of gas	= 0.13 gms/cm^2.sec.

Table 3a Data Employed in the Matrix Model Simulating O-xylene Oxidation in a Tubular Reactor

$$n = 5$$

$$D_T = 2(n - 1)d = 2.4 \text{ cms.}$$

$$K \ (= h.A_s) = 0.0050$$

(By use of the subsidiary program simulating a packed bed heat exchanger, this K value was found to correspond to an overall heat transfer coefficient of 0.0022 cals/cm^{2}sec.$^\circ$C. Froment calculated his overall coefficient to be 0.0023 cals/cm^{2}sec.$^\circ$C (82.7 K.cal/m^2.hr.$^\circ$C))

$$C_p = 7.45 \text{ cals/gm.mol.}^\circ\text{C}$$

Table 4 Performance of an Isothermal Plug Flow Reactor based on Froment's Kinetic Data

Temperature (°C)	Maximum yield of phthalic anhydride	Selectivity at maximum yield	Reactor length for maximum yield (cms)
355	0.739	0.785	964
365	0.721	0.769	701
375	0.715	0.765	472
385	0.710	0.761	339
395	0.701	0.755	244

Note: These results are based on the data of Table 3 and are calculated as described in Appendix 1.

Froment himself, of modifying the temperature profile by catalyst dilution in such a way that the hot spot can be diminished or eliminated while maintaining a high (or higher) average reactor temperature.

This suggestion of Froment's appeared at a time when catalyst dilution was being investigated at Edinburgh in connection with the ammoxidation of naphthalene and the control of exothermic reactions generally (see next section), and provided the starting point for the work reported in this thesis. The remainder of this chapter will deal with the history of the use of catalyst dilution, the theory, and the application to the phthalic anhydride synthesis.

2.2 History of catalyst dilution

Catalyst dilution has been employed extensively in laboratory kinetic studies for the purpose of maintaining isothermal conditions in flow reactors. A large excess of inert material is normally used, and the degree of dilution is almost always uniform throughout the reactor space. (Under certain conditions errors may result from this procedure due to by-passing of feed round the active catalyst particles - a situation equivalent to a cross-flow reactor: an analysis has been given by van der Bleek et al[56].)

An early reference to the industrial use of dilution occurs in a patent granted to a Czechoslovakian company[57]. The diluents suggested are heat conducting materials such as aluminium and these are to be either intimately mixed with the catalyst or alternated with it in a series of layers. The principle example quoted is the contact process for sulphuric acid manufacture in which the reactor employs countercurrent cooling. It is stated that the temperature near the entrance of such a reactor may rise above the optimum level and subsequently fall well below the optimum, thus

spot, increased the total conversion of naphthalene, and gave an improved yield of phthalonitrile. At lower temperatures the effect of dilution was deleterious. Gilliatt concluded that at the hot spot temperature the combustion of ammonia was so dominant that insufficient oxygen remained for naphthalene reaction.

2.3 Dilution and the one dimensional reactor - theory

(Most of the results of this section and subsequent sections of this chapter have been published in References 61 and 62.)

As before we consider a single first order irreversible reaction and neglect radial temperature and concentration gradients. We define the catalyst dilution by

$$R' = \frac{\text{Total weight of packing}}{\text{Weight of active catalyst}} \qquad (9)$$

In general R' is a function of reactor length. Equations (2) and (3) can then be replaced by

$$F.\pi R^2.N_A.dX = r.dW = K.N_A.P(1 - X)\rho_B.\pi R^2.dZ/R' \qquad (10)$$

$$\frac{dT}{dZ} = \frac{\Delta T_{ad}.K.P.\rho_B(1 - X)}{F.R'} - \frac{2U(T - T_j)}{F.R.Cp} \qquad (11)$$

Equation (11) permits us to calculate the dilution required at a given value of conversion to achieve any temperature gradient within the range:

$$\frac{-2U(T - T_j)}{F.R.Cp} \leq \frac{dT}{dZ} \leq \frac{\Delta T_{ad}.K.P.\rho_B(1 - X)}{F} - \frac{2U(T - T_j)}{F.R.Cp}$$

For example, the dilution required to achieve isothermality is

$$R' = \frac{\Delta T_{ad}.K.P.\rho_B(1 - X)R.Cp}{2U(T - T_j)} \qquad (12)$$

(Note that in this case the feed must be preheated above the jacket temperature unless the reactor is infinitely long). A more useful

relation can be obtained by substituting (12) into (10) and integrating

$$\frac{dX}{dZ} = \frac{K.P.\rho_B(1 - X)}{F} \cdot \frac{2U(T - T_j)}{\Delta T_{ad}.K.P.\rho_B(1 - X)RCp}$$

$$\frac{X}{Z} = \frac{dX}{dZ} = \frac{2U(T - T_j)}{\Delta T_{ad}.F.R.Cp} = \text{Constant} \qquad (13)$$

It is seen that the conversion varies uniformly with distance along the reactor, and hence that the rate of reaction is constant. Now it would normally be desirable to use pure catalyst at the exit of the reactor, in order to achieve a high reaction rate. Hence from (12)

$$R' = \frac{1 - X}{1 - X_o} \qquad (14)$$

where X_o is the final conversion. Combining (13) and (14) we obtain

$$R' = \frac{1 - Z(X_o/Z_o)}{1 - X_o} \qquad (15)$$

The temperature difference necessary to achieve conversion X_o isothermally in length Z_o is given from (13) by

$$T - T_j = \frac{\Delta T_{ad}.F.R.Cp.X_o}{2U.Z_o} \qquad (16)$$

and the operating temperature is found from (12) and (16) with $R' = 1$, $X = X_o$

$$T = \frac{E}{R_G \log_e \left[\frac{A.Z_o.P.\rho_B(1 - X_o)}{F.X_o}\right]} \qquad (17)$$

where A is the pre-exponential factor of the rate constant.

The average catalyst dilution for the entire reactor is defined by

$$\overline{R'} = \frac{Z_o}{\int_o^{Z_o} \frac{dZ}{R'}}$$

and for the isothermal case this gives

$$\overline{R'} = -\frac{X_o}{1 - X_o \cdot \log_e(1 - X_o)} \qquad (18)$$

As an example of the isothermal reactor Table 5 shows the results of some calculations for o-xylene oxidation based on Froment's data (see Table 3) but neglecting the combustion reactions. The temperature difference, operating temperature, inlet and mean dilutions are shown which enable various conversions to be achieved in a 3 metre long, 1 inch diameter reactor.

The analytical approach can be extended to cover other simple reactions, e.g. a second order irreversible reaction, and in fact it is possible to treat some more complex reaction schemes. Equations (19), (20) and (21) are derived in Appendix 2 and give the conditions for isothermality in Froment's simplified scheme for o-xylene oxidation. Equation (20) gives the appropriate temperature

$$Z = \frac{(\Delta T_3 - \Delta T_1)\left[K_1 U - \frac{K_1}{K_1 + K_3 - K_2}\left((K_1 + K_3)U^{\frac{K_2}{K_1 + K_3}} - K_2 U\right)\right] + \frac{\Delta T_3 (K_1 + K_3)(1 - U)}{\left(U_o^{\frac{K_2}{K_1 + K_3}} - U_o\right)}}{\frac{N_B \cdot \rho_B}{F}.(K_1 + K_3)\left[\Delta T_3 (K_1 + K_3)U_o - (\Delta T_3 - \Delta T_1)\left(K_1 U_o - \frac{K_2 K_1}{K_1 + K_3 - K_2}\right)\right]} \qquad (19)$$

$$T - T_W = \frac{N_B \cdot \rho_B \cdot Cp \cdot R}{2h}\left[\Delta T_3 (K_1 + K_3)U_o - (\Delta T_3 - \Delta T_1)\right.$$

Table 5 Catalyst Dilutions to Achieve Isothermal Conditions for O-xylene Oxidation in a Tubular Reactor (neglecting the combustion reactions)

Yield of phthalic anhydride	$T - T_j$ (°C)	T_j (°C)	Catalyst dilution at the inlet	Mean catalyst dilution
0.2	2.4	322	1.25	1.12
0.4	4.8	349	1.67	1.30
0.6	7.2	372	2.50	1.64
0.8	9.6	405	5.00	2.49

Note: The results in Tables 5 and 6 were calculated using the data of Table 3 and also taking:

C_p = 7.45 cals/gm.mol.°C

Z_o = 300 cms

U = 0.0022 cals/cm^2.sec.°C

Table 6 Catalyst dilution Schedule to Achieve Isothermal Operation at 402°C with an 88% Conversion of O-xylene in a Tubular Reactor (taking account of the combustion reactions)

Z/Z_o	Conversion of o-xylene	Yield of phthalic anhydride	Catalyst dilution
0.0	0.000	0.000	4.08
0.2	0.207	0.182	3.38
0.4	0.403	0.348	2.69
0.6	0.592	0.500	2.02
0.8	0.753	0.614	1.46
1.0	0.880	0.686	1.00

$$(K_1U_o - \frac{K_2K_1}{K_1 + K_3 - K_2}(U_o^{\frac{K_2}{K_1 + K_3}} - U_o))\Big] \qquad (20)$$

$$R' = \frac{\Delta T_3(K_1 + K_3)U - (\Delta T_3 - \Delta T_1)(K_1U - \frac{K_2K_1}{K_1 + K_3 - K_2}(U^{\frac{K_2}{K_1 + K_3}} - U))}{\Delta T_3(K_1 + K_3)U_o - (\Delta T_3 - \Delta T_1)(K_1U_o - \frac{K_2K_1}{K_1 + K_3 - K_2}(U_o^{\frac{K_2}{K_1 + K_3}} - U_o))} \qquad (21)$$

difference for any selected combination of reaction temperature and final (total) conversion of xylene. Equations (19) and (21) give corresponding values of reactor length and catalyst dilution at intermediate conversions down the reactor. A single set of results is shown in Table 6. (It may be noted that since the reactor is isothermal the selectivity to phthalic anhydride can readily be obtained from the results of Appendix I.) The final conversion of o-xylene is 88% and a phthalic anhydride yield of 68.6% is obtained in a 3 metre reactor. This represents a high yield and (of course) the hot spot has been completely eliminated. In view of this, and also the fact that the temperature difference is only 16°C, one would guess that the reactor should be fairly unresponsive to small disturbances and also that the one dimensional approximation is not wholly inappropriate. The investigation of the two dimensional reactor model discussed in the next section throws light on both these points.

2.4 Dilution and the two dimensional reactor - theory

2.4.1 Choice of model

There are two basic reactor models which have been used to allow for radial variations of temperature and concentration in calculations on catalyst packed reactors. The first of these

treats the reactor as pseudo-homogeneous, i.e. as if the catalyst was finely dispersed throughout the reaction space, and involves the solution of the set of non-linear, second order partial differential equations for mass and energy conservation. A numerical solution is required and problems of stability of the solution can arise but the Crank Nicolson implicit difference procedure is normally found to be satisfactory. This was the approach used by Froment[10].

The second approach is that of the cell model, first introduced by Deans and Lapidus[63]. A wedge shaped section of the reactor, as indicated in Figure 6 is divided into a number of over-

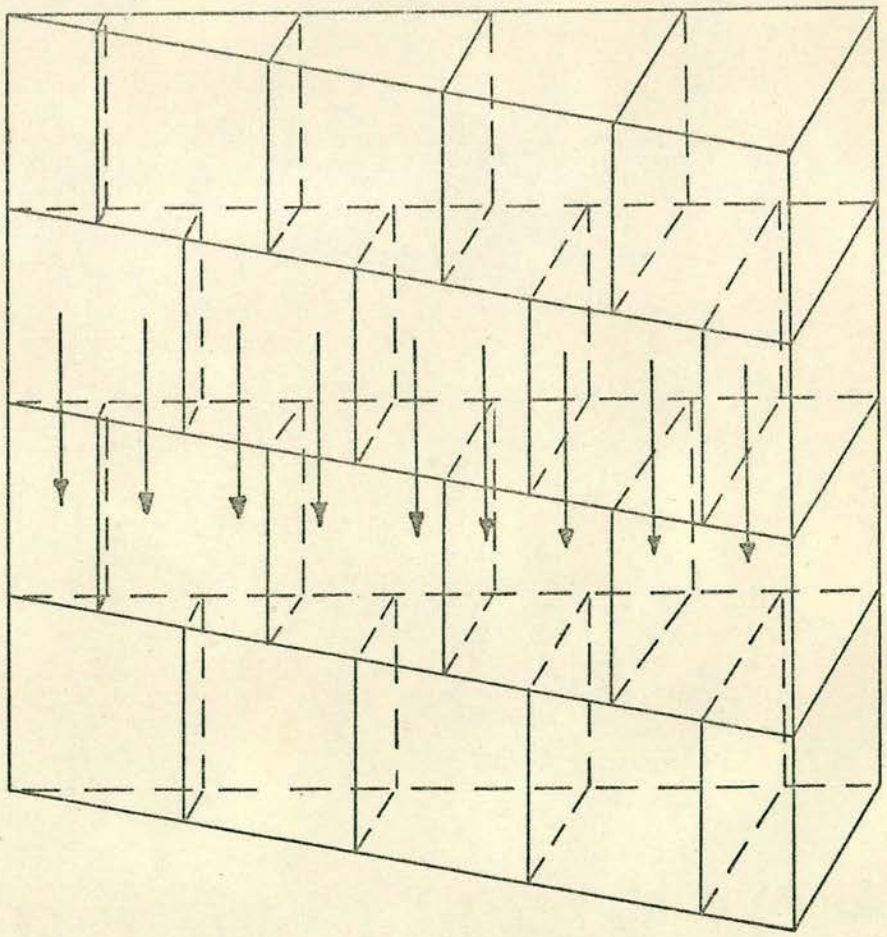

Figure 6

lapping cells, whose dimensions are related to the catalyst particle diameter. Each cell feeds the two adjacent cells in the next row and hence a degree of lateral mixing is introduced into the model: the cell size is so calculated that this lateral mixing matches experimental heat (or mass) transfer data. Within each cell the concentrations and temperature are supposed uniform.

Both of these approaches have something to recommend them: a detailed discussion has been given by Valstar[64]. In the case of a highly reactive system, however, where an appreciable degree of conversion may occur across a single particle, it becomes important that the quantity of catalyst contained in a cell (or what corresponds to a cell in the pseudo-homogeneous approach) should be exactly equal to the weight of a catalyst particle. This is certainly impossible to arrange with the Deans and Lapidus model, where the cell size is determined by mass/heat transfer requirements, and may not be possible with the pseudo-homogeneous model because the step length is limited by solution stability considerations. For this reason a cell model was adopted in which the cell constituted a single spherical catalyst particle. In addition to meeting the requirement mentioned above - which seemed likely to be important in the case of o-xylene - such a model could very rapidly be extended to take account of heat and mass transfer resistance inside and at the surface of the catalyst particle.

This model, hereinafter referred to as the matrix model, is described more fully in the following section.

2.4.2 The matrix model

It is supposed that the particles in the reactor (whether catalytic or inert) are of uniform size, spherical, and arranged in the hexagonal-closest-packed (hcp) form. Each particle

is assumed to behave as an ideal adiabatic stirred tank reactor. Mixing is accounted for by a three way flow of fluid as shown in Figure 7, so that each particle receives an equal stream of fluid

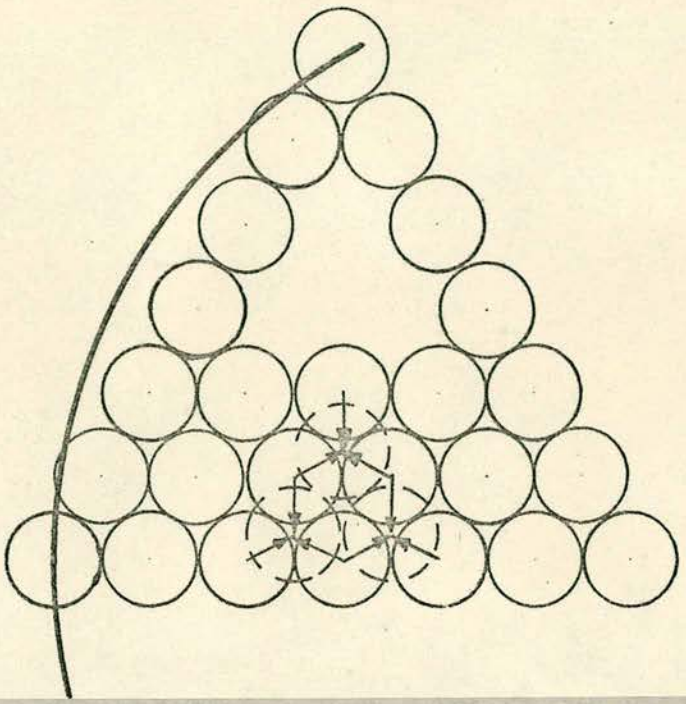

Figure 7

from the three particles in the previous row. Mixing is complete before the commencement of reaction at each stage. Appendix 3 demonstrates that this mixing pattern gives rise to a Peclet number value of 9.8 for both heat and mass transfer, in good agreement with experimental findings. This is the sole reason for employing the three way mixing pattern.

A major disadvantage of the model arises because the hcp arrangement cannot be fitted exactly into the circular cross-section of the tubular reactor. The best regular arrangement to approximate the circular form is a hexagonal matrix as illustrated in Figure 8. Adopting the nomenclature of this diagram the tube diameter may be approximated by

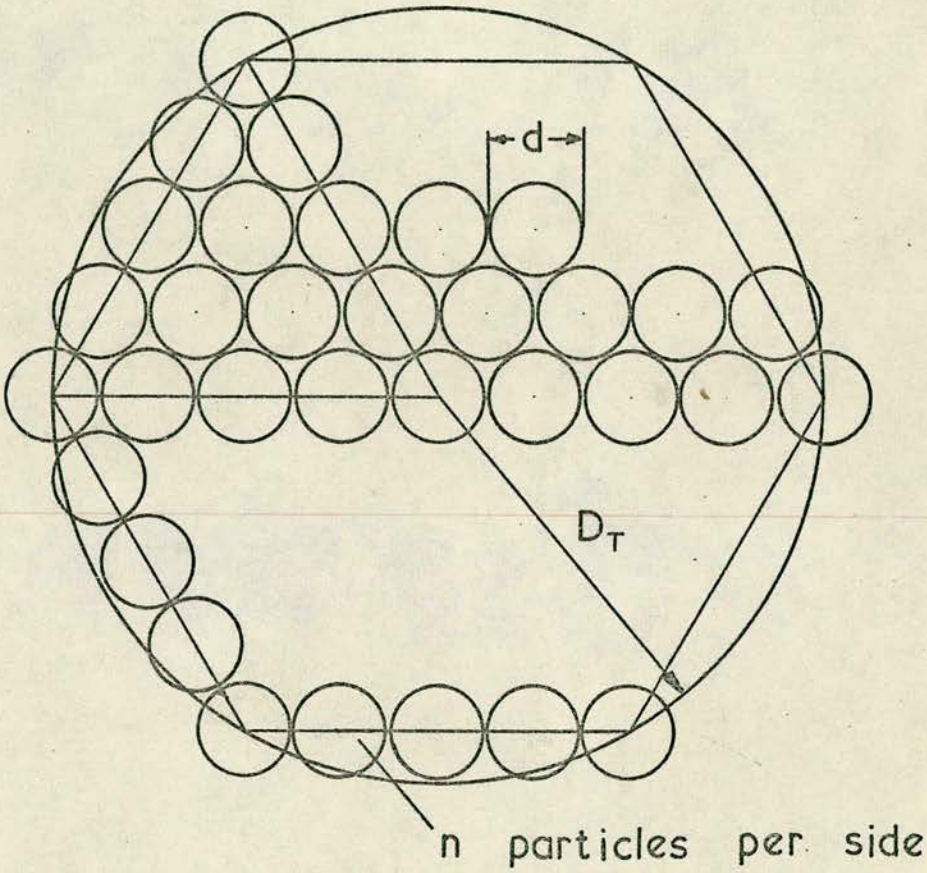

FIGURE 8 — THE MATRIX MODEL

$$D_t = 2(n - 1)d$$

Calculations on the matrix may be simplified by considerations of reactor symmetry. Since no net transfer of heat or mass takes place across a radial line in a reactor with axial symmetry only a triangular portion of the matrix (see Figure 7) need be considered. This simplification is not wholly justifiable: a discussion of the errors introduced is included in Appendix 4.

We have referred to the three way mixing pattern which accounts for both heat and mass transfer in the bulk of the bed. At the reactor wall mixing equations must be introduced which provide for the retention of matter within the reactor and the transfer of heat to the surroundings. In both cases this is effected by by-pass streams at the wall, so that where a stream would otherwise cross the boundary it is instead considered to pass along the tube wall and to arrive at a particle in the next row but one.

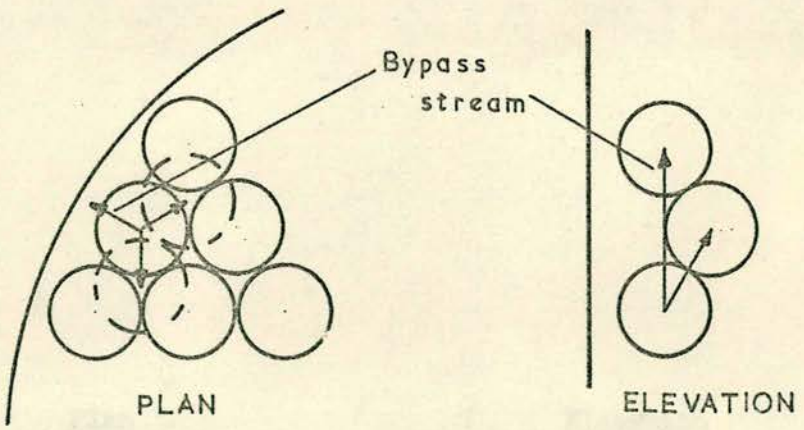

For heat transfer alone an allowance is made for exchange across the boundary wall: the calculations are identical to those applicable to a standard heat exchanger.

Let

T_j = jacket temperature

T_1, T_2 = initial and final temperatures of bypass stream

f = flow rate of bypass stream

A_s = area for heat exchange

h = an overall heat transfer coefficient

therefore

$$h.A_s . \frac{T_1 - T_2}{\log_e(\frac{T_1 - T_j}{T_2 - T_j})} = f.Cp.(T_1 - T_2)$$

$$T_2 = T_j + (T_1 - T_j).e^{-\frac{h.A_s}{f.Cp}} \qquad (19)$$

The parameter h cannot be identified with the wall heat transfer coefficient - although the two are obviously closely related - and due to the hexagonal matrix approximation to the circular tube there is some doubt about the correct value to assign to A_s. Hence a single unknown parameter K was introduced, defined by

$$K = h.A_s$$

and this was determined by a trial and error matching procedure. A subsidiary computer program was employed in which the matrix model simulated a packed tube heat exchanger having identical dimensions and characteristics to the reactor which it was desired to simulate. An arbitrary choice of inlet temperature and jacket temperature is made for this exchanger and the outlet (mixed mean) temperature is then determined for a particular choice of the parameter K. The program then calculates the overall heat transfer coefficient U from the standard equation

$$U = \frac{F.Cp}{\pi.D.Z.} \log_e(\frac{T_1 - T_j}{T_2 - T_j})$$

and compares it with the desired value of U obtained from some correlation. K is adjusted and the program repeats until a match is obtained. (The results are, of course, independent of the initial choice of inlet and jacket temperature.) Leva's correlation was normally employed to provide values of U_o[64*].

The matrix model, in common with all cell models, suffers from the disadvantage that the Peclet numbers for heat and mass transfer are fixed and unalterable without radical changes to the mixing equations. Experimental evidence does suggest that the Peclet numbers are constant and both approximately equal to 10 if $Re_p > 100$ (see, e.g. (65)). This condition was satisfied in the work reported here: nevertheless it must be admitted that pseudo-homogeneous models are superior by virtue of greater flexibility in this respect.

In retrospect it appears that the disadvantages of the matrix model discussed here and in Appendix 4 more than outweigh the single advantage of giving stepwise changes over a reactor space of the dimensions of a catalyst particle. Despite this conclusion there is no reason to suppose that the model fails to represent qualitatively the behaviour of a packed catalytic reactor, and the results quoted later show that under "mild" reaction conditions the results from it agree reasonably with those from a pseudo-homogeneous model.

2.4.3 Computer programs based on the matrix model

A number of computer programs based on the matrix model were written to simulate reactor behaviour. Most of the routines employed were common to all programs: these are listed in Table 7, together with a brief account of the purpose of each routine. The programs themselves appear as Appendix 5.

Table 7 List of Routines Employed in the Computer Programs Based on the Matrix Model

Name of Routine	Description
CATALYST SELECTION	Selects a specified number of particles as active within a triangular matrix. The selection process is pseudo-random but a bias is introduced so that the particle at the tube axis is chosen one sixth as often and particles on the radial boundaries one half as often as the rest. (See Appendix 4)
CONVERSION	An iterative procedure is used to calculate the conversions and temperature of a gas stream leaving a single pellet, given the input values of these variables. The pellet is assumed to behave as an adiabatic ideal stirred tank reactor. (In some early work the assumption of adiabatic plug flow behaviour was made. A comparison showed very minor differences under the conditions employed.)
AVERAGE	The mixed mean temperature (or conversion) is calculated by averaging the values over the whole matrix. As with CATALYST SELECTION a bias is introduced.
ENCOUNTER 1 ENCOUNTER 2 ENCOUNTER 3	These routines calculate the inputs to a row of particles in the matrix from the outputs of the last (or last two) rows. ENCOUNTER 1 gives both temperature and conversion inputs to an even numbered row. ENCOUNTER 2 gives the temperature input to an odd numbered row (allowing for heat transfer at the wall). ENCOUNTER 3 gives conversion inputs to an odd numbered row with bypassing at the wall.

The first program entitled 'Xylox' was written to develop the routines of Table 7 and to simulate the xylene oxidation reaction in a reactor packed with pure catalyst. Results from this were compared (a) with those obtained by Froment[10] and, (b) with those given by a program based on a pseudo-homogeneous model.

The second program under the title 'Xylox 2' was an extension of this which allowed for the introduction and optimization of catalyst dilution. In theory one might wish to vary the dilution in a continuous fashion along the reactor. This would not be practicable, however, and so the compromise was adopted of dividing the reactor into ten sections of equal length: within each section the dilution was uniform but variation between sections was permitted. It was recognised that chance groupings of active or inactive particles might exert an appreciable influence on the reactor behaviour and so (although the dilution within a section remained the same from layer to layer) within each layer the active particles were selected by a random process. Similar random fluctuations in catalyst density could also occur in practice in the axial direction: to allow for this in the program would have increased storage requirements and computation time.

The 'optimization' of the catalyst dilution profile consisted in maximising the yield of phthalic anhydride from each section of the reactor without exceeding an (arbitrary) upper temperature limit at any point. There is no guarantee that this procedure will discover the true optimum but even this simple method required up to 25 minutes CPU time on a KDF 9. Moreover an inspection of the results given in Table 4 for the yield under isothermal conditions over a range of temperatures indicates that the optimum is likely to be rather flat.

The last program (entitled 'Xylox 3') was used to

examine the stability of the diluted reactor when subjected to jacket temperature fluctuations. The data for this program consisted of the optimum dilution profile discovered by the previous program for a particular set of conditions. Identical conditions were employed, except for a variation in the jacket temperature, and the program determined the resultant temperature profile.

2.4.4 Results

Temperature profiles obtained from the matrix model simulating the pure catalyst reactor are shown in Figure 9 and Froment's results are shown for comparison. (These were obtained from a small scale graph in Ref. 10 and hence may be displaced slightly.) The matrix model results show temperature runaway at 353°C compared with 360°C from Froment. This discrepancy is not surprising because (apart from other differences between the models) Froment used a Peclet number of 5.25 compared with 9.8 in the matrix model: thus the effective thermal conductivity of the bed is nearly twice as large in Froment's calculations. By way of compensation a very high wall heat transfer coefficient was used in the matrix model so that the overall heat transfer coefficients matched. (The relation between the overall coefficient, the wall coefficient and the bed effective thermal conductivity is

$$U = \frac{\beta_1^2 . Ke}{D_T} + \frac{F.Cp.D_T}{4Z} \log_e \left[\frac{\beta_1^2(\beta_1^2 + A^2)}{4A^2} \right]$$

where β_1 is the first root of

$$xJ_1(x) = AJ_o(x)$$

and

$$A = R.h_w/Ke$$

See, for example, Ref. 66). Despite this matching of the overall

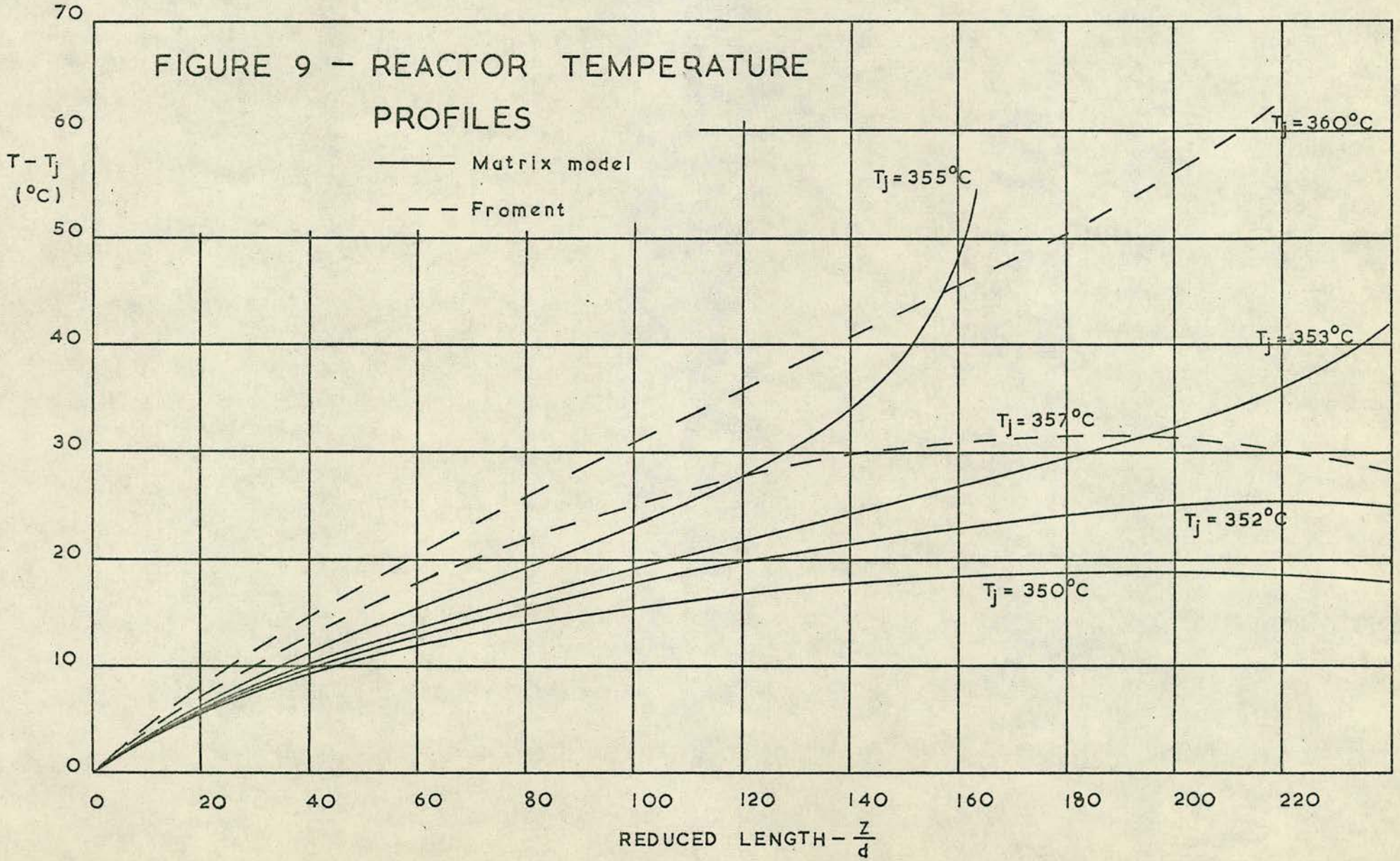
FIGURE 9 – REACTOR TEMPERATURE PROFILES
Matrix model
Froment
T – Tj (°C)
Tj = 360°C
Tj = 355°C
Tj = 353°C
Tj = 357°C
Tj = 352°C
Tj = 350°C
0
10
20
30
40
50
60
70
0
20
40
60
80
100
120
140
160
180
200
220
REDUCED LENGTH – Z/d

coefficient under pure heat transfer conditions the fact remains that in the matrix model a hot spot will be dispersed less readily, and so we should expect that it will predict a lower runaway temperature as indeed it does.

The data on which the graphs of Figure 9 are based are shown in Table 3a. (Parameters not given here may be assumed to have the same value as taken by Froment, Table 3).

Figure 10 shows a further comparison between the results from the matrix model program and a program based on a pseudo-homogeneous model. (The computational procedure used was that described by Petersen[67]). These two programs had been checked against each other and found to agree exactly as regards

(a) The conversions achieved in a given length under isothermal conditions

(b) The mixed mean temperature profiles in the absence of chemical reaction when gas entering at 400°C was cooled by contact with the jacket at 0°C.

Despite this close agreement on both counts Figure 10 shows quite an appreciable divergence of temperature profiles between the two programs for non-isothermal operation. This divergence emphasizes the phenomenon of parametric sensitivity and the qualitative nature of the results in general.

The effect of catalyst dilution may be seen by comparison of the temperature profiles of Figure 9 with those of Figure 11: the corresponding conversion profiles are shown in Figure 12. Reaction parameters are identical in all cases apart from the presence or absence of diluting material among the catalyst particles. In particular the reactor length is identical. Figure 9 shows that the maximum operating temperature for an undiluted reactor is 352°C and the corresponding yield (in 3 metres) is about 60% (Figure 12). On the other hand Figure 11 shows that operation with a

FIGURE 10 — REACTOR TEMPERATURE PROFILES

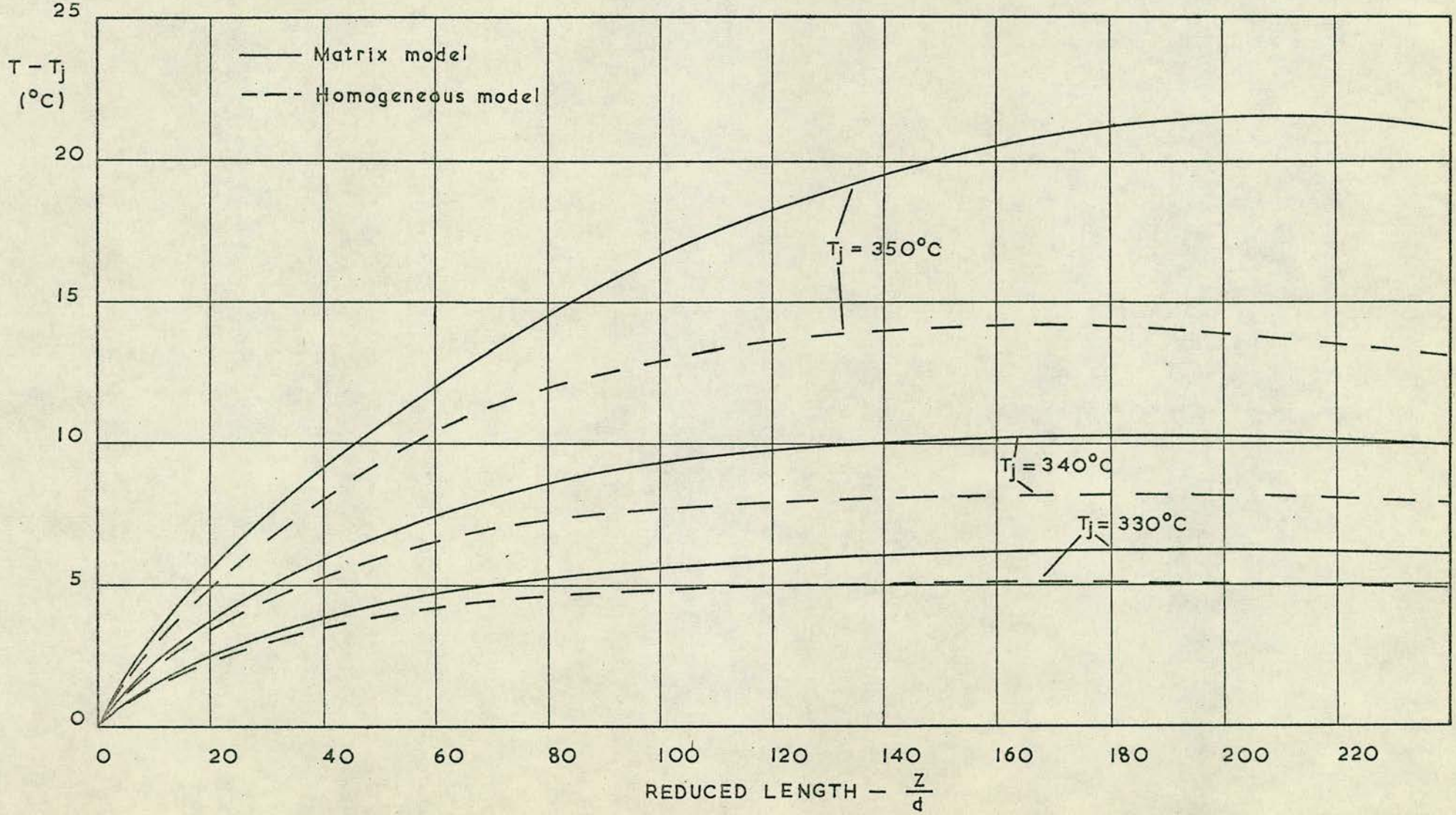

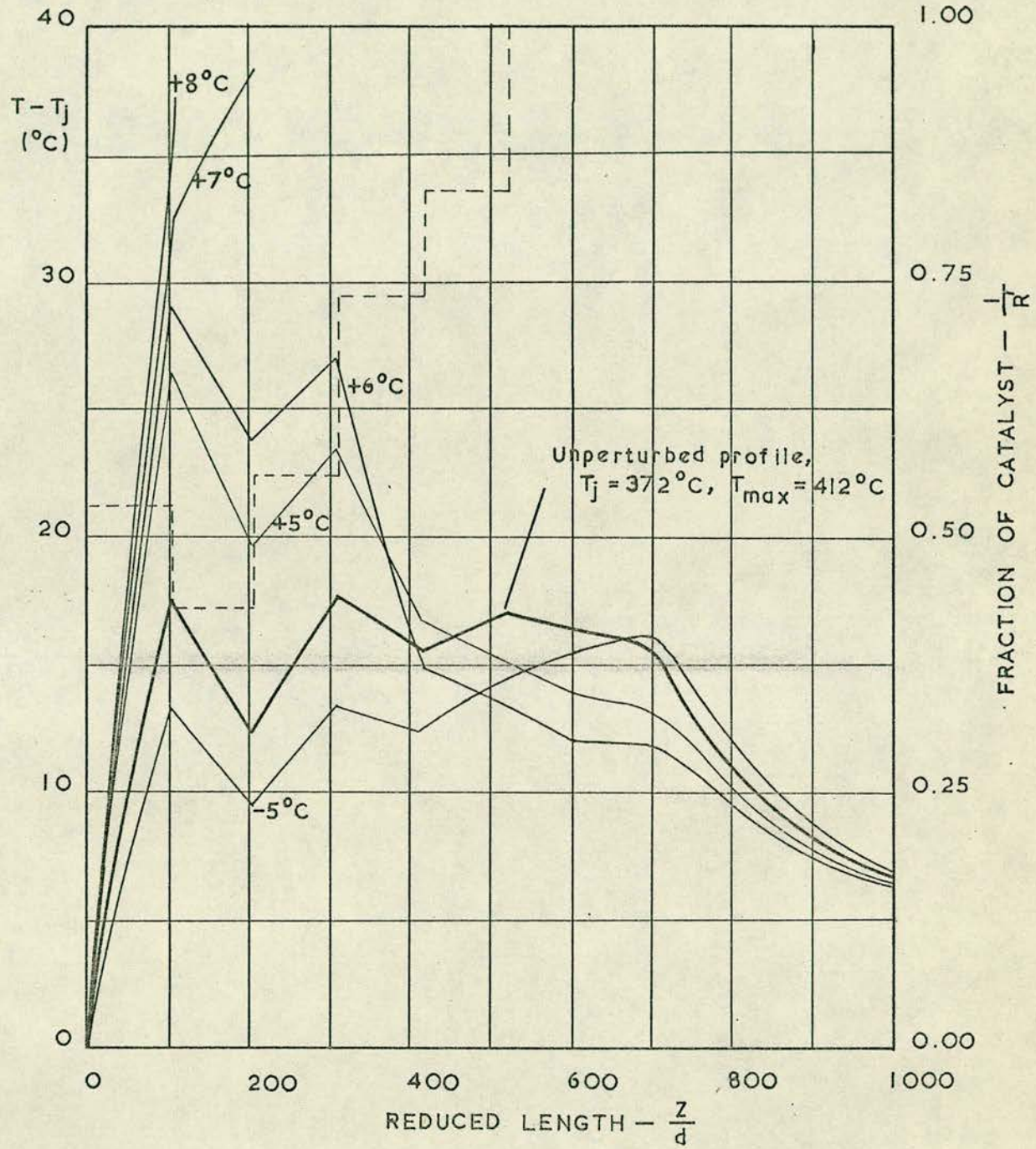

FIGURE II — TEMPERATURE PROFILES FOR A DILUTED CATALYST REACTOR

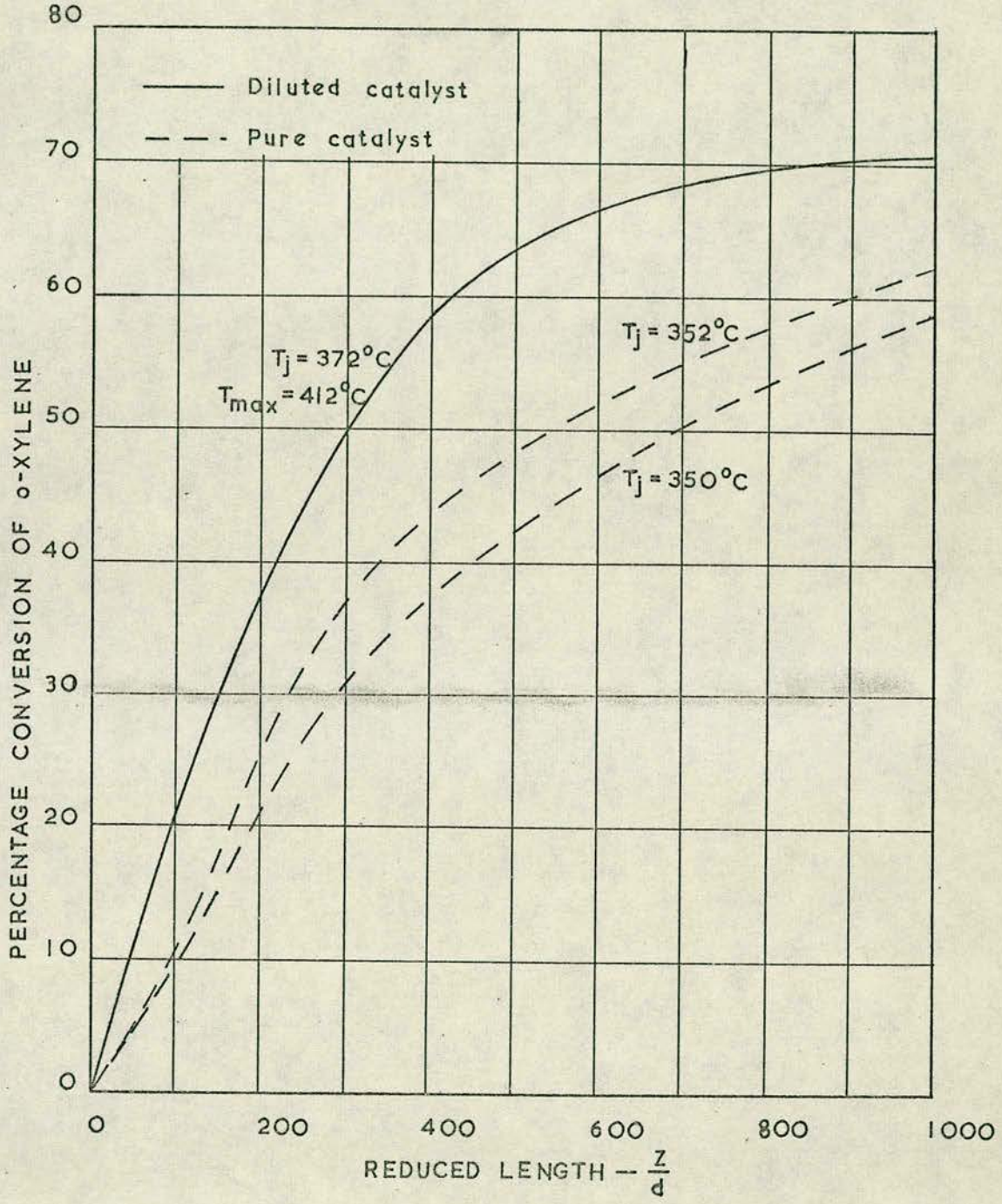

FIGURE 12 — CONVERSION PROFILES FOR PURE AND DILUTED CATALYST REACTORS

jacket temperature of 372°C is perfectly feasible with a diluted reactor and the yield (Figure 12) is increased to about 70%. The optimal catalyst dilution profile for the jacket temperature of 372°C is also shown in Figure 11.

It is seen therefore that the two dimensional model broadly confirms the predictions of the one dimensional model. An exact comparison is not possible since the two dimensional model does not show isothermal behaviour and moreover the feed enters at the jacket temperature: the table below gives a rough idea.

	Jacket temperature (°C)	Reactor temperature (mean) (°C)	Reactor temperature (max.) (°C)	Yield %
One dimensional model	386	402	402	68.6
Two dimensional model	372	390 (approx)	412	69.4

The effect of perturbations of jacket temperature on the temperature profile are also seen in Figure 11. A 7°C increase in jacket temperature is necessary to cause temperature runaway (whereas, of course, the undiluted reactor at 352°C is unstable to a 1°C increase in jacket temperature).

The results reported here for the diluted reactor were obtained by imposing the constraint

$$T_{max} < 412^{\circ}C$$

on the temperature at all points in the reactor. This constraint is arbitrary and so is the choice of jacket temperature. The effect of varying these parameters was examined and can be stated as follows. A considerable range of values may be employed for both parameters without significantly affecting the yield obtainable from a given length of reactor - the dilution profile varies in a compensatory manner. However, if these parameters are chosen with values close

together (within about 20°C) the yield declines. If the maximum permitted temperature is increased the stability to jacket temperature perturbations decreases.

2.5 Conclusion

It has been demonstrated that the use of dilution enables the average temperature level in a tubular catalyst packed reactor to be raised, and hence the yield from a given reactor length may be increased. The technique should be applicable to all exothermic reactions where there is some constraint on the upper temperature but where a high yield is required from a single pass. In particular the yield of phthalic anhydride from o-xylene may be markedly improved by dilution if the reaction model employed is adequate.

The experimental work reported in the next chapter was undertaken to determine the truth of this conclusion.

CHAPTER 3 EXPERIMENTAL WORK:

An account of the equipment and experimental techniques

3.1 Scale of the experimental work

As stated at the end of the last chapter it was decided to initiate an experimental program to verify (or otherwise) the theoretical findings on catalyst dilution with o-xylene oxidation. These findings were of great potential interest to the manufacturer of phthalic anhydride and hence it was important that the experimental work should be convincing. Obviously a bench scale reactor is so far removed from an industrial plant that results from it would be open to question. It was decided to conduct a large scale experiment on a single tube reactor of dimensions comparable with those of a tube from an industrial multi-tube reactor, employing (if possible) an industrial catalyst, and using gas flows and reactant concentrations of the range employed in practice.

3.2 The catalyst and the diluent

The existence of the two basic types of catalyst was known and clearly (since Froment's data and the calculations reported in Chapter 2 were based on the 'German' type of catalyst) the German catalyst was a more appropriate choice. However, no very definite distinction could be made between the two types (see Chapter 1) apart from the increased activity associated with the American type of catalyst. By virtue of this increased activity the American catalyst might indeed be considered a suitable case for treatment ... Preference aside it was not easy to find a manufacturer able and willing to supply a sample of catalyst. Ultimately a one litre sample was obtained. This was a surface coated promoted V_2O_5 on silicon carbide catalyst in the form of irregular granules roughly in the size range 0.3 - 0.8 cms. The mean particle diameter was 0.63 cms.

FIGURE 13

THE REACTOR

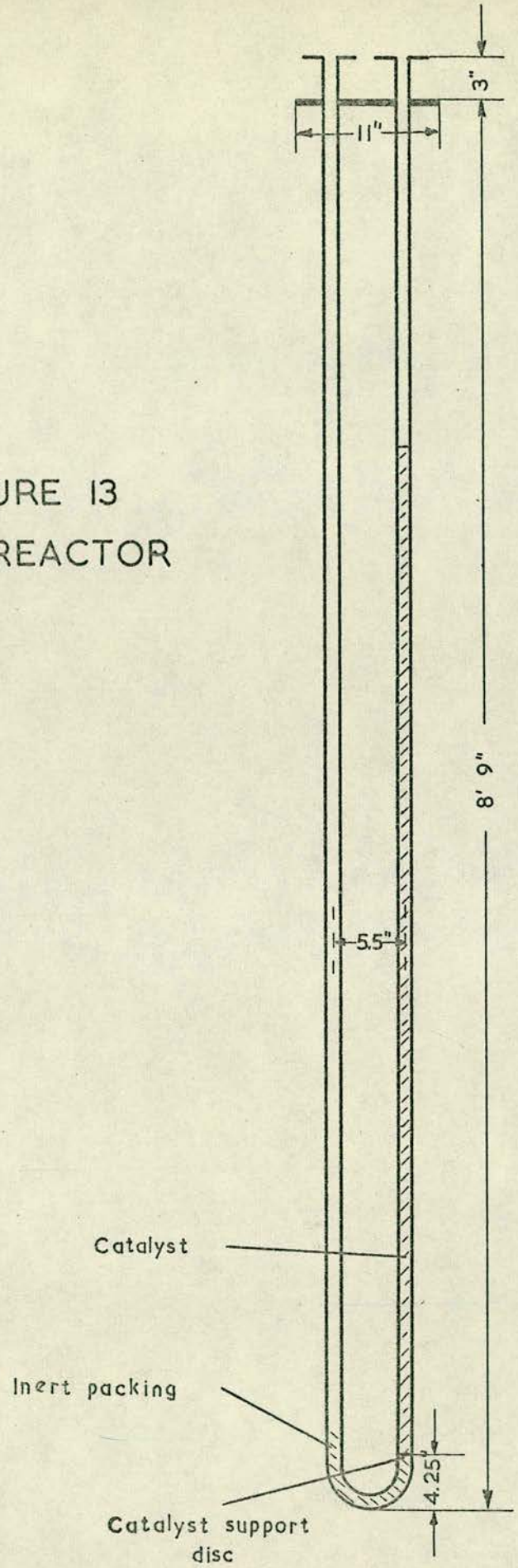

FIGURE 14
THERMOCOUPLE
LOCATIONS

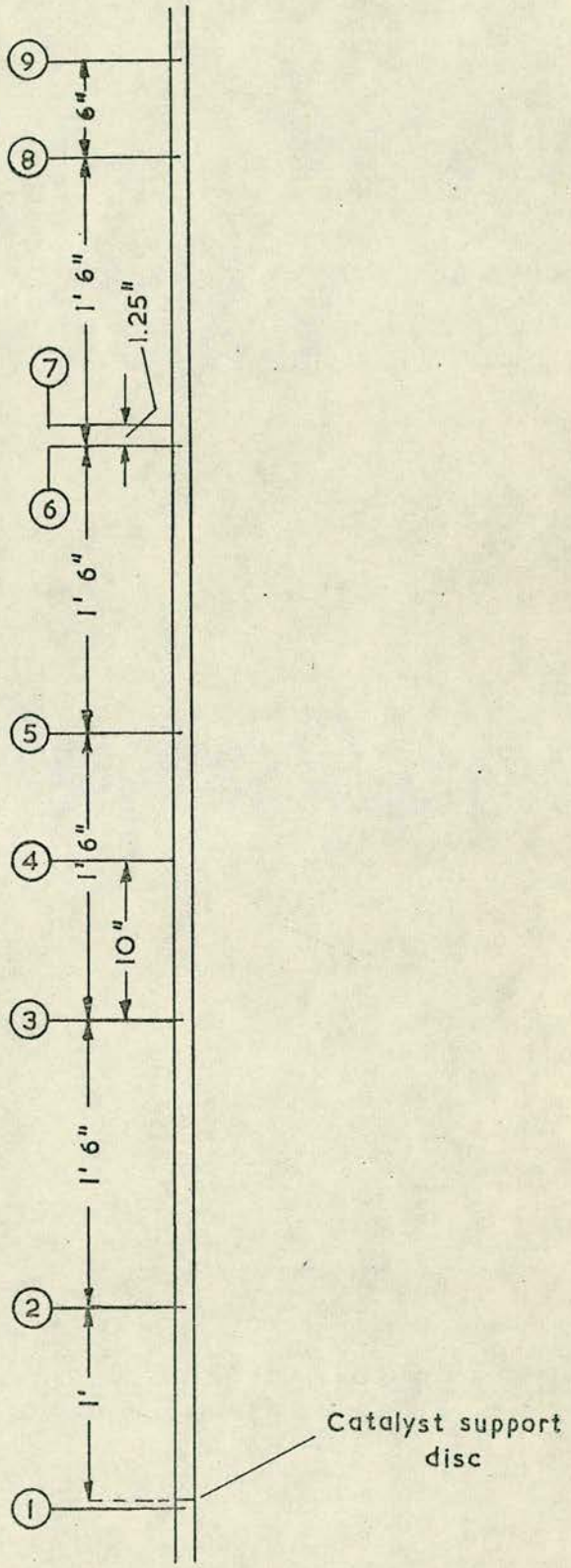

and other characteristics are listed below

Surface area	0.2 m^2/gm (approx.)
True density (He)	2.84 gm/cm^3
Particle density (Hg)	2.55 gm/cm^3
Pore volume	0.04 cm^3/gm
Pore radius	4444 $\mathring{A}$

The description indicates that the catalyst may be classified as of American type, apart from the use of a promoter. It is not known whether this catalyst is, has been, or will be employed industrially but it was supplied by a firm making industrial catalysts.

The catalyst suppliers were not able to provide inert material for use as a diluent of the same size and shape as the catalyst itself. The diluent actually employed was 3/16 inch alundum spheres supplied by Norton Abrasives Ltd. The characteristics are shown in the accompanying table.

Supplier	:	Norton Abrasives Ltd.					
Catalogue No.	:	S.A.201					
Size	:	3/16" dia. spheres					
Composition	:	Al_2O_3	SiO_2	Fe_2O_3	TiO_2	CaO	Na_2O	K_2O
		90.4	8.46	0.26	0.28	0.04	0.33	0.09
Apparent porosity:		39 - 45%						
Surface area	:	$< 1\ m^2/gm$						
Apparent S.G.	:	3.5 - 3.7						

This material was not entirely satisfactory in that some segregation tended to occur on mixing with the catalyst, but this was not considered to be a serious disadvantage.

3.3 Equipment

3.3.1 Reactor and reactor shell

The reactor is illustrated in Figure 13 and consisted of a Type 321 seamless stainless steel tube having the dimensions

Internal diameter	1.000"
External diameter	1.125"
Wall thickness	1/16"

This tube was bent into the form of a U with the axes of the two legs five inches apart. Catalyst was contained in one leg only, being supported on a stainless steel disc drilled with many 1/32" dia. holes on a 1/16" square pitch: this disc was located close to the U bend and was inserted by cutting the tube and welding it into place.

At intervals along the reactor a number of 5/64" dia. holes were drilled for the purpose of inserting thermocouples. These were located in the plane of the tube leg axes and on the inside of the leg - the exact positions are indicated in Figure 14. Both legs of the reactor terminated in 3/8" thick, 4½" dia. flanges for connection to the feed and product collection systems. 'Metaflex' gaskets were used on these joints because of the high temperatures involved. Three inches below these flanges the two legs passed through and were welded to a circular mild steel plate of diameter 11" and thickness ½". This was drilled with 8 5/8" holes on a P.C.D. 8½" and served to bolt the reactor into position in its shell.

The reactor shell itself is illustrated in Figure 15. It was a cylindrical M.S. vessel, thickness 1/8", of internal diameter 18", 9 feet long, and flanged at both ends. This shell contained the reactor and a heated fluidized bed of sand to provide a constant temperature jacket. The sand was supported on a stainless steel sintered plate of diameter 2.0' bolted between the lower flange of the reactor shell and the upper flange of the shell support drum.

FIGURE 15.
REACTOR SHELL

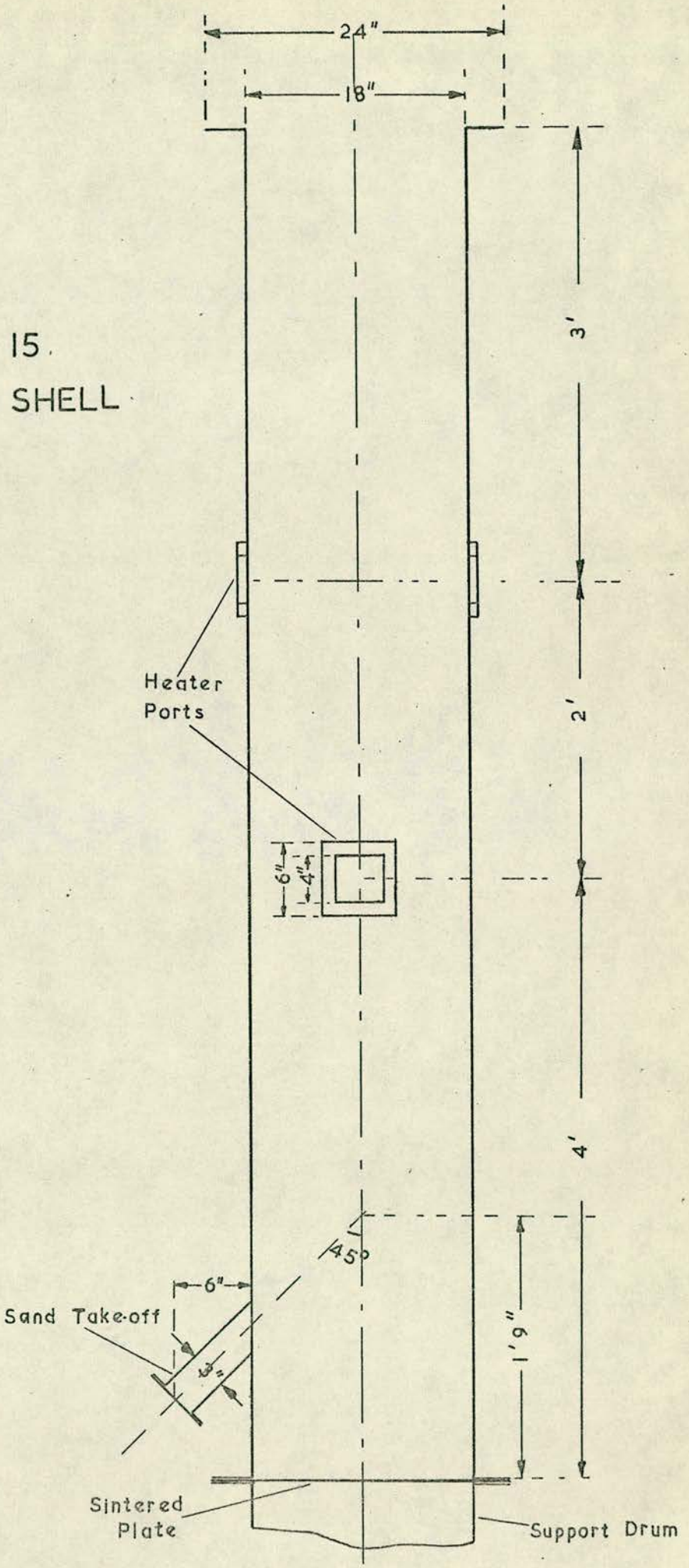

This plate was supplied by Sintered Products Ltd. and had the characteristics

Diameter	24"
Thickness	0.1"
Micron rating	40
Ultimate tensile strength	12 tons/ins^2

The sand was heated by four 'Pyrobar' heating elements of approximately 2½ kw. rating. These elements were each 8 feet long and were bent into a U form with tails of approximately 6" length at right angles to each leg (see Figure 16). The tails passed through and were fixed by mechanical fixing nipples to a 6" square plate which could be bolted over a corresponding entry port in the reactor shell. Thus the heaters were vertically aligned within the shell and about 2-3 inches from the shell wall.

The upper end of the reactor shell was closed by a plate bolted to the shell flange. This was of 1/4" M.S. and is shown in Figure 17. A central hole of diameter 7 inches was cut in this plate and through this the reactor could be inserted into the shell. Eight ½" studs on a P.C.D. 8½" were let into this plate around the central hole and these clamped the reactor into position. The shell cover plate was also provided with a branched exit port which had the dual purpose of taking off the fluidizing air and admitting sand to replenish the bed.

Near the bottom of the reactor shell a side take off point was provided through which the sand could be discharged when necessary.

The reactor shell support drum was three feet long and eighteen inches in diameter. It was attached by steel studs to a three quarter inch M.S. base plate twenty six inches square which rested on the concrete floor. A side entry was provided for the

UNIV. EDINBURGH EX BIBL

FIGURE 16

ARRANGEMENT OF HEATING ELEMENTS

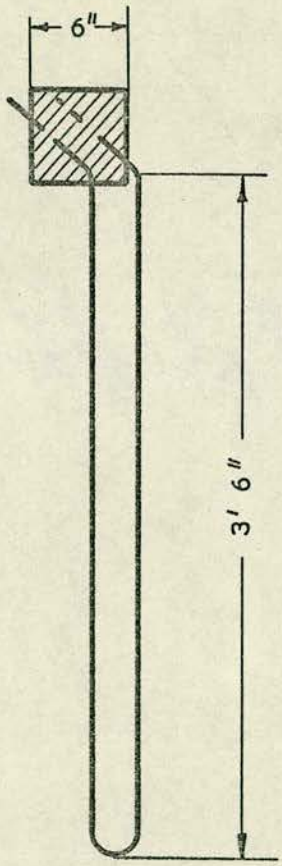

FIGURE 17
REACTOR SHELL COVER PLATE

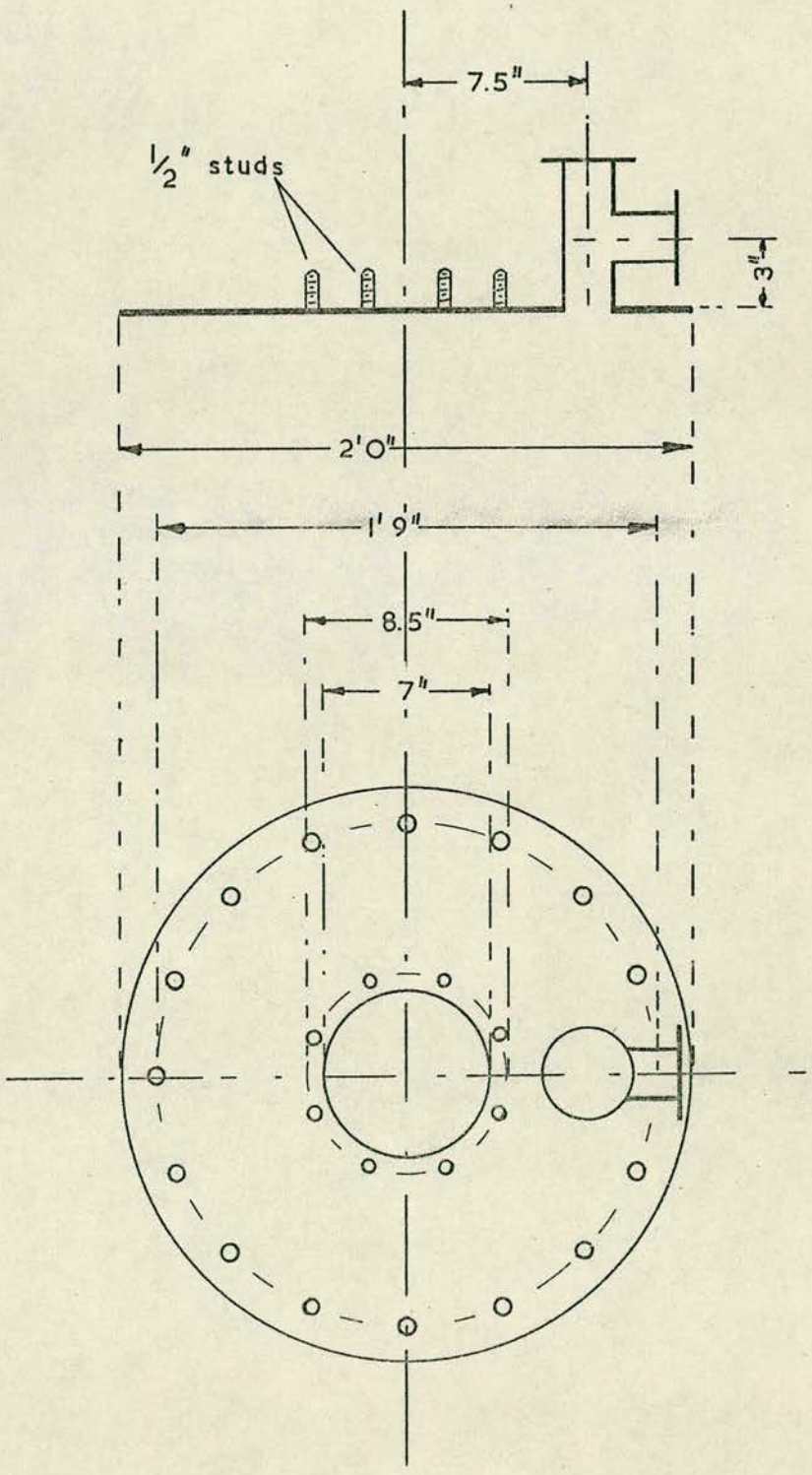

fluidizing air.

All permanent joints were rendered air tight with high temperature jointing compounds. Asbestos string and 'Suprete' paste were used in some cases: 'Lion' Universal Jointing Paste No. 434 in others. Less permanent joints - e.g. between the reactor plate and reactor shell cover plate - were sealed with gaskets cut from 'Twillsteel' material.

The whole assembly was insulated with approximately three inches of Superlight Plastic Insulation applied in layers over a wire mesh former. The heater ports were left clear of insulation. The cover plate had no permanent insulation but a woven asbestos jacket was provided to fit over it.

There were two platforms beside the rig approximately seven and nine feet respectively off the ground. These provided access to the top of the rig and also supported it by means of stays.

The sand in the reactor shell was "-120" sand supplied by A.L. Curtis (ONX) Ltd. of Cambridgeshire. A sieve test on a single sample, not necessarily representative of the reactor shell contents, gave the following analysis

B.S. Sieve Mesh Numbers	+100	-100+120	-120+150	-150+170	-170
Weight %	6.8	32.2	25.4	29.6	6.1

Making the assumptions that the two end fractions were -85 mesh and +200 mesh respectively, the weighted mean particle diameter of the sand was calculated to be 0.118 mms.

3.3.2 Fluidizing Air system

The air feed to the fluidized bed was supplied by a Holmes TG 336 blower rated 75 c.f.m. at a discharge pressure of 7 p.s.i.g., driven by a 5.5 H.P., three phase motor. A pressure

switch was set to trip the motor at a delivery pressure of 8 p.s.i.g. A tee junction downstream of the blower had one arm discharging to atmosphere via a 3 inch steam valve which could thus be used to regulate the air supply to the sand bath. (Figure 18 gives a flow diagram for the fluidizing air). The air flow rate could be measured with a 65X Metric Series Rotameter, rated at 53 c.f.m. maximum throughput.

A heat exchanger was installed to preheat the fresh air to the fluidized bed with the air leaving the system. This was a vertically mounted shell and tube exchanger with the cold gas on the shell side. The rated duty and description are given below

Duty	50 c.f.m. of air (on both sides) to be heated/cooled through 280°C with a constant temperature difference of 100°C.
Shell diameter	6 inches
Tube length	7 feet
Tubes	121 tubes, 3/8" O.D. x 16 S.W.G.
Pressure drops	negligible ($<$ 0.2" W.G.)
Material	tubes and end shells in stainless steel, shell in mild steel

The exchanger was over-designed for the actual duty. The reason for this (and also for the part stainless steel construction) was that experiments with a much larger diameter reactor were contemplated and it was planned to discharge the bulk of the reactor gas through the heat exchanger.

Air leaving the fluidized bed passed downwards through the tubes of the exchanger (to avoid accumulation of entrained sand) and thence to a cyclone separator. The cyclone discharged into a polythene vessel of capacity 20 inches by 10 inches diameter: the dimensions of the cyclone are given in Figure 19. Finally, the air was scrubbed by countercurrent passage to a trickle of water in a

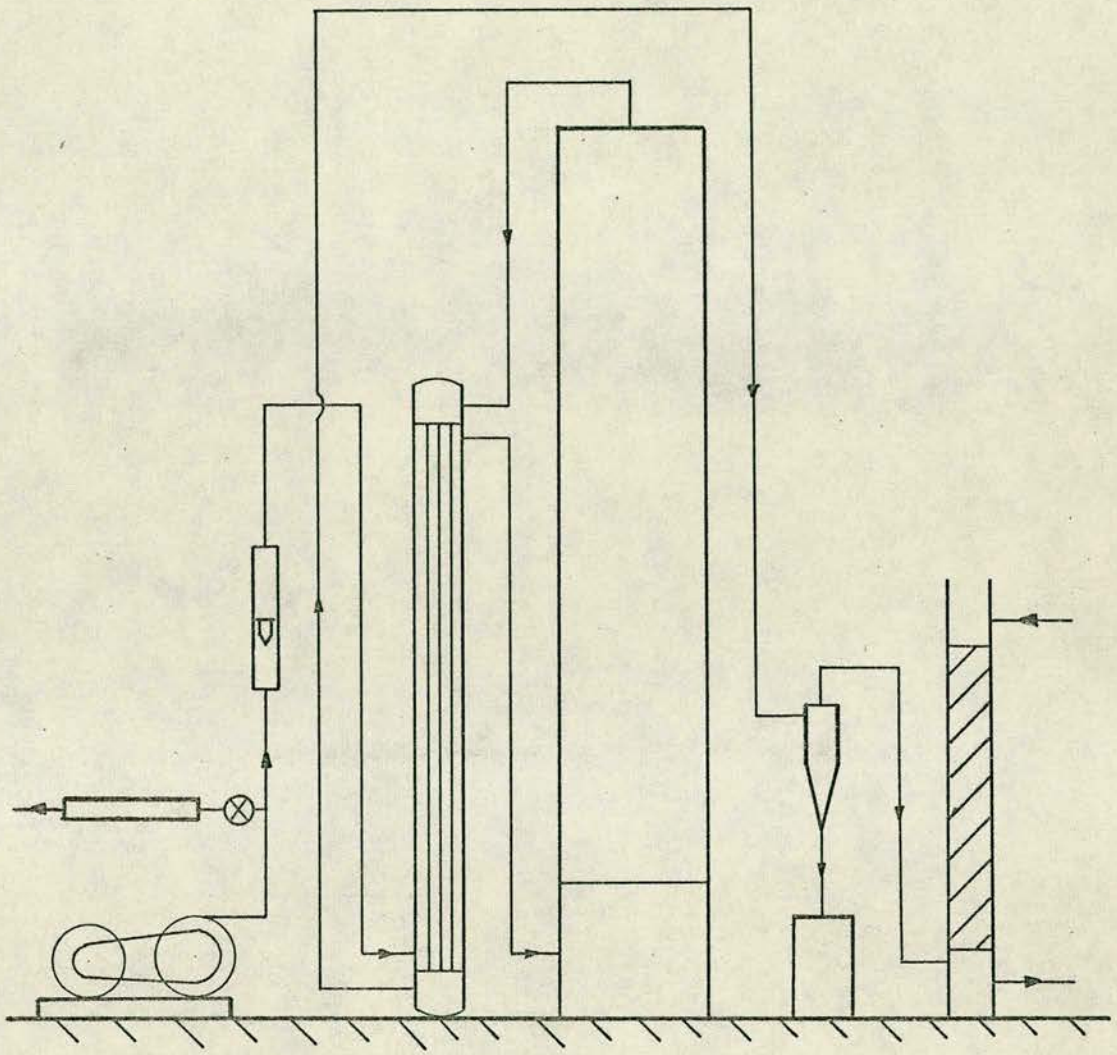

FIGURE 18

FLOW DIAGRAM FOR FLUIDISING AIR

FIGURE 19 - CYCLONE DIMENSIONS

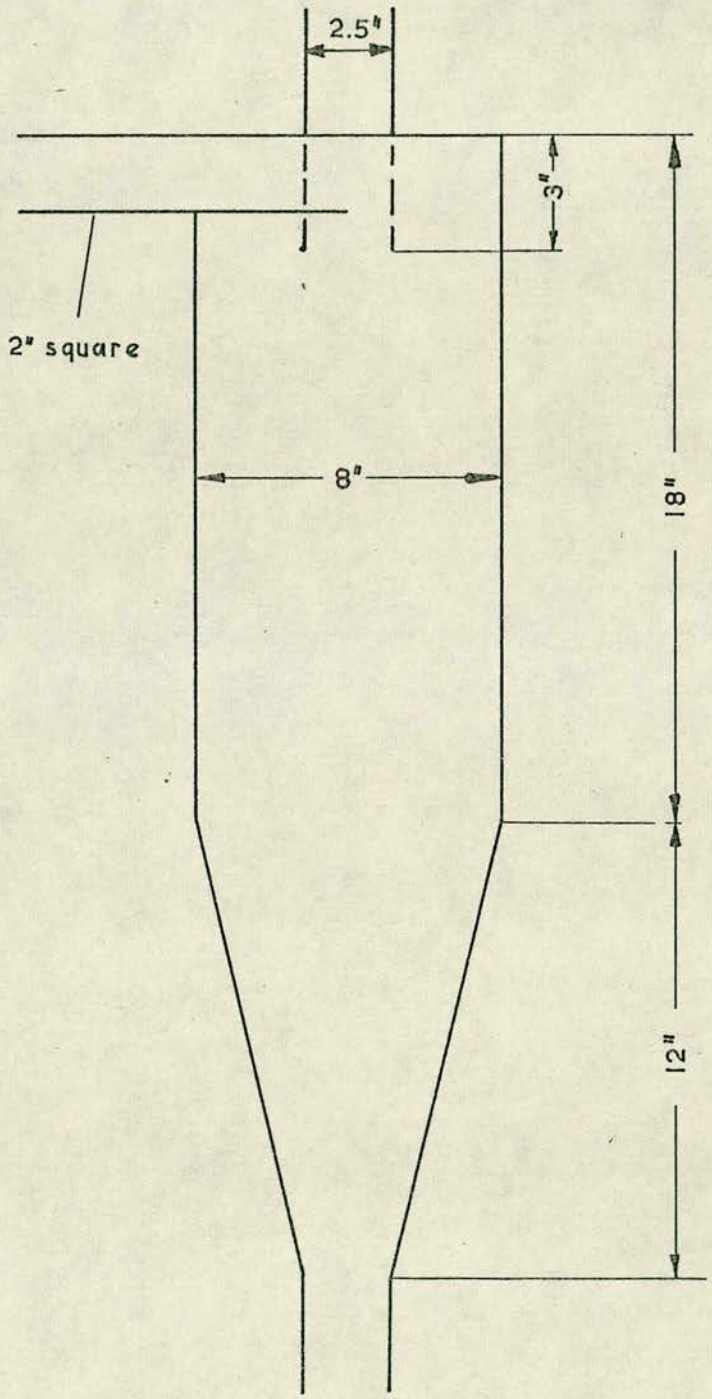

Q.V.F. glass column. The column contained approximately 3 feet of packing (multi-turn glass helices) supported on a perforated plate, and was 9 inches in diameter.

The connecting pipework was mostly of approximately 3 inch bore and the hot sections were lagged.

3.3.3 Reactor air system

A flow diagram is provided as Figure 20.

Air from an Edwards RB5 vane type blower was filtered over glass wool to remove entrained oil and passed via a tee junction with control valve to a 14X Metric Series Rotameter. Both valve and Rotameter were mounted on the control panel.

After the Rotameter the air entered a preheater, consisting of a rectangular mild steel box of internal dimensions 14 inches by 6 inches by 6 inches. The preheater box was flanged and a cover plate was bolted to this flange. Formed 'Pyrobar' heating elements were fixed to this plate by the same technique used for the fluidized bed heater. There were four of these elements each rated at 0.75 kw. For the purpose of insulation the preheater was enclosed within an outer box constructed of 'Sindanyo' and packed with glass wool.

From the preheater a short well-lagged pipe conducted the air directly to the reactor. The connections were such that the air passed down the empty leg of the reactor U tube and then up through the catalyst bed in the other leg. Between the preheater and the reactor was an injection point for the o-xylene feed (see later).

Air leaving the reactor passed through a short pipe to a three way cock. The flow could be directed either to a collection system (see later) or to waste. In the latter event

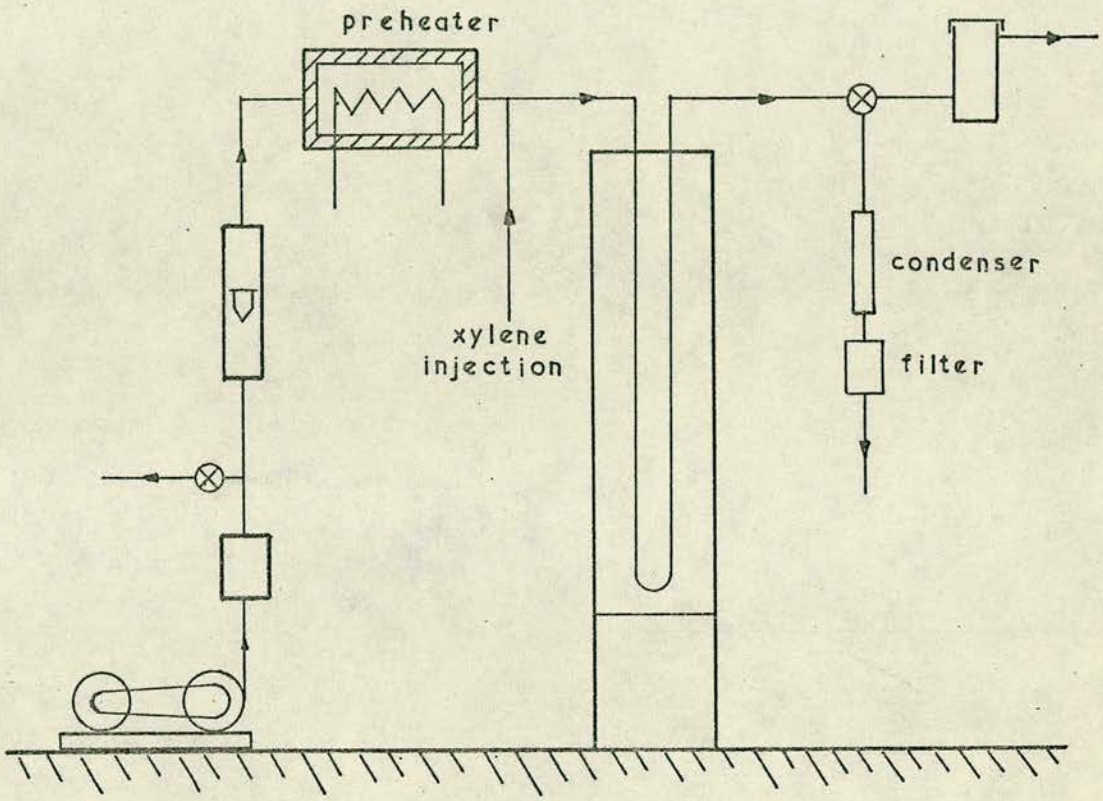

FIGURE 20

FLOW DIAGRAM FOR REACTOR AIR

it entered at the base of a metal drum 17 inches high by 10½ inches diameter in which the bulk of the phthalic anhydride deposited as long needle crystals. A PVC hose from the top of this drum vented to the outside of the building, and the drum had a loose fitting lid which was readily removed in order to clean out the contents. The pipework between the reactor and the waste drum/collection system was lagged near the reactor and heated with 'Thermocord' around the three way cock and points downstream. The temperature was maintained above 130°C at the exit to the collection system.

The pipework was half inch B.S.P. up to the preheater and one inch B.S.P. thereafter.

3.3.4 O-xylene injection system

The o-xylene employed in all experiments was supplied by the Aldrich Chemical Co. ~~and~~ was 99%+ grade. Impurities were presumably mostly other xylene isomers.

A 100 ml. burette broken off just above the top was mounted on the control panel and o-xylene was filled into this as required. Quarter inch copper tubing led the xylene via a 1/4" 'Straitflow Strainer' (containing a 40 mesh filter) to the suction side of a Hughes type 'M' metering pump located behind the control panel and about 18 inches lower than the bottom of the burette. A drain cock was fitted just before the pump entry point.

The pump was rated at 750 mls/hour (maximum delivery) with a continuous adjustment possible by varying the stroke length. This adjustment could be made with the pump operating and was effected by rotating a micrometer thimble. For the most part the pump was run at or about 90 mls/hour.

From the pump the o-xylene passed directly to the injection point in the air line. Initially a fine needle was

fitted at the injection point to try and smooth the flow, but it was found that this became choked over a period of time (causing the pump output to fall steadily at a given setting) and consequently the needle was discarded. No trace of the pulsed input could be observed in the reactor behaviour.

3.3.5 Product collection system

Whereas a complete analysis of the entire range of reaction products is always of interest the principal purpose of the experiments was to determine the influence of catalyst dilution on the yield and temperature profile of the reactor. Accordingly attention was focused on the principal product of the reaction, phthalic anhydride, though some attempts were also made to obtain information about the extent of o-xylene reaction and the importance of the complete combustion reactions.

The maximum anticipated phthalic anhydride content in the reactor exit gas was about 1% by volume. At this level (and a total pressure of 760 mm.Hg.) condensation would commence at about 130°C. For this reason the pipework before the collection system was maintained above 130°C. Similar calculations showed that to make a better than 99% recovery of phthalic anhydride (with the same inlet concentration) the temperature would have to be dropped below 60°C in the collection system.

A number of ideas were tried and the most satisfactory system (used in almost all the experiments reported here) was as follows. The heated pipework from the reactor terminated in a machined stainless steel cone. A simple jacketed tube condenser was constructed in aluminium alloy with a socket connection mating with the steel cone. A steady flow of cold water was maintained through the jacket during experimental runs. The condenser termin-

ated in a machined cone which fitted the socket of a cylindrical can packed with glass wool. The condenser was 30 inches long overall with a jacketed length of 18 inches and the bore was 1 1/4 inches; the can was 5 inches long by 4½ inches diameter.

Apart from those products condensing with the phthalic anhydride (notably phthalide) other products (including o-xylene) were not collected in the apparatus as finally employed. A detailed discussion is given later in Section 3.4.2.

3.3.6 Control and instrumentation

As described in Section 3.3.1 the fluidized bed in the reactor shell was heated by four Pyrobar elements. The two lower elements were wired in parallel and on a different circuit from the two upper elements (also in parallel). The two sets could be switched on and off independently from the control panel. The upper set of elements were connected through a 7.5 KVA 'Variac' mounted on the control panel frame, so that a fine control over the fluid bed temperature was possible by adjustment of the voltage across these elements. Both heater circuits incorporated a 'Sunvic' 26 amp. hot wire switch activated by the Holmes blower motor: the heaters therefore did not function unless the blower supplying the fluidized bed was running.

A similar arrangement was adopted in the case of the reactor air preheater. Two spearate circuits with switches on the control panel supplied two sets of two heating elements in parallel. One circuit was wired through a 2 KVA 'Variac'. Both circuits were connected through different poles of a contactor activated by the reactor air blower motor.

The temperature at seven points along the reactor axis and at two points on the reactor wall was measured with 'Pyrotenax'

Ni-Cr/Ni-Al thermocouple units. Exact locations are shown in Figure 14. The units were of 0.041 inches diameter and varied in length up to a maximum of 12 feet. Since these units were subjected for much of their length to the buffeting of the fluidized bed it was considered advisable to give them additional support by sheathing them with stainless steel needle tubing. This tubing, supplied by Accles and Pollock Ltd. in 10 foot lengths, was of 0.0525 inches inside diameter, 0.0725 inches outside diameter. The mode of installation of the sheathed units is indicated in Figure 21. In the first place the thermocouple was inserted through the needle tubing. This was a difficult task and required the thermocouple to be carefully straightened and freed from kinks beforehand. Lubrication with a thin oil was found helpful and in the case of the longer units it was necessary to use two or three lengths (say 4 feet each) of needle tubing and cover the joints with collars subsequently. The assembled unit was then passed through a small hole (with minimum clearance) in the reactor cover plate. The end of the unit was inserted into the reactor tube and the tip of the thermocouple (projecting very slightly out from the sheath) reached the axis. Hard solder was applied to fix the needle tubing to the reactor tube wall and finally the unit was tacked with hard solder to the opposite leg of the reactor U tube at intervals of 12-18 inches. It will be noted that in addition to providing extra strength to the thermocouple unit the needle tubing served to keep the full heat of the gas torch off the thermocouple during soldering. The restricted passage between thermocouple and needle tubing was sealed with 'Araldite' at the point where the latter terminated - well above the reactor cover plate, and hence not subjected to high temperatures. Thermocouples measuring the wall temperature were installed with a similar procedure except that the tip was inserted

FIGURE 21 - THERMOCOUPLE INSTALLATION

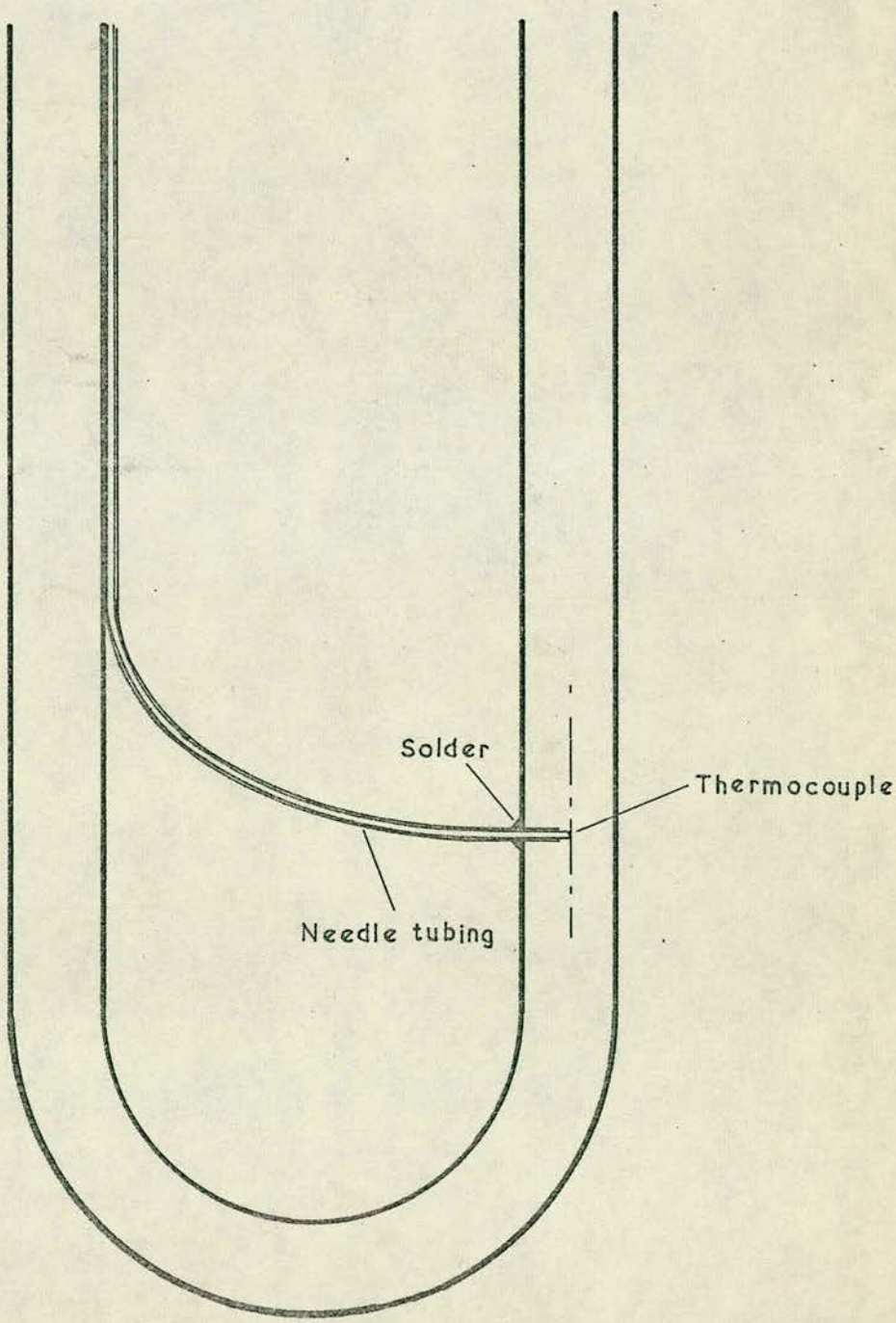

into a narrow groove cut longitudinally into the reactor tube wall and then soldered into position. Before use the reactor was subjected to a pressure test with compressed air at 20 p.s.i.g. to check for leaks past the thermocouples.

The installed thermocouple units terminated about three feet above the reactor cover plate. After the reactor had been located in its shell the units were connected to a barrier terminal strip in a junction box. From there insulated Ni-Cr/Ni-Al cables connected with a 12 point Kent Mark 3 temperature recorder on the control panel: this had a range of 300-450°C in early experiments but was subsequently changed to 350-500°C. The print cycle was 5 seconds so that each temperature was obtained at least once a minute and some could be obtained at 30 second intervals. The chart speed was adjustable but a speed of 15 inches per hour was found satisfactory.

In addition to these thermocouples on the reactor a further unit was inserted directly into the fluidized bed through a hole drilled in the cover plate over the sand removal tube. About 15 inches of thermocouple projected into the bed so that the tip was in a region of good mixing. This thermocouple was also connected to the Kent recorder and the readings from it were used to make manual adjustments to the controlling 'Variac'.

A mercury in steel thermometer measured the temperature of the air leaving the fluidized bed. The reading on this was found to be anything from 30 to 50°C lower than the fluidized bed temperature, depending on the air flow rate, degree of insulation, etc. Nevertheless this instrument was quite useful when the system was heating up from cold and the temperatures were below the range of the Kent recorder.

A similar instrument measured the temperature of the air leaving the pre-heater. The controlling 'Variac' was normally adjusted so that this temperature was 400°C.

A pressure gauge with a 0-30 p.s.i.g. scale measured the reactor air pressure after the filter and immediately before the rotameter.

The flow controls for reactor air, fluidized bed air and o-xylene have already been described.

3.4 Operation of the equipment

3.4.1 Typical experimental schedule

Starting from cold the fluidized bed required up to ten hours to reach operating temperatures. It was therefore switched on the day before an experiment was planned and was often left running for five days on end. All the heaters, of course, were fully on during the initial warming up period, but overnight the power was reduced to 6-8 kw. to avoid overheating. An input of 5-7 kw. (roughly) would maintain operating temperatures between 370-430°C. The reading on the fluid bed rotameter would normally fall off during this heating up period. This was presumably due to the increased bed resistance at higher temperatures.

Sand entrainment from the fluidized bed was quite heavy and it was necessary to empty the cyclone receiver once per day to maintain the bed level. This involved shutting off the equipment for about 10 mintues and caused a drop of about 10-15°C in the fluid bed temperature. The operation was usually carried out in the morning so that the reactor tube was covered to the maximum extent.

Following this the fluidized bed heaters were ad-

justed to bring the temperature to the desired starting level. This normally required up to an hour: simultaneously the reactor air would be switched on and the preheater brought up to 400°C. If reaction products were to be collected the condenser and filter can would be prepared and weighed (to 0.1 gms) during this period. The Thermocord would be switched on and also the Kent recorder. Gases leaving the reactor were diverted to the waste drum.

When both fluidized bed and preheater temperatures were steady at the desired levels and all flow rates corrected the o-xylene would be switched on. A delay of some minutes might ensue before any response was observed owing to the tendency of the xylene to evaporate from the feed line over a period of time, particularly when the rig was at high temperature.

After reaction began the reactor would be allowed to settle before collecting a sample. Two hours were often required for this and occasionally as much as seven or eight hours. The burette on the control panel would require to be replenished with o-xylene from time to time. The flow rate of o-xylene also required to be checked (by taking readings on the burette over a timed interval) periodically.

When steady conditions obtained (as judged by the Kent recorder) a sample would be collected: this was normally taken over a thirty minute interval. The gas flow would be diverted to the collection system for the measured period and the input of o-xylene would be recorded from the burette readings at the commencement and end of the period. (In fact, since the three way cock for switching the gas flow was located on an access platform and the burette was at ground level, the burette was normally read exactly 30 seconds after operating the cock.)

Following the sample collection, the o-xylene would

be switched off, the condenser and filter can removed, the water emptied carefully from the condenser jacket, and compressed air blown through the jacket to dry it before weighing. The rest of the sample treatment procedure is described in the section on Product Analysis.

The reactor air was not switched off until all the thermocouples in the reactor showed a uniform reading at the fluid bed temperature. All equipment except for the Holmes blower and fluidized bed heaters would then be shut off.

3.4.2 Experimental difficulties and equipment modifications

Some trouble was experienced with the Pyrobar heaters in the fluidized bed. Six elements burned out and were replaced in the course of the experimental work. Unfortunately replacement was a lengthy process, since the sand had to be let out of the bed and it was also necessary to remove the reactor assembly so that the thermocouples would not be damaged when inserting the heaters through the entry ports.

The cause of the failures is attributed to an insufficient air supply leading to loss of fluidization and local overheating of the elements. In each case the element was found to have fractured completely and an agglomeration of sand particles was observed adhering to the broken ends. Such failures were not prevented by the safety cut-out on the heaters which only operated if the blower motor stopped. On at least one occasion failures occurred because belt slip developed on the Holmes blower.

The original elements were rated at 3 kw. On failure they were replaced with elements of 2½kw. but these also were subject to failure - in one case after quite a short period. No point on the element appeared to be particularly subject to failure.

Alternative protective devices for the heaters were considered. A high temperature cut-out was rejected since it can only sense the temperature at one point whereas the total immersed length of element is about 32 feet. A differential pressure switch (which would cut off the heaters if the air flow rate became too small) might be feasible but would require the incorporation of a deliberate restriction in the line in order to secure a large enough pressure differential.

The fluidized bed design was deficient in that insufficient freeboard was allowed at the top of the bed to prevent sand losses by entrainment. In effect this meant that the bed operated with about 16-18" freeboard and the last two thermocouples in the reactor were above the sand level. (Fortunately this turned out not to be very important.) The cyclone, which was a late addition to the equipment, was totally effective in collecting the entrained sand at the air flow rates employed. A direct discharge from the cyclone to the fluidized bed was considered but there was insufficient head room between the top of the rig and an overhead crane. Moreover, even without such a modification, access to various parts of the top of the rig was quite difficult.

Sand leakage from joints was never entirely eliminated. This was mostly from the joint between the reactor shell and the reactor cover plate. A jointing compound was not used here because the reactor had to be taken out fairly often. It was found best to use two or three gaskets cut from 'Twillsteel' and to ensure that all faces were wiped off before bolting down the plate.

The temperature range of the Kent recorder was originally selected as 300-450°C (prior to any experimental work). The catalyst proved to be more or less inactive below about 380°C and the range was subsequently adjusted to 350-500°C. In retro-

spect, a range of 350-600°C would have been ideal.

A number of thermocouple breakages occurred, particularly in the early stages of assembling the equipment. These first breakages were simply due to not securing the units sufficiently well, so that fractures occurred through metal fatigue. When this was corrected the incidence of breakages dropped considerably.

The product collection system (and waste collection system) undoubtedly presented the major experimental difficulty. It was in a state of evolution throughout the course of the work and it must be admitted that no satisfactory solution was found to the problems. The principal difficulty consisted in the conflict between achieving effective solids removal and maintaining an unrestricted passage for gas flow all within an apparatus of reasonably small dimensions. Moreover it was necessary for the collection system to function satisfactorily over a half hour period.

The final arrangement gave a reasonably effective removal of phthalic anhydride, provided that the can filter was correctly packed with glass wool. Some losses occurred in the first minute or so of collection. Once the phthalic anhydride had formed a deposit filtration was very effective. Inevitably as time went on the flow area became restricted and the increased pressure drop caused changes in the flow rate. These were sometimes sufficiently large to seriously disturb the reactor temperature profile. A larger collection system would help to overcome these difficulties, but this of course would make it more difficult to work up the products for analysis.

Similar difficulties were experienced with the waste collection system. As the phthalic anhydride deposited in the waste drum (and also the PVC tube from this drum) the resistance to flow increased so that it was difficult to maintain steady conditions. The point of exit from the drum was particularly prone to blocking up.

Frequent emptying of the drum (once a week at least) and unblocking the PVC tube every day kept this problem to a minimum.

Under conditions of incomplete reaction a brown liquid deposited as well as phthalic anhydride: these combined to give an impervious cake on the filter. Neither the waste drum nor the product collection system worked effectively when this occurred.

The worst difficulty of all was that a sudden pressure change tended to occur on switching over the flow from the waste drum to the collection system. One might wait several hours for the reactor temperature profile to become steady only to have it completely changed by the action of sampling. No solution was found to this problem other than to keep all passages as clear as possible: part of the difficulty may lie in the restricted flow through the three way cock. It might be worth increasing the pipe diameter after the reactor to $1\frac{1}{2}$ inches in future work.

In early experiments an attempt was made to collect other reaction products (in particular the unreacted o-xylene) by freezing out with "dry-ice" in acetone. Various shapes of condenser of both metal and glass construction were used. The principal difficulty was that the reaction products froze to the consistency of snow and were blown out of the apparatus by the gas flow: lower gas velocities could not be used because no larger Thermos flask could be obtained to house the condenser. Secondary difficulties were that the freezing mixture was consumed at an inordinate rate and almost constant attention was necessary to replenish it. It became clear that it was not practicable to collect the volatile components in toto. A chromatographic analysis of a side stream sample was considered but no chromatograph was available at the time. Moreover by this stage the reactor temperature profiles already obtained indicated that the bulk of the xylene was reacting and fairly

good yields of phthalic anhydride were being achieved. A complete analysis of the minor products was not considered necessary.

3.5 Analysis of the products

The total amount of reaction products collected was determined by weighing the collection vessels before and after each experimental run. Following the weighing each vessel was washed out with acetone into a two litre standard flask. Typically about 10-15 gms. of products were recovered from the filter can and 20-30 gms. from the condenser. The filter can was washed by sealing it with a rubber bung and shaking up with acetone, this operation being repeated three or four times.

The colour of the made-up solution varied from a very pale pink or yellow through a deep red to a nearly opaque black. The darker colours were obtained with low reaction temperatures.

The temperature of the exhaust gases from the collection system was never less than 50°C. At this level no o-xylene or tolualaldehyde would be found in the products and maleic anhydride would only appear if its yield was greater than 23% - a most unlikely event. Phthalic anhydride, phthalide and other carboxylic acids should be obtained quantitatively.

Analyses for the acid content (reported as phthalic anhydride) and for phthalide were carried out on all samples. The procedure was as follows. A 25 ml. aliquot of the standard solution was taken in a conical flask and the sides washed down with a little acetone. Two drops of phenolphthalein indicator were added and the solution titrated against 0.1 N sodium hydroxide until a pink colour persisting for a few seconds was obtained. This titre gave the total acid content. An (exactly measured) excess of sodium hydroxide was then added (normally about 10 mls.) and the solution allowed

to stand for ten minutes to hydrolyse phthalide according to the equation -

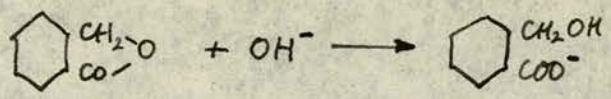

The phthalide was then determined by back titrating the excess sodium hydroxide with 0.1 N hydrochloric acid until the original endpoint was reached.

A series of five determinations using this procedure were carried out on a synthetic solution containing 1.698 gms. of phthalide and 2.139 gms. phthalic anhydride made up to 250 mls. in acetone. The standing times allowed for hydrolysis were varied.

Determination	PA found	Error in PA	Standing time	PI found	Error in PI
1	2.175 gms.	+1.7%	29	1.690 gms.	-0.47%
2	2.145	+0.28	22	1.770	+4.24
3	2.139	0.00	17	1.745	+2.77
4	2.162	+1.08	12	1.690	-0.47
5	2.148	+0.42	9	1.622	-4.48

The results are shown in the above table. Good accuracy was achieved for phthalic anhydride and fairly good accuracy for phthalide. In practice the accuracy for phthalic anhydride would be slightly lower than this because the colouration of the solution tends to obscure the endpoint. Accuracy for phthalide would be very much worse, partly for the same reason but largely because the amount present was always small.

Other synthetic solutions were tested to which quantities of xylene, tolualdehyde and maleic anhydride had been added. The results were not significantly different from the above.

Several of the experimental solutions were analysed qualitatively on a Perkin-Elmer F11 chromatograph. Apart from phthalic anhydride and phthalide only traces of other components were found. Toluic acid seemed to be present in one sample and a high boiling point compound in another - possibly a tribasic acid.

In a few of the experimental runs a determination of the oxygen content of the gas leaving the collection system was made. A sample of the gas (taken just prior to the exit of the system) was withdrawn by a hand aspirator, passed through cotton wool filters and silica gel and fed to a direct reading Servomex OA101 Mark 2 oxygen analyser. The quoted accuracy of this instrument is 0.1% oxygen.

CHAPTER 4 EXPERIMENTAL RESULTS

4.1 The experimental program

Apart from preliminary experiments when the equipment was being assembled, the reactor was charged with catalyst (and inert material) on four occasions during the course of the work. All experimental results are therefore coded with a preliminary number between 1 and 4, corresponding to the reactor charge from which they were obtained. These numbers follow the correct temporal sequence, as do the secondary numbers which distinguish the different experimental runs on the same batch of catalyst.

Table 8 gives the details of each reactor charge.

This program was not determined in advance apart from the first two charges of catalyst. The later work was suggested by the results already obtained.

The reactor air rotameter was calibrated after each packing of the reactor; at the same time the joints in the air line were checked for leaks. The calibrations were performed with both the fluidized bed and the preheater at 400°C, because of the variation in pressure drop across the system with temperature. A wet gas meter of appropriate size was connected to the reactor discharge via a hose of sufficient length to cool the air to ambient temperature before it reached the meter.

The fluidized bed rotameter was set at a scale mark of 6 in all runs after 1-12. (Prior to this it was set at 4.) It is calculated (see Appendix 6) that the air flow to the fluidized bed under standard conditions was therefore 18.4 c.f.m. and the heat transfer coefficient to the reactor was 50 B.t.u./hr.ft^2 °F. There must have occurred some slight variations in these figures in the course of the work, however, because the sand level in the bed

Table 8 Reactor Packing Details

Charge Number	Date of packing	Total packed length	Total catalyst in charge	Comments
1	14.5.69	6'2½"	945.7 gms.	Pure catalyst throughout
2	27.1.70	6'1½"	830 gms.	First section of length 1'0 1/8" contained 152 gms. catalyst. Second section of length 1'5 3/4" contained 114 gms. catalyst and 144 gms. inert material. Third section of length 3'7 5/8" contained 564 gms. catalyst.
3	24.3.70	6'1 3/4"	691 gms.	First section of length 3'3 1/4" contained 247 gms. catalyst and 312 gms. inert material. Second section of length 2'10½" contained 444 gms. catalyst.
4	30.4.70	Not measured	913 gms approx	This was charge 1 (less a few gms.) replaced in the reactor. No dilution.

fluctuated (probably over a range of six inches) and the different bed temperatures employed would also affect the results. The heat transfer coefficient was probably rather low compared with the values obtained industrially which one would guess to be greater than 100 B.t.u./hr.ft^2 $^\circ$F.

4.2 The dynamic behaviour of the reactor

The reactor was operated for some three hundred hours with continuous monitoring of the temperature profile, and for most of that period it exhibited unsteady state behaviour. Clearly it is impossible to tabulate or otherwise record within these pages all (or even most) of the results so obtained. A highly selective summary has been prepared after examining the complete output from the Kent recorder during the experimental work; it is believed, however, that this summary gives an adequate qualitative description of the dynamic responses of the reactor.

A feature of the reactor which rapidly became apparent (and which had not been anticipated) was the phenomenon of reaction ignition and extinction. On many occasions it was observed that a lengthy induction period (or pseudo-steady state period) intervened between start-up and the reaction 'taking hold' or igniting. This is illustrated in Figures 22-25. Figure 22 depicts temperature profiles at time intervals during the start-up of an undiluted catalyst reactor. The jacket temperature was 386°C rising to 387°C throughout: the xylene feed first reached the reactor (as judged by the thermocouple responses) at time zero. It may be seen that after about 8 minutes a pseudo-steady state profile is achieved which persists more or less undisturbed until about 64 minutes after start-up. In the ensuing 20-30 minutes the reaction ignites with marked and rapid alteration of the temperature profile.

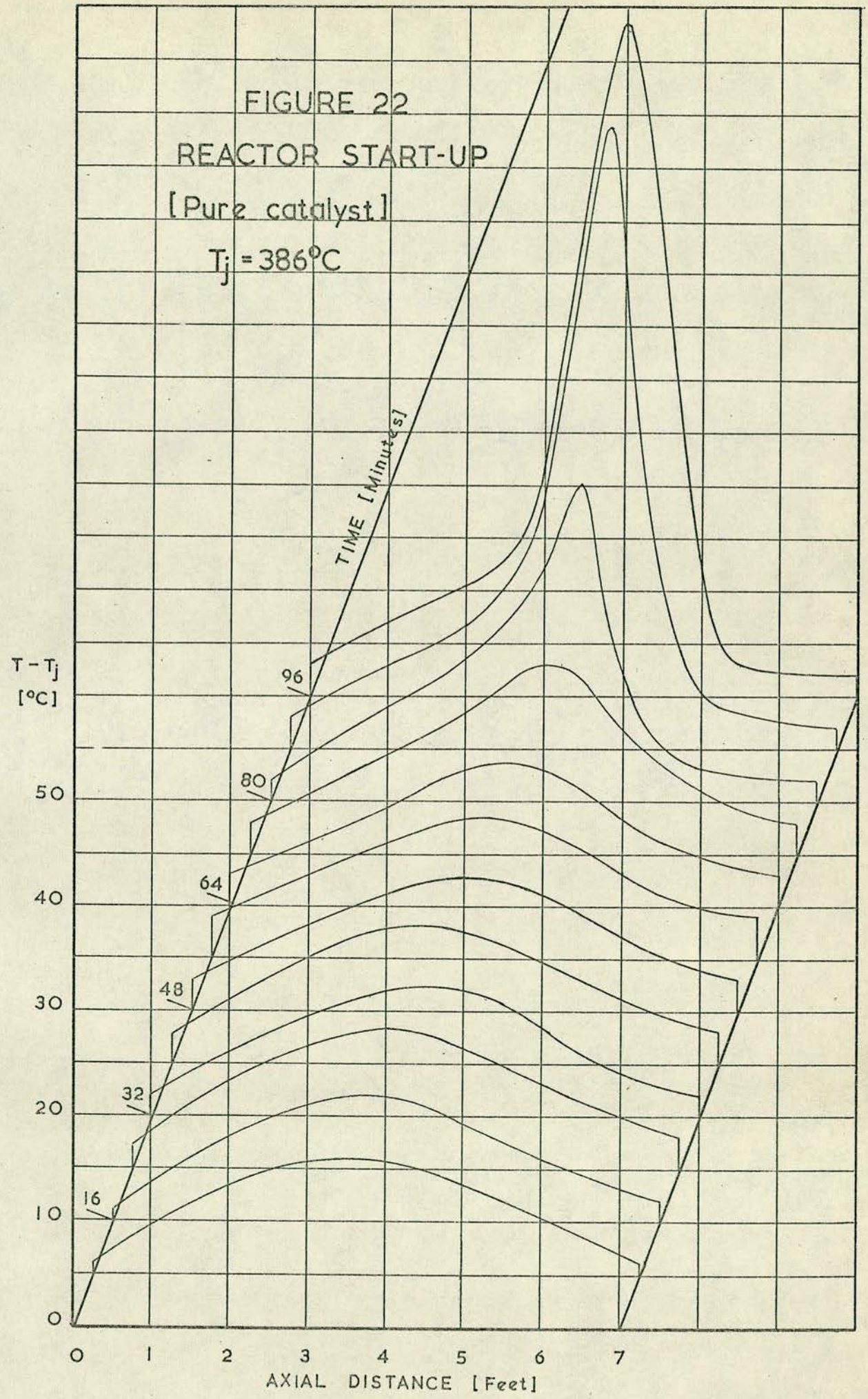
FIGURE 22
REACTOR START-UP
[Pure catalyst]
T_j = 386°C
TIME [Minutes]
96
80
64
48
32
16
T - T_j [°C]
0
10
20
30
40
50
0
1
2
3
4
5
6
7
AXIAL DISTANCE [Feet]

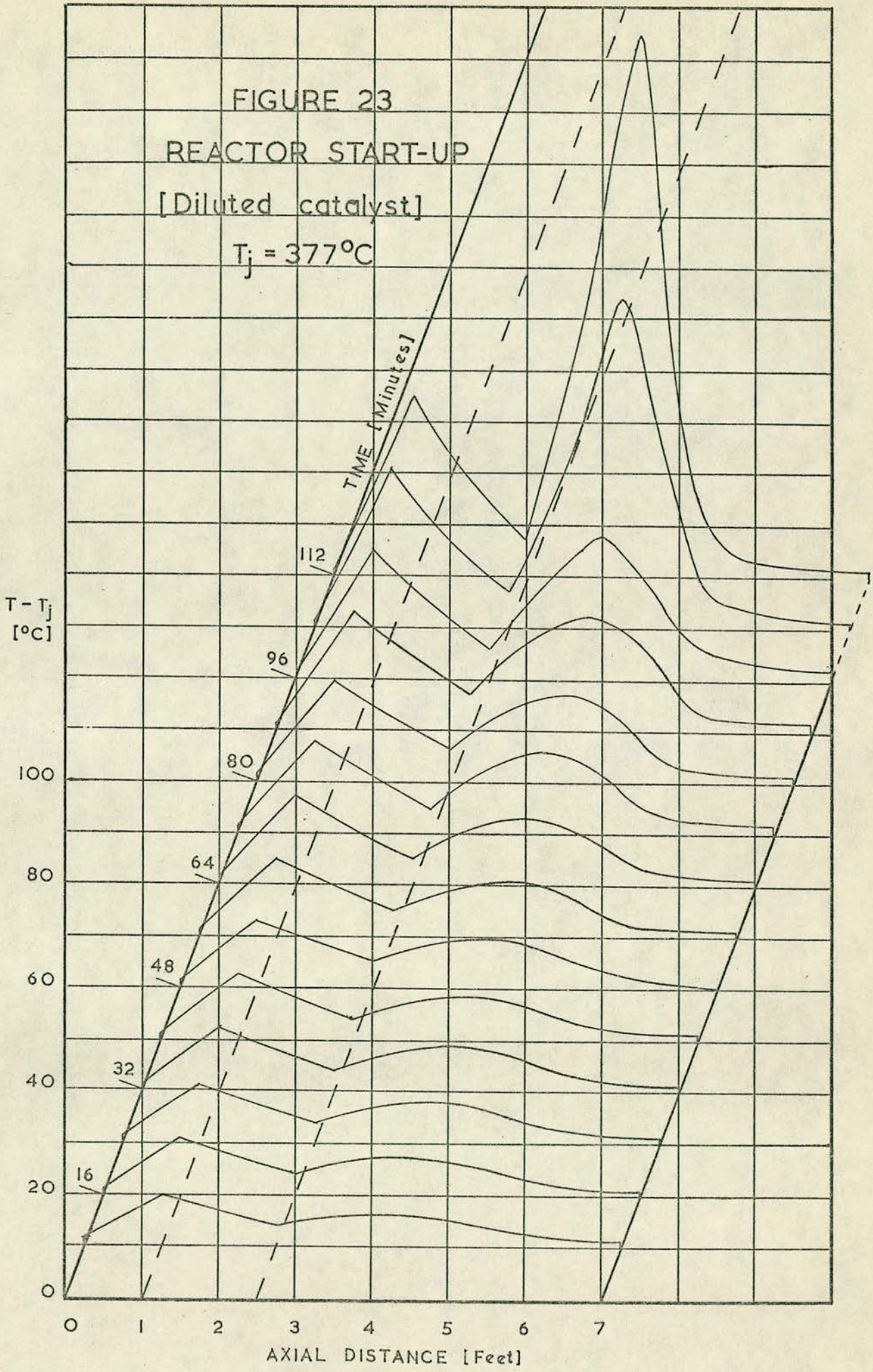
FIGURE 23
REACTOR START-UP
[Diluted catalyst]
T_j = 377°C
TIME [Minutes]
112
96
80
64
48
32
16
T - T_j [°C]
0
20
40
60
80
100
0
1
2
3
4
5
6
7
AXIAL DISTANCE [Feet]

FIGURE 24

REACTOR START-UP (Pure catalyst)

$T_j = 393\,^{\circ}C$

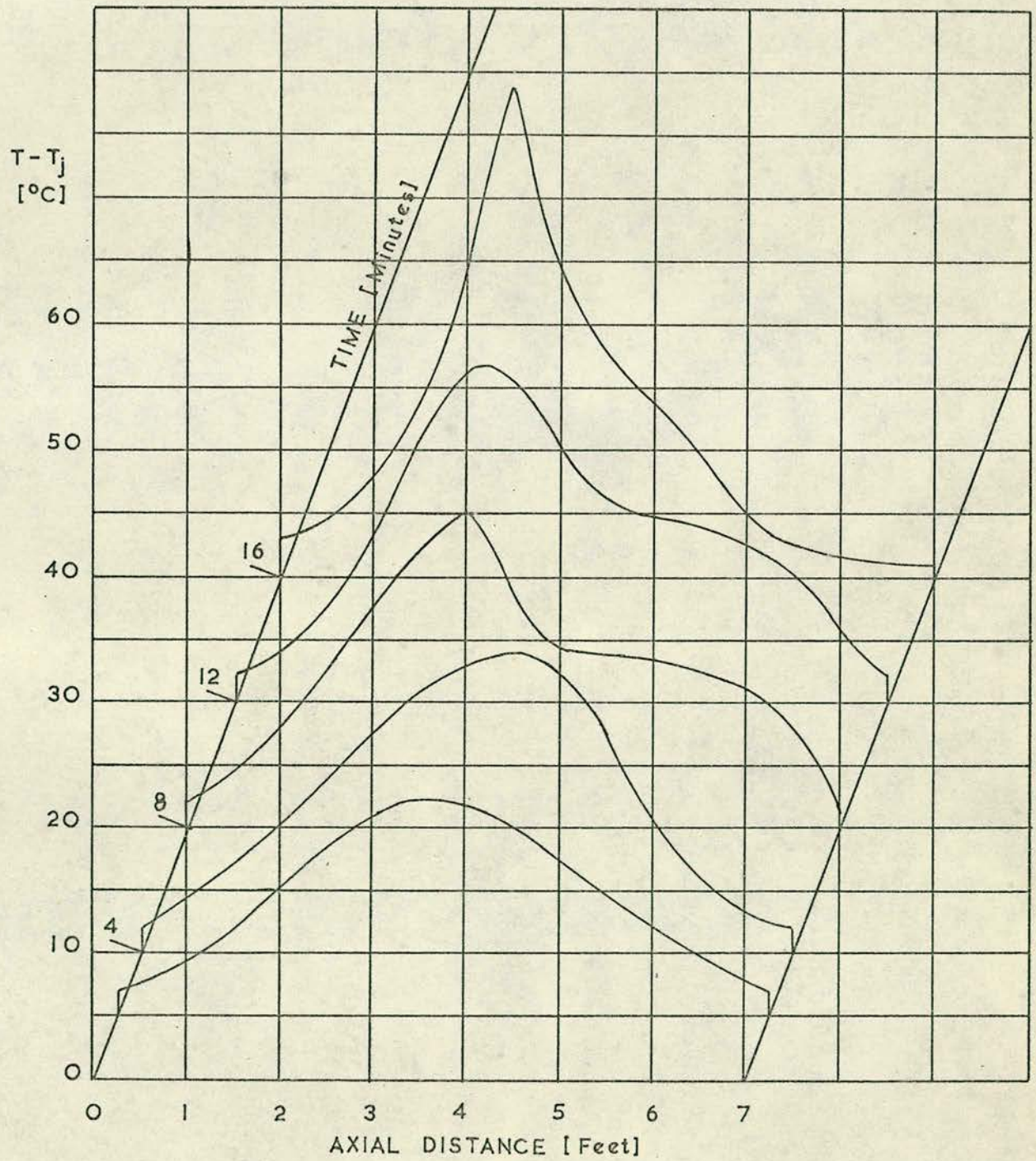

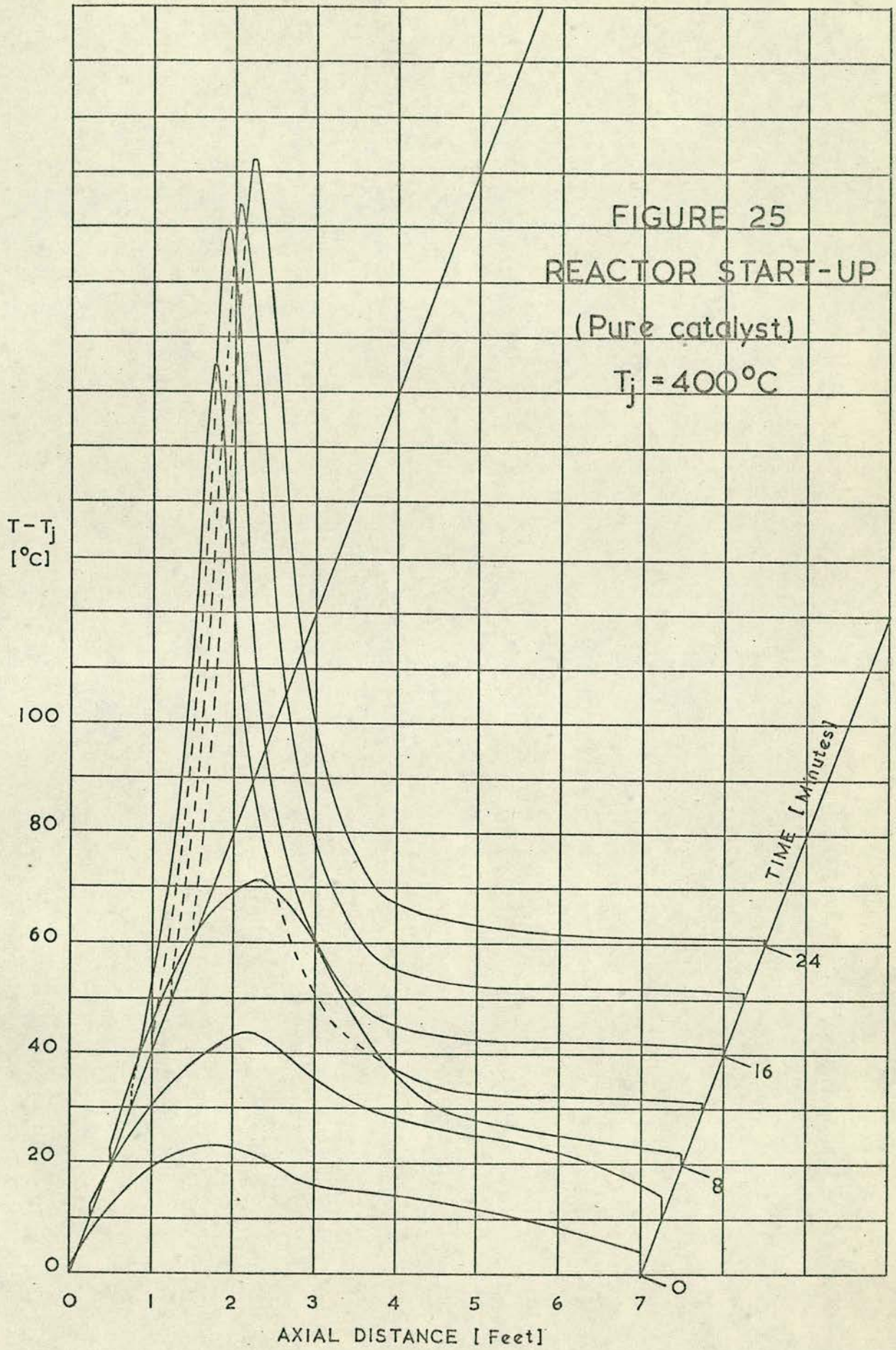
FIGURE 25
REACTOR START-UP
(Pure catalyst)
$T_j = 400°C$
$T - T_j$ [°C]
0
20
40
60
80
100
0 1 2 3 4 5 6 7
AXIAL DISTANCE [Feet]
TIME [Minutes]
0
8
16
24

Figure 23 provides an even more striking illustration of the same phenomenon. The ignition occurs a full 90 minutes after start-up in this case in which the jacket temperature was 377°C. The unusual temperature profile is due to the fact that the reactor was here diluted over an 18 inch section beginning 12 inches down from the inlet. Figure 23 shows more clearly than Figure 22 that there is a slight (but definite) upward trend in the general temperature level of the reactor throughout the induction period.

In contrast, Figures 24 and 25 (which both refer to an undiluted reactor) show start-up profiles with no hint of an induction period: there is an immediate ignition. Reaction conditions were identical in all four cases with the exception of the jacket temperature: it was 393°C for Figure 24 and 400°C for Figure 25.

The start-up behaviour of the reactor may therefore be described as follows. At low temperatures, below approximately 375-385°C the reactor rapidly (3-5 minutes) attained steady state conditions with a peak temperature not exceeding about 15°C above the jacket temperature. Between approximately 380°C and 395°C the reactor attained a pseudo-steady state in 3-5 minutes; an induction period of up to 90 minutes duration followed by an eventual fairly rapid ignition to a high reaction state. The higher the jacket temperature, the shorter was the duration of the induction period. With jacket temperatures greater than about 390-400°C the reactor ignited immediately.

It will be noted that the temperatures which delimit the various categories of behaviour are given very imprecisely. A good deal of time was devoted to attempting to obtain precise limits, but it was eventually concluded that in this, as in many other respects, the reactor was not able to give reproducible results.

This may be taken as support for the view of a variable catalyst activity, dependent on the previous history of operation. One general effect that was observed was that a fresh charge of catalyst required a relatively high jacket temperature to produce reaction ignition. For example, in Run 1-2 on July 3rd 1969, with a jacket temperature of 393°C, the maximum recorded temperature 55 minutes after start-up was 18°C above the jacket temperature. (14°C above the jacket temperature 4 minutes after start-up.) This may be compared with the results of Run 1-21 seen in Figure 24 which refers to the same batch of catalyst, the same jacket temperature and identical flow rates. Here the maximum recorded temperature already exceeds the jacket temperature by 38°C only 16 minutes after start-up.

Another generally observed effect was that activity was retained by the catalyst for a short period - perhaps two hours - after shutting down the reactor. In consequence a return to a high level of reaction could be achieved fairly easily (i.e. at a low jacket temperature) if the reactor were re-started within this period. Figure 23 provides an example of this, where ignition is (eventually) achieved at the abnormally low jacket temperature of 377°C. In this case the xylene feed had been closed off one hour previously after operating with a high reaction level, and the reactor air had been left on over the intervening period.

Returning to the phenomenon of reaction ignition and extinction an example of extinction is provided by Figure 26. This refers to an diluted catalyst reactor. At the zero point on the time scale the maximum temperature in the reactor was about 140°C above the jacket temperature, and the temperature profile had been reasonably steady over the previous 25 minutes. Between 2 and 4 minutes after time zero the jacket temperature was dropped by 1°C

FIGURE 26

REACTION EXTINCTION (Diluted catalyst)

T_j = 376-375 °C

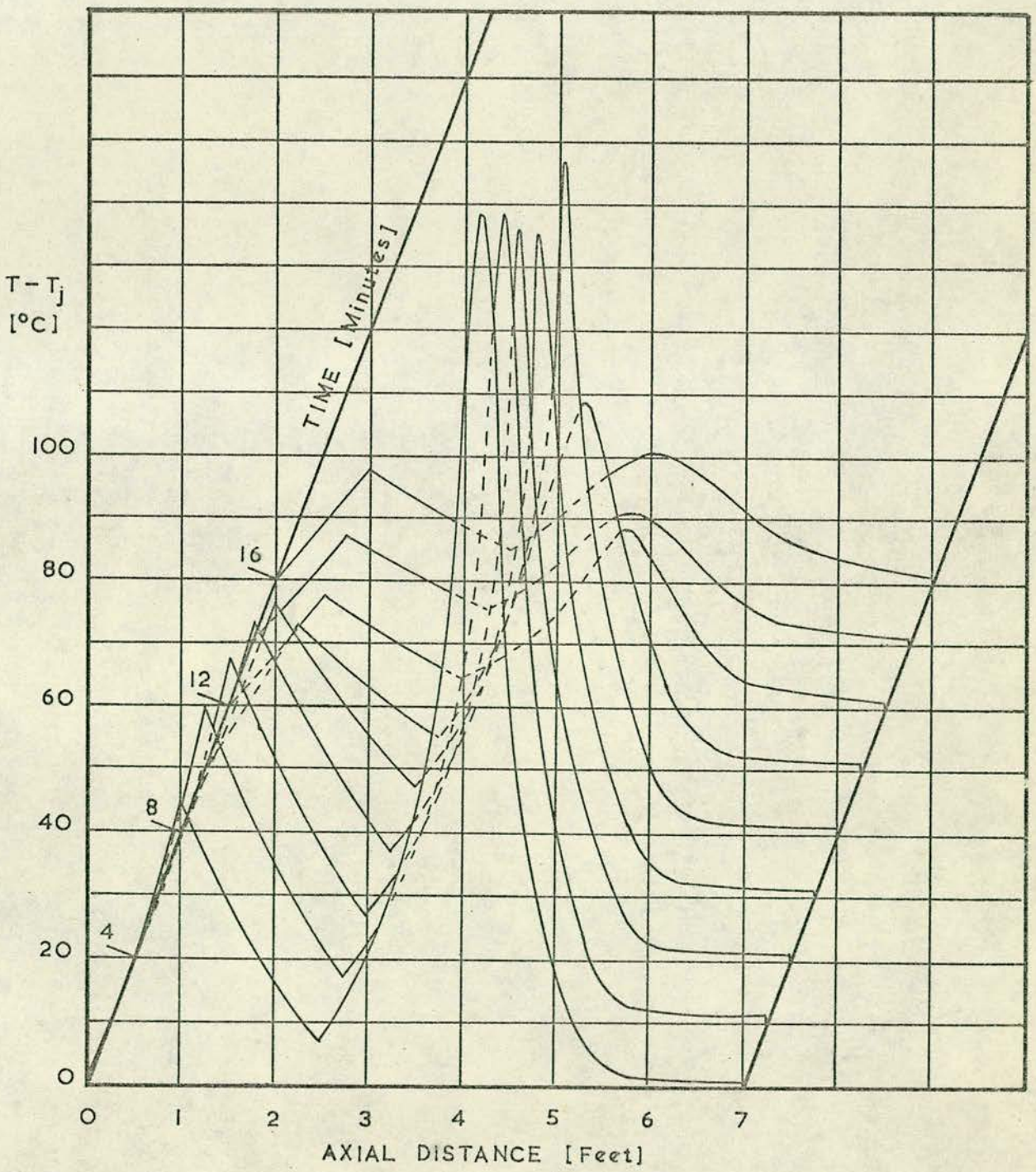

from 376 to 375°C. After 8 minutes the three-way cock was turned to collect a sample of the product and the temperature profile immediately collapsed to give a final peak temperature of 21°C. The direct cause of this collapse was undoubtedly the action of sampling - but the reactor must have been operating on the verge of extinction due to the drop in jacket temperature. It may be noted that the smaller of the two temperature peaks had begun to decline before the action of sampling.

A question that is bound to be raised in connection with ignition-extinction phenomena is whether hysteresis also occurs. It seems certain that it is exhibited by this reaction system but the magnitude of the lag is uncertain. In Run 1-15 the reaction ignited with a jacket temperature of 386-7°C after a delay of about 90 minutes (Figure 22). It subsequently proved possible (in the course of the same run) to maintain a high level of reaction down to a jacket temperature of 380°C. This lag of 6-7°C was found in a number of other runs; the maximum and minimum observed values were 10°C and 2°C respectively.

A further example of reaction extinction is shown in Figure 27. At the beginning of the time period shown the temperature profile had been steady for 40 minutes: no change was made to the operating conditions and for no apparent reason the temperature profile collapsed, with the peak temperature declining from about 70°C to about 30°C. (A sample of product was subsequently taken with the profile more or less at the final level shown in Figure 27. The yield of phthalic anhydride was 17.9%). This phenomenon of apparently stable operation suddenly proving to be highly unstable was observed on a number of occasions.

The type of behaviour illustrated in Figure 27 is analogous to the supersaturation of a liquid solution on slow cooling;

FIGURE 27

REACTION EXTINCTION (Pure catalyst)

$T_j = 376\,^{\circ}C$

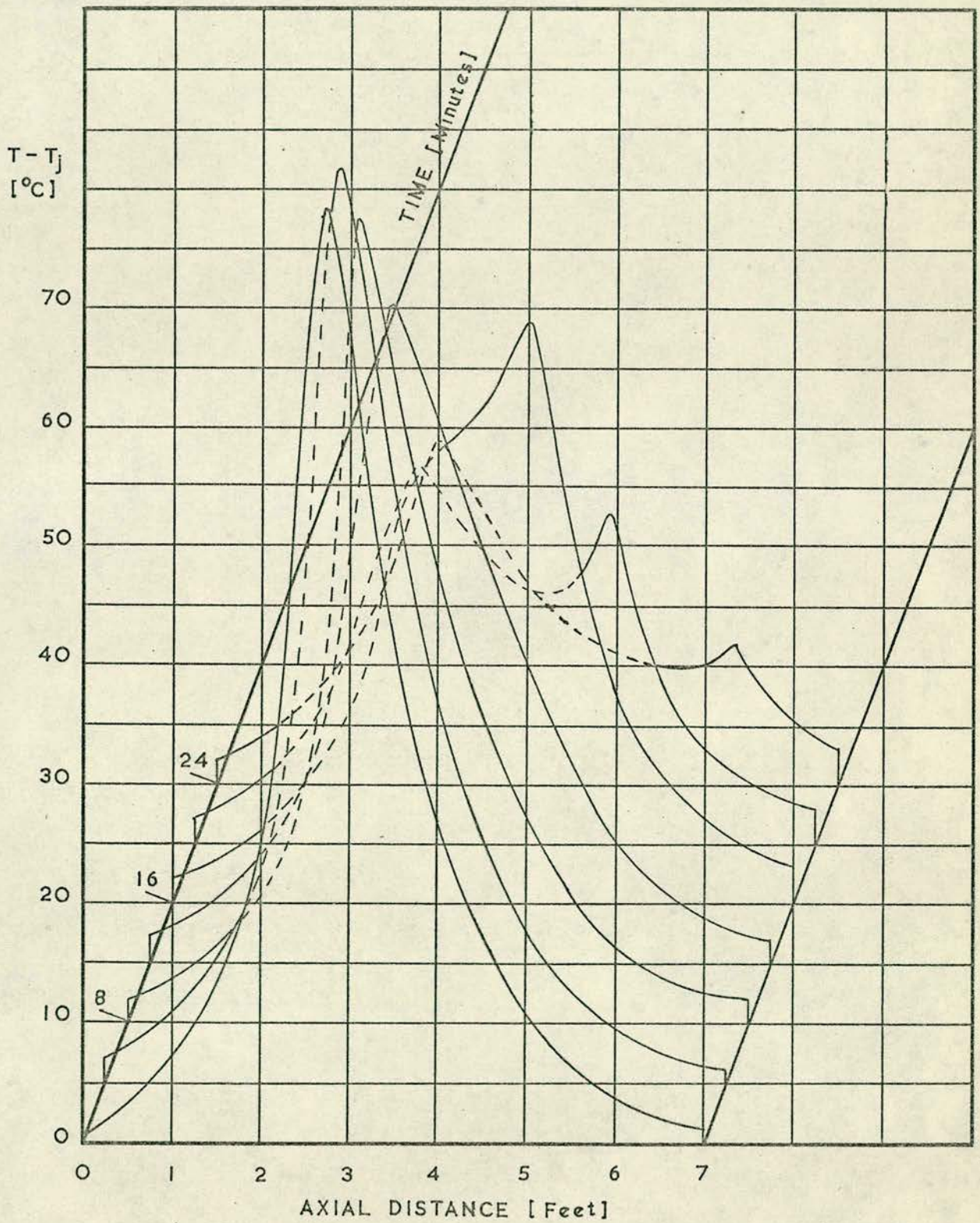

there is a very abrupt collapse in the profile. A different mode of extinction was also observed on occasion: this is typified by the results of Figure 28. An initial hot spot is present at a point near the inlet of the reactor. On lowering the jacket temperature the hot spot begins to be displaced towards the exit. Typically, the peak declines in magnitude and moves with increasing rapidity until it finally disappears out of the tail end of the reactor. A by no means exhaustive examination of this phenomenon indicated that it is most likely to be produced by a rapid lowering of the jacket temperature: a very gradual downward movement produces the "supersaturation" effect of Figure 27. In the case of Figure 28 the jacket temperature was lowered from 390°C to 376°C in the space of 28 minutes, and was then held constant: time zero in the diagram is the time when the jacket temperature first reached 376°C. (This cooling rate of 0.5°C/minute was the greatest that could be achieved by turning off all the heaters). Attempts were made to arrest the movement of the hot spot and cause it to travel back towards the inlet by raising the jacket temperature but this was never achieved. What did happen was that a new hot spot grew up around the initial position, and the increased reaction at this point - leading to depletion of reactant further downstream - caused the 'old' hot spot to die away more rapidly.

Hot spot movements of the kind just described were only properly observed with the undiluted catalyst reactor. The presence of diluted catalyst distorted the phenomenon considerably. Ignition and extinction phenomena were observed with all catalyst charges.

The effects of a number of parameter variations on the temperature profile were observed in a qualitative manner. An increase in the flow of air to the fluidized bed caused a diminution

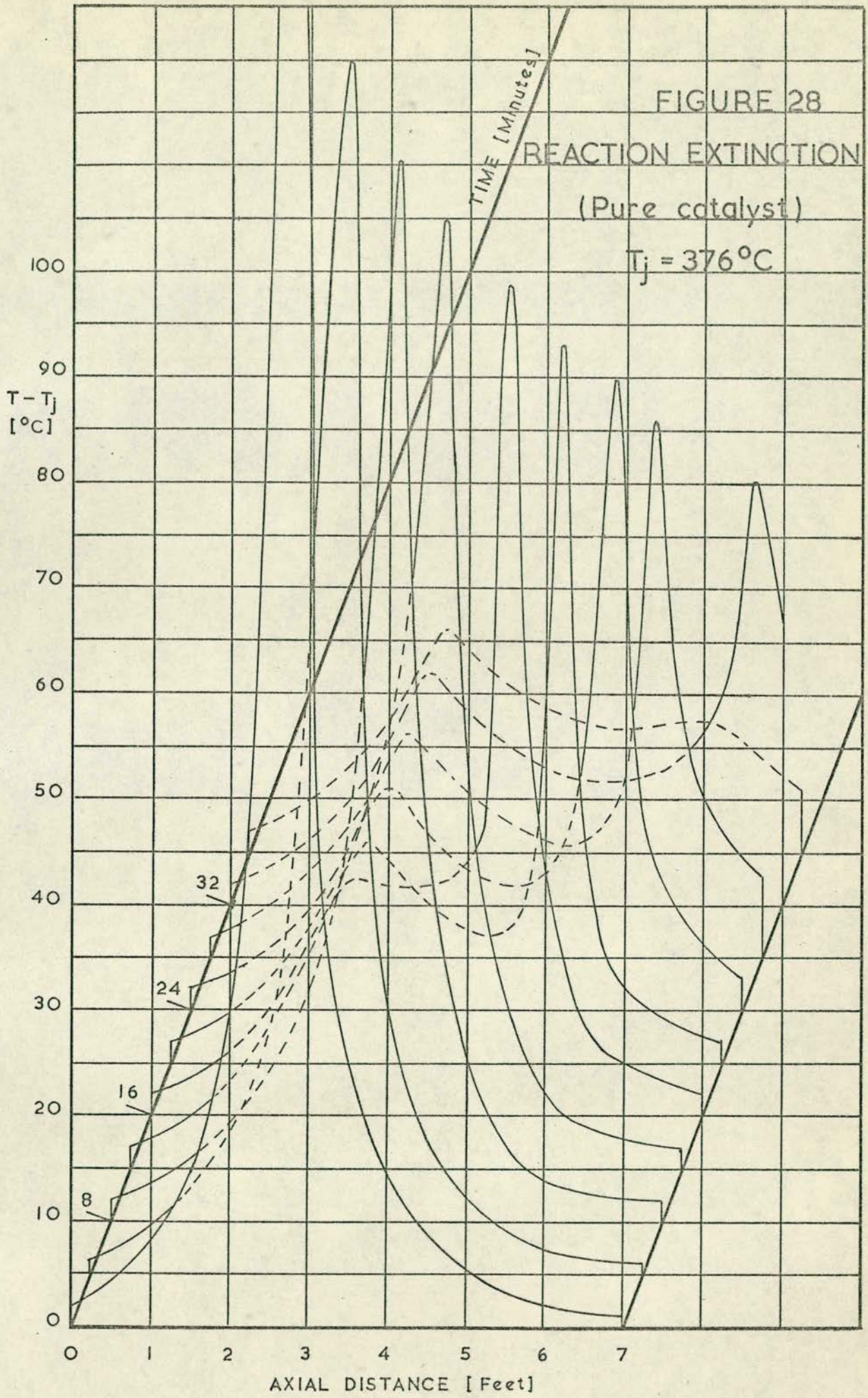
FIGURE 28
REACTION EXTINCTION
(Pure catalyst)
$T_j = 376°C$
TIME [Minutes]
$T - T_j$ [°C]
100
90
80
70
60
50
40
30
20
10
0
32
24
16
8
0
1
2
3
4
5
6
7
AXIAL DISTANCE [Feet]

of the general temperature level in the reactor. From this it may be concluded that the shell side coefficient is of comparable magnitude to the inside wall coefficient and packed bed resistance. Heavy sand losses by entrainment precluded the use of a larger fluidizing air flow over long periods of time.

Although the total flow through the reactor was varied in a number of runs this change was usually made at the outset: on only one occasion was the flow varied after steady state condition had been achieved. The results of making a 30% cut in the total flow rate (whilst keeping the air:xylene ratio constant) is shown in Figure 29, which shows the steady state profiles before and after the change. The transition between the two profiles was smooth and monotonic. Unfortunately, owing to the limited number of thermocouples in the bed, there is here (as in a number of other cases) some uncertainty about the position and magnitude of the hot spot. The curves have been drawn to indicate that the effect of a flow cut is to increase the peak temperature and displace it towards the reactor inlet. It must be admitted that (aside from intuitive feelings in the matter) the curves could equally well have been drawn to indicate a decrease in the peak temperature and a movement towards the exit. The only evidence to support the chosen presentation is the slight but definite increase of $2^{\circ}C$ in the temperature at the inlet - presumably due to increased back mixing of heat from the nearer and larger hot spot.

The effect of a change in the o-xylene concentration in the feed was observed under a variety of conditions and some most interesting results obtained. Where a high level of reaction had been achieved a decrease in xylene concentration had the anticipated effect of generally reducing the temperature. On the other hand at low levels of reaction - during the induction period for example -

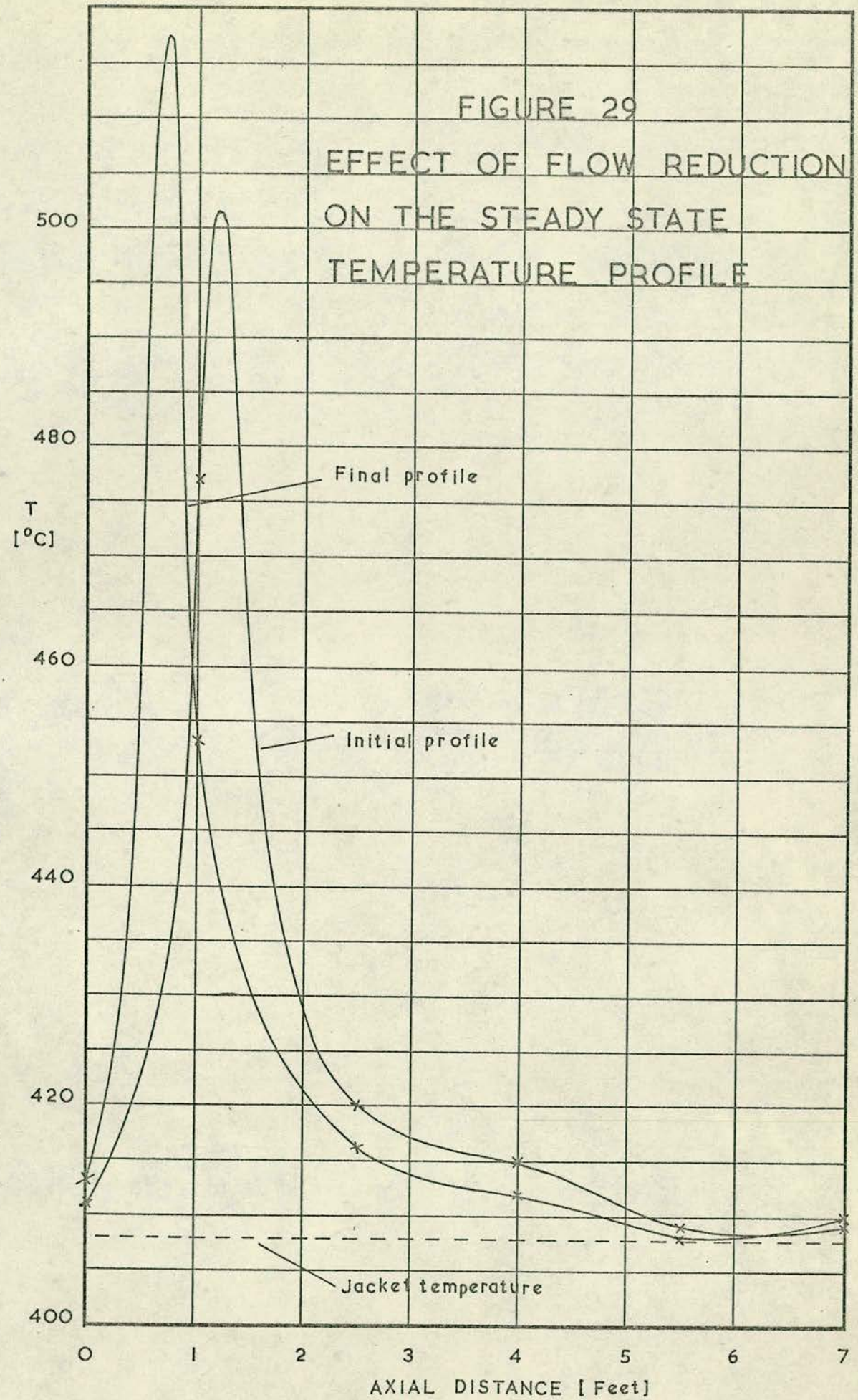
FIGURE 29
EFFECT OF FLOW REDUCTION ON THE STEADY STATE TEMPERATURE PROFILE
500
480
460
440
420
400
T [°C]
Final profile
Initial profile
Jacket temperature
0
1
2
3
4
5
6
7
AXIAL DISTANCE [Feet]

cuts of more than 50% in the feed rate of o-xylene had absolutely no apparent effect on the reactor temperatures. This was observed on two separate occasions, one with a diluted catalyst charge and one with a pure catalyst charge. The temperature-time profiles are shown in Figure 30 for the diluted catalyst charge.

4.3 The steady state behaviour of the reactor

The dynamic behaviour of the reactor reported in the previous section was observed (for the most part) whilst endeavouring to bring the reactor to steady state operation with high yields but a restrained temperature profile. At the outset of the experimental work the theoretical predictions of the Froment model - and the reports of tube burnouts and other disasters - were very much in the forefront of the author's mind. It appeared from theoretical studies that the temperature rise in the reactor should be limited to 30-40°C, and since the catalyst was found to become active in the 380-400°C range it seemed appropriate to set 450°C as the 'danger level' above which the reactor temperature must not rise. (Particularly in view of the fact that 450°C was the upper limit of the Kent recorder range in the early part of the work!) In consequence, throughout most of the Series 1 Runs this limit was observed, but considerable difficulties were encountered due to the complete inability of the reactor to perform in the prescribed fashion.

In a typical experimental run the reaction would ignite (after a greater or lesser induction period) and one of the thermocouple readings would then climb above 450°C fairly rapidly. This would be checked by the short term remedy of reducing (or completely stopping) the xylene feed for a limited time period. At the same time the jacket temperature would be lowered to a level where all temperatures remained below 450°C. Herein lay the

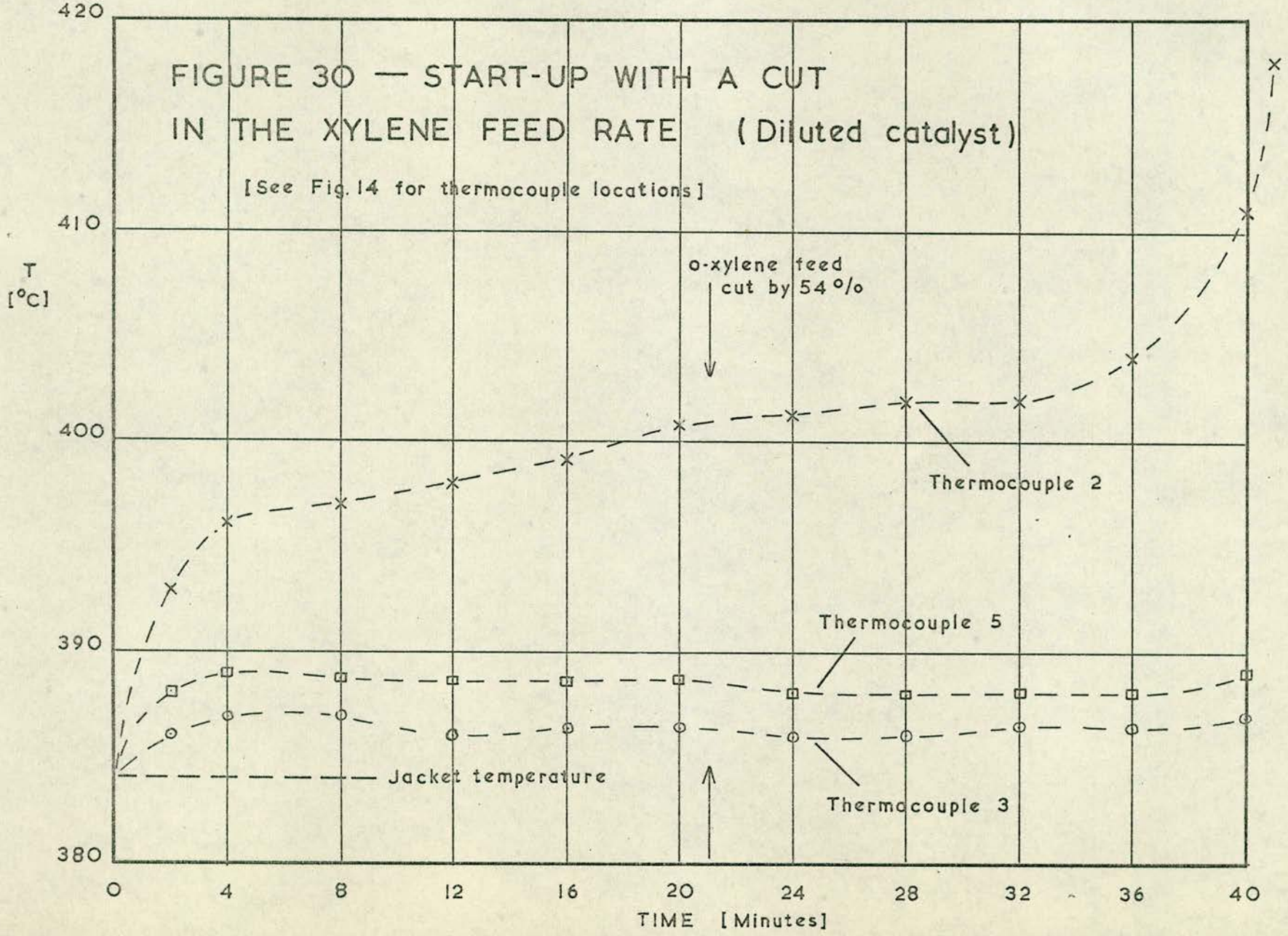
FIGURE 30 — START-UP WITH A CUT
IN THE XYLENE FEED RATE (Diluted catalyst)
[See Fig. 14 for thermocouple locations]
T
[°C]
420
410
400
390
380
o-xylene feed
cut by 54 %
Thermocouple 2
Thermocouple 5
Jacket temperature
Thermocouple 3
0
4
8
12
16
20
24
28
32
36
40
TIME [Minutes]

difficulty, because frequently no jacket temperature proved satisfactory until eventually the reaction became totally extinguished.

Had the type of behaviour described in the previous paragraph been observed in every case the final conclusion might have been reached considerably earlier. However, in a number of runs it did appear possible to achieve maximum temperatures of 30-50°C above the jacket temperature but still below 450°C. The difficulty in these cases was that the peak temperatures (for here there were always two thermocouples indicating appreciable excess temperatures) were persistently unsteady, so that fluctuations of 20°C or more occurred even when all conditions had been held constant for a long period. It now seems certain to the author that in fact the hot spot was located more or less centrally between two thermocouples and was considerably in excess of 450°C: the sensitivity of the thermocouples is not difficult to understand because with such severe peaks the slightest displacement of the hot spot will cause a great change in the reading at a point on the shoulder of the peak. This conclusion is confirmed by the fact that one of the thermocouple readings would increase if the jacket temperature were raised (causing the hot spot to move to the inlet), and the other would increase if the jacket temperature were lowered.

In the later of the Series 1 Runs (where higher jacket temperatures were employed) and in all other later work temperatures of up to 560°C were observed, and there is no reason to suppose that the actual hot spot - which of course does not necessarily coincide with a thermocouple - may not have been higher. (As reported earlier, the range of the Kent recorder was changed from 300-450°C to 350-500°C, and temperatures higher than this were followed with a potentiometer). No ill effects on the catalyst or reactor were observed as a consequence of these high values.

It is concluded that the form of the steady state profile is "discontinuous" in its variations with respect to temperature. The peak temperature is either less than about 15-20°C or greater than about 100°C. These limits (which are not known with precision) apply to an undiluted reactor. A diluted catalyst reactor shows the same qualitative behaviour. The discontinuity is, of course, due to the ignition/extinction phenomenon reported in Section 4.2.

The yield of phthalic anhydride was determined by collecting the products during many of the runs: this was done as far as possible under steady state conditions. Results are given in Table 9 which shows the yield and the reaction conditions and gives an indication of the stability of the temperature profile during the period of product collection.

These results are also presented graphically in Figures 31 and 32 in which the yield of phthalic anhydride is plotted against the jacket temperature. Figure 31, which refers to the undiluted catalyst, shows a clear break at a jacket temperature of about 378°C: below this level the yield is very poor. Above this level a yield of about 60% is obtained and it is remarkable how insensitive this is to changes in jacket temperature. Three of the points shown refer to flow rates 20% above or below the 'standard' flow rate: these seem to fall naturally on the curve and suggest that the yields are independent of flow rate at the conditions used.

A comparison of Figures 31 and 32 reveals that the improvement in yield due to catalyst dilution is marginal - possibly zero. The rather large scatter in the points in Figure 32 makes it difficult to decide on this. The general form of the yield-temperature curve is the same in both cases but the indications are that the break point in the curve occurs at a rather higher temper-

Table 9 Reactor Performance under Steady State Conditions

A. Pure Catalyst

Run No.	Air Flow (litres/min)	Total o-xylene injected (cm^3)	Jacket temperature (°C)	Maximum Recorded+ Reactor Temperature (°C)	Yield %
1-13	30.0	45.5	385	$430^{+}_{-}3$	58.0
1-14	29.8	46.2	389	$432^{+}_{-}8$	58.0
1-15	29.9	46.1	380	$434^{+}_{-}6$	46.9
1-16	29.9	46.3	387	$431^{+}_{-}3$	58.0
1-17	29.8	46.5	384.5	$438^{+}_{-}6$	58.8
1-18	23.8	37.0	386.5	$443^{+}_{-}6$	59.2
1-20	35.8	55.25	382	$436^{+}_{-}3$	52.3
1-21	29.8	46.55	383.5	$432^{+}_{-}12$	59.7
1-22	29.8	30.9*	380.5	$410^{+}_{-}4$	52.5
1-25	35.9	55.65	377.5	$413^{+}_{-}3$	21.5
1-26	29.8	45.8	371	$395^{+}_{-}1$	14.0
1-28	29.8	45.65	375	$407^{+}_{-}7$	14.1
1-29	29.8	45.7	376	$408^{+}_{-}5$	17.9
1-30	23.8	37.2	378	$397^{+}_{-}2$	48.9
1-35	30.1	46.05	384	$520^{+}_{-}17$	56.7
1-36	30.5	45.9	383	$520^{+}_{-}26$	57.0
4-1	29.5	45.2	400	$472^{+}_{-}5$	61.1
4-2	29.5	45.4	410	$463^{+}_{-}3$	58.95
4-3	29 .1	45.55	405	$458^{+}_{-}2$	60.6
4-4	29.3	45.6	415	$457^{+}_{-}3$	57.3

* Sample collected for 20 minutes only: 30 minutes in all other runs

\+ The chart reading was noted down at five minute intervals. The value here is the mean of these readings, and the deviation given is that of the worst case.

ature in the case of the diluted catalyst - say 385°C as opposed to 378°C. The low temperature region was insufficiently studied with diluted catalyst charges. It should be remembered that the results of Figure 32 refer to catalyst charges diluted in different ways, but there is no strong indication of a difference in results. As with Figure 31 some of the points refer to non-standard conditions - variations in flow rate or in feed concentration - and again there is no indication of a dependence on these parameters.

Mention has already been made of the lack of reproducibility of reactor behaviour in respect of the effect of jacket temperature on the time required to achieve ignition. The steady state profiles achieved under apparently the same conditions also showed greater or lesser variations: the hot spot showed a tendency to shift its position and/or magnitude - discrepancies of 20-30°C in the value of the maximum recorded temperature were not uncommon. The most striking variation of profile was achieved with one of the diluted charges, in which the first 3 feet (approx.) of reactor had a catalyst concentration which was 50% of the concentration in the last undiluted section (Run series 3). With identical jacket temperatures, flow rates and feed concentrations the hot spot was - on different occasions - observed in the diluted and undiluted sections of the catalyst. This is shown in Figure 33. The two runs in which the peak occurs in the latter part of the reactor were carried out one before and one after the run in which the peak is in the diluted section. The mode of obtaining these profiles was as follows. In Run 3-1 (the first after packing the reactor) the jacket temperature was raised steadily from 394°C to 410°C when the peak developed naturally in the latter part of the reactor. The jacket temperature was then lowered to 395°C. In the next two or three runs the hot spot remained in this part of the reactor but

Table 9 Cont.

B. Diluted Catalyst

Run No.	Air flow (litres/min)	Total o-xylene injected (cm^3)	Jacket temperature (°C)	Maximum Recorded Reactor Temperature (°C)	Yield %
2-1	30.2	45.7	400	456±3	59.5
2-2	30.3	45.8	398.5	454±3	60.6
2-9	29.4	46.3	382	456±14	56.9
2-11	29.6	38.3*	384	457±8	53.5
3-1	29.7	45.7	395	498±3	60.2
3-2	29.7	45.05	392	494±6	59.5
3-4	29.6	44.8	407.5	467±2	65.1
3-5	28.8	44.7	400	470±2	64.8
3-6	29.2	45.55	418	478±2	62.5
3-7	29.4	45.6	395	458±3	62.0
3-8	29.7	45.55	404	463±2	59.0
3-9	29.7	45.0	412	475±2	59.0
3-10	29.7	28.6	409	449±1	57.5
3-11	29.7	65.4	409	478±2	61.5
3-12	29.3	45.6	409	474±1	59.7
3-13	29.7	44.95	405	464±1	60.1
3-14	29.7	45.5	391	419±1	46.0
3-15	20.6	31.85	408	453±1	58.0
3-16	29.3	44.4	430	483±3	56.0
3-17	29.1	45.05	390	416±2	48.2
3-18	29.3	45.1	386	420±3	48.9
3-19	29.7	45.2	382	437±2	50.3

* Sample collected for 25 minutes only: 30 minutes in all other runs.

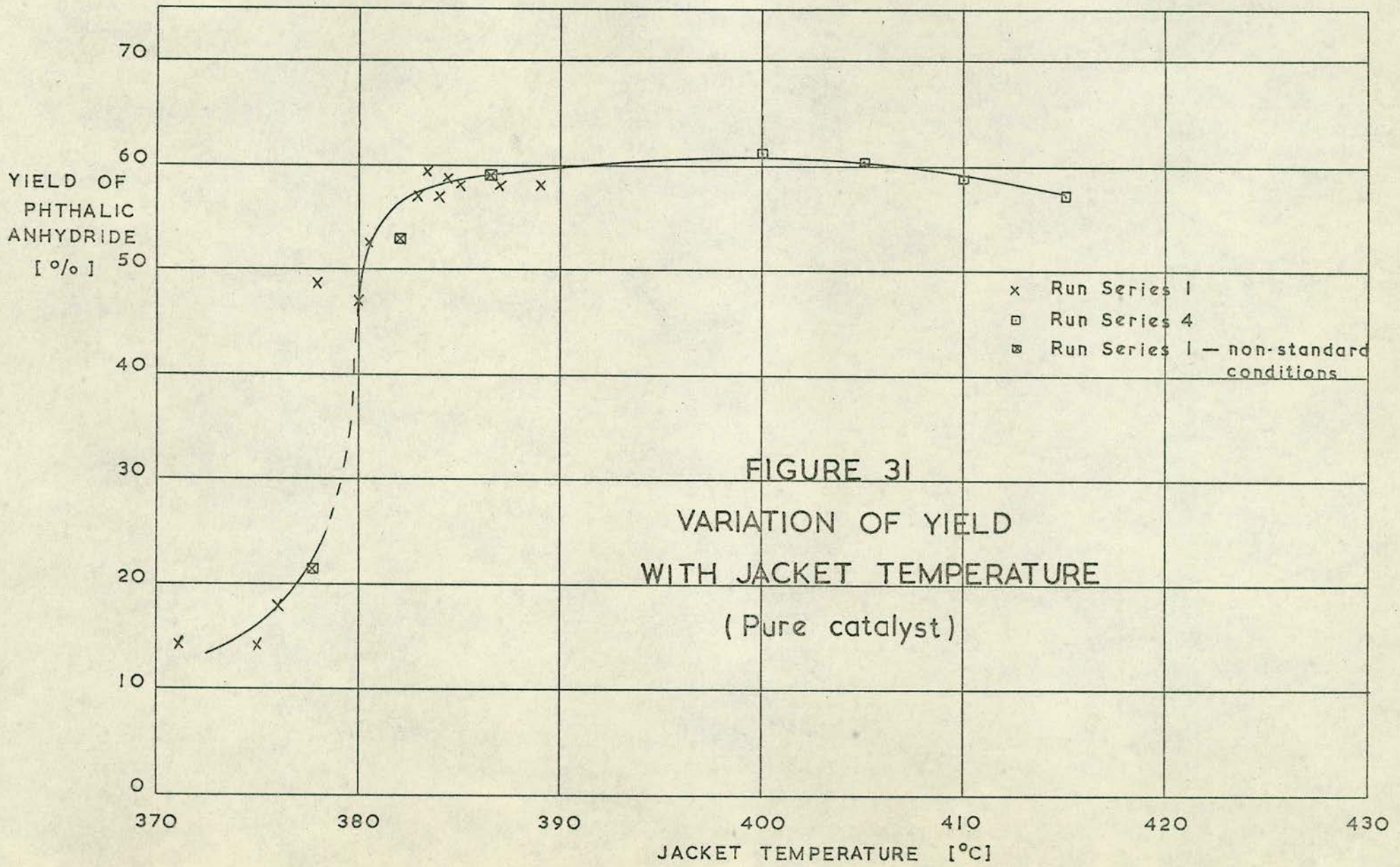

FIGURE 31

VARIATION OF YIELD WITH JACKET TEMPERATURE

(Pure catalyst)

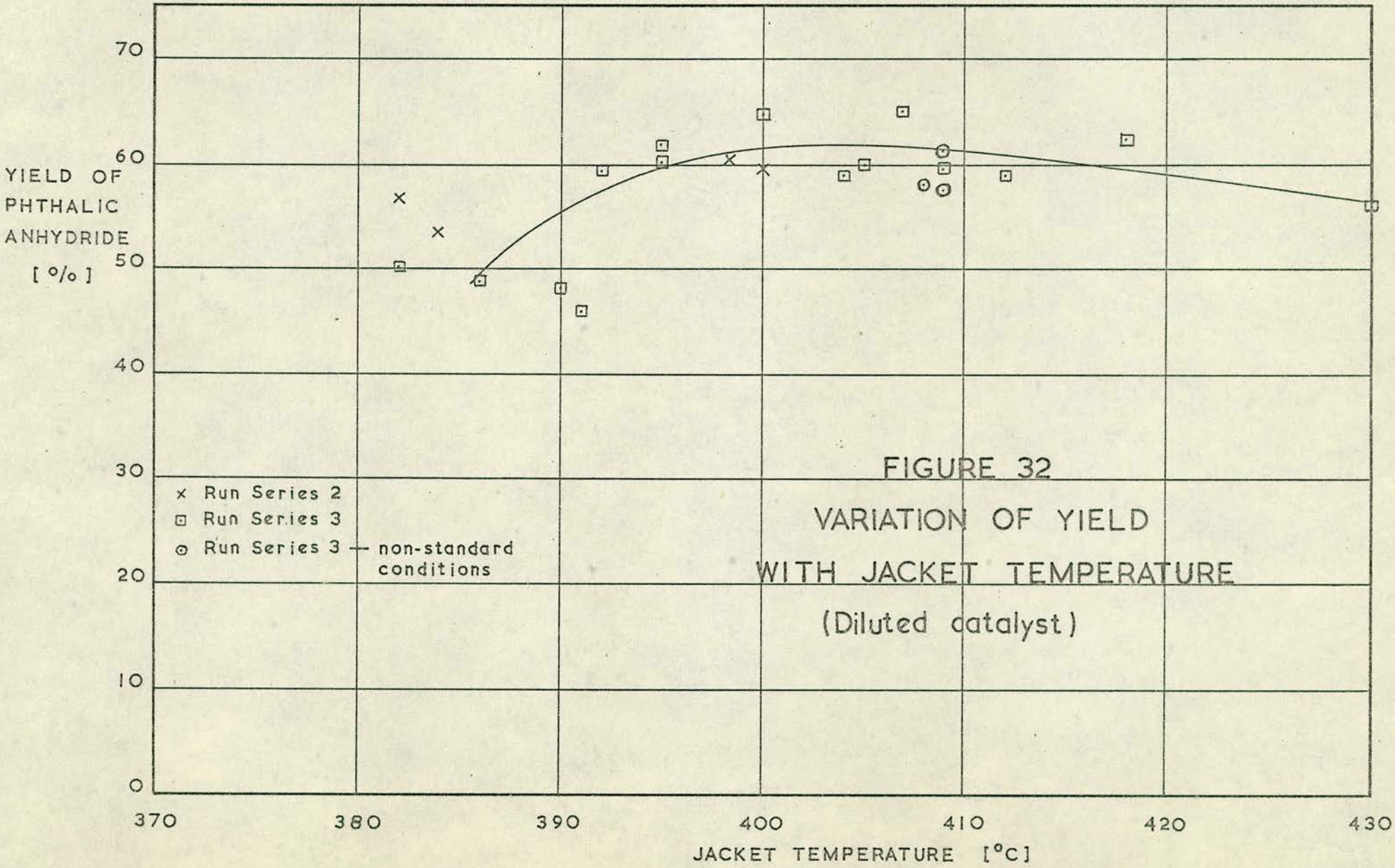

FIGURE 32

VARIATION OF YIELD WITH JACKET TEMPERATURE

(Diluted catalyst)

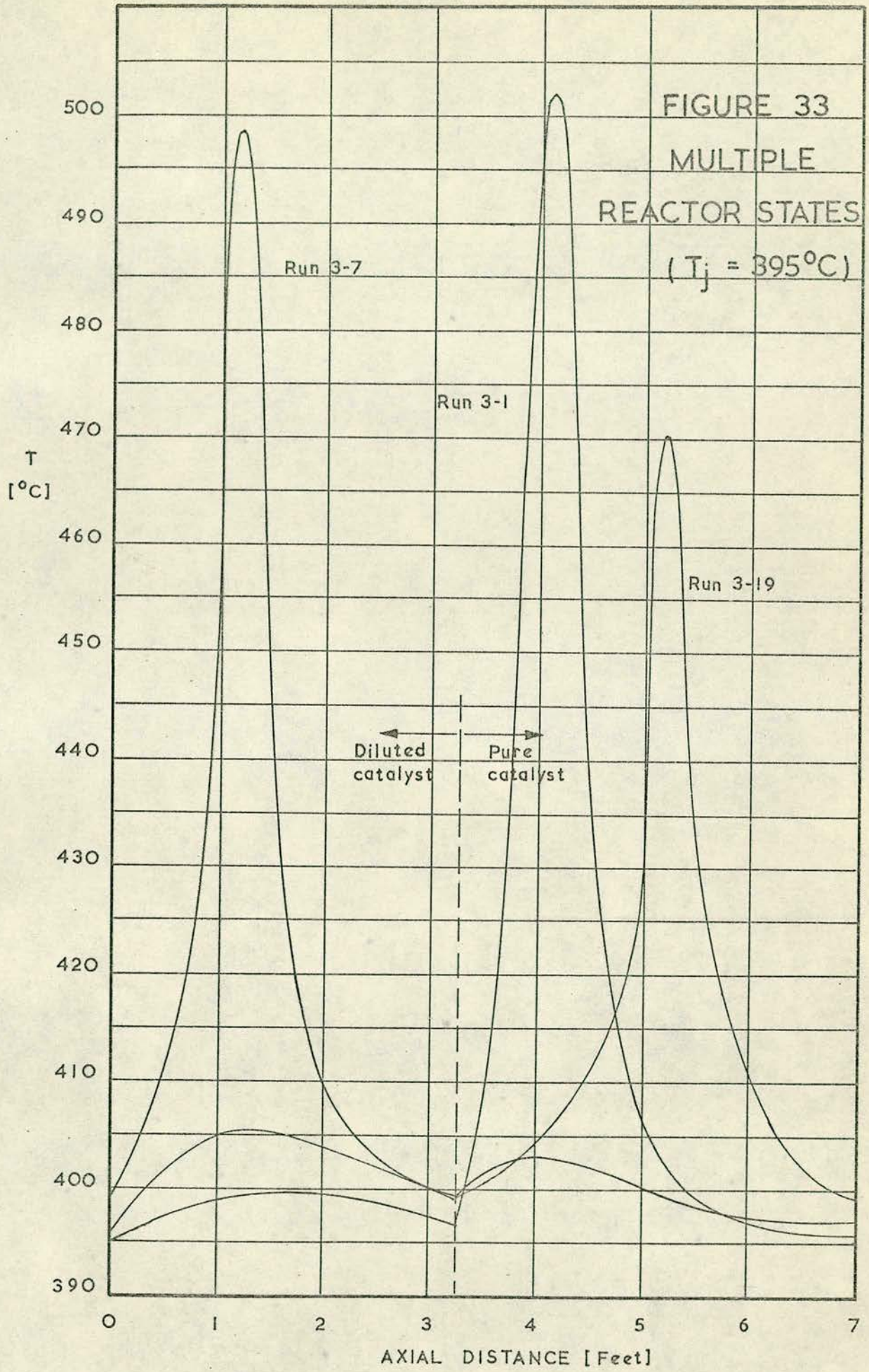
FIGURE 33
MULTIPLE
REACTOR STATES
(T_j = 395°C)
Run 3-7
Run 3-1
Run 3-19
Diluted catalyst
Pure catalyst
T [°C]
500
490
480
470
460
450
440
430
420
410
400
390
0
1
2
3
4
5
6
7
AXIAL DISTANCE [Feet]

it was not necessary to raise the jacket temperature as high as 410°C to achieve ignition. It was found that by continuing to raise the jacket temperature after ignition had occured a peak began to develop in the diluted section and this, of course, killed the peak in the later part of the reactor. In subsequent runs (including 3-7) the peak developed naturally in the diluted section, as if the catalyst had now been activated at that point. This situation persisted so long as the jacket temperature was maintained above about 395°C. Still later, however, the reactor was subjected to a period of prolonged operation with jacket temperatures of 390°C and lower. At first this seemed to extinguish the reaction altogether but gradually the hot spot built up again in the latter part of the reactor. Run 3-19 was performed under these conditions.*

This multiplicity (or at least duplicity) of steady state profiles may well be due to variations in catalytic activity. That variations did occur was seen by examination of the catalyst pellets as they were removed from the reactor. Whereas the fresh catalyst was a bright yellow ochre colour, most of the pellets on withdrawal had darkened to some extent. Some indeed had become blackish-blue in colour: these were principally found at the place where the hot spot formed. After the Series 3 runs some very dark pellets were found at the very beginning of the reactor. (A jacket temperature of 430°C was reached with this catalyst charge). It was interesting to observe that variations in pellet colour occurred quite locally, so that blackish coloured pellets

---

*N.B. The conditions for which the profiles of Figure 33 are drawn are not necessarily those listed in Table 9, which gives only the final conditions under which a sample was taken. (Conditions were often varied in the course of an experimental run.)

were found near pellets almost unchanged in colour.

4.4 Summary of the results

(1) Above a certain critical jacket temperature (about 380°C for an undiluted reactor and perhaps 390°C for a diluted reactor) the yield of phthalic anhydride is approximately 60%. This is virtually independent of jacket temperature, catalyst dilution, flow rate and feed concentration of o-xylene.

(2) There is no evidence that high jacket temperatures are harmful - whether to the yield, the catalyst or the reactor.

(3) In contrast to the yield, the steady state temperature profile is not reproducible. There is strong evidence of multiple steady states.

(4) The catalyst appears to be altered by reaction in a non-uniform manner throughout the reactor.

(5) The dynamic behaviour of the reactor indicates an abrupt variation in the reaction state akin to the ignition and extinction of a flame, albeit much less pronounced.

CHAPTER 5 DISCUSSION OF THE RESULTS

The experimental program had been undertaken with the objective of determining whether a more favourable form of temperature profile could be realised through catalyst dilution - one in which excessively high temperatures were avoided, thus preventing over-oxidation, catalyst deactivation, etc., but where the average temperature level was raised, leading to a higher yield of phthalic anhydride. The results obtained demonstrated conclusively (for the particular catalyst employed) that in the first place high temperatures were essential for phthalic anhydride production, secondly that there appeared to be no serious disadvantages of high temperature operation - the traditional bogeys of phthalic anhydride production failed to materialise, and finally that no improvement in the yield was possible.

In a sense, therefore, the results may be considered disappointing, since the expected advantages were not confirmed. But it is abundantly clear from the results that the behaviour of the catalyst used in these experiments is totally unlike that described by Froment's kinetic data, on which the theoretical predictions were based. The merit or otherwise of catalyst dilution still remains undecided, therefore, since it has clearly been demonstrated that if a catalyst exists to which Froment's data is applicable then its performance can be improved by dilution. On the other hand the present experimental work has served to elucidate some aspects of phthalic anhydride manufacture which have been hitherto undisclosed, if not unknown.

The ignition/extinction phenomena reported in Chapter 4 serve to show that we are here concerned with a catalyst whose activity is so high that the rate of reaction may be, at high temperatures, controlled by the rates of transport of heat and matter between the bulk gas and the active surfaces. (Since the catalyst

in this case has a very low total surface area and was prepared by surface coating, we may be fairly certain that the active surface is largely external to the particle.) For this situation it has been demonstrated that a catalyst particle can (subject to the fulfillment of certain conditions) exist in either of two steady states, thus leading to instability, ignition phenomena, etc. Such behaviour is also well known from work on flames and the autothermal stirred tank reactor. It would seem that Wagner was the first worker to describe the phenomena in catalyst beds[68]; much of the recent work is associated with the name of Wicke[69,70,71]. Petersen gives an account in English[72]. A simple presentation will be given here.

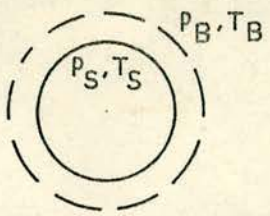

We consider a single first order reaction occurring on a spherical non-porous catalyst particle. Conditions at the surface of the pellet are uniform, as also in the bulk of the gas, but reaction is sufficiently rapid for gradients of temperature and concentration to occur across the film surrounding the particle. There is transfer of the reacting component from the bulk gas to the surface, and of heat from the surface to the surrounding gas. Under steady state conditions the pellet is isothermal, and transport of heat into the pellet may be neglected. (Under non-steady state conditions this is a major factor in determining the dynamic behaviour.)

Let

P_B, P_S = bulk and surface partial pressures of reacting component (atm.)

T_B, T_S = bulk and surface temperatures ($^\circ K$)

K = rate constant for chemical reaction (gm.mols/gm.sec.atm.)

h = film heat transfer coefficient (cals/cm^2sec$^\circ$C)

K_g = film mass transfer coefficient for the reacting component (gm.mols/cm^2sec.atm.)

a = surface area per unit mass of catalyst (cm^2)

ΔH = heat of reaction (cals/gm.mol.)

By mass balance on the reacting component at the steady state

$$K.p_S = K_g.a(p_B - p_S) \qquad (1)$$

therefore

$$p_S (K + K_g a) = K_g a.p_B$$

therefore

$$p_S = \frac{K_g.a.p_B}{K + K_g a}$$

Hence the rate of heat production per unit mass of catalyst is given by Q_P where

$$Q_P = K.p_S(-\Delta H) = \frac{K_g.a.p_B}{K + K_g a}.K.- \Delta H$$

The maximum possible rate of heat production, Q_M, is achieved when $p_S \longrightarrow 0$

therefore

$$Q_M = K_g.a.p_B.- \Delta H$$

therefore

$$Q_P/Q_M = \frac{K}{K + K_g a} = \frac{1}{1 + K_g a/K} \qquad (2)$$

Similarly a heat balance gives

$$Q_R = K.p_S.- \Delta H = h.a(T_S - T_B) \qquad (3)$$

where Q_R is the rate of heat removal per unit mass of catalyst.

Now from above

$$Q_M = K_g.a.p_B.- \Delta H$$

$$= K_g.a.P.\Delta T_{ad}.C_p$$

therefore

$$Q_R/Q_M = \frac{h}{K_g.P.C_p} \cdot \frac{T_S - T_B}{\Delta T_{ad}} \qquad (4)$$

Equations (2) and (4) may be plotted as functions of T_S on the same graph. Equation (2) is an S shaped curve, the function $\frac{1}{1 + K_g a/K}$ tending to zero at low T_S and to unity at high T_S. Equation (4) is linear in T_S, cutting the abscissa at T_B which is conveniently taken to be the origin. The qualitative appearance of the diagram is shown in Figure 34. A single line has been drawn

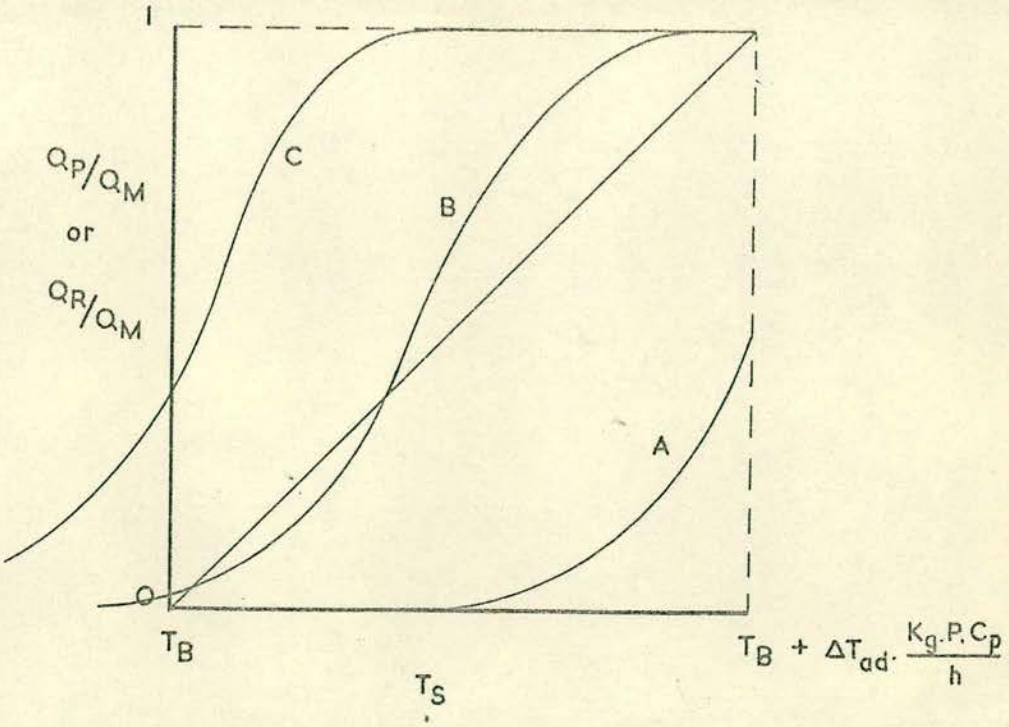

Figure 34

for the heat removal, but three curves labelled A, B and C have been drawn for the heat production to distinguish three different possibilities.

In the case of curve A there is but a single intersection (in the range $T_B \leq T_S \leq T_B + \Delta T_{ad} \cdot \frac{K_g.P.C_p}{h}$) between the curve and the heat removal line. This occurs at $T_S \approx T_B$. Hence there is only one possible solution to the problem and one set of conditions to describe the steady state of the catalyst particle. Since $T_S \approx T_B$ it follows from (3) that $K.p_S$ is small, and hence from (1) that $p_S \approx p_B$. Clearly the situation depicted by the relative positions of Curve A and the heat removal line indicate a low rate of reaction.

With Curve C on the other hand there is again only a single intersection but this occurs with $T_S \approx \Delta T_{ad} \cdot \frac{K_g.P.C_p}{h} + T_B$ It is readily seen from (3) and (1) that $p_S \longrightarrow 0$. We have here a single operating state for the particle with a very high rate of surface reaction. With a very exothermic reaction the surface temperature of the pellet may be some hundreds of degrees above the bulk gas temperature. As noted by Wicke, the surface temperature may exceed the bulk temperature by an amount which is greater or less than the adiabatic temperature rise, according as the factor $\frac{K_g.P.C_p}{h}$ is greater or less than unity(70).

Finally the possibility represented by Curve B shows three intersections with the heat removal line and hence three theoretical stationary operating states for the catalyst pellet. The lower and upper states can readily be identified with those discussed for Curves A and C. The central intersection, however, represents an unstable solution since the slightest displacement of surface temperature leads to an imbalance in the rates of heat production and removal which does not tend to restore the original condition. Thus an increase of surface temperature causes the rate of heat production to exceed that of heat removal, leading to a further rise in surface temperature and eventually bringing the

particle to the upper (stable) condition. Equally a decrease in surface temperature would drop the particle to the lower solution.

In the case of Curve B, therefore, there are two possible operating conditions, but which of these is adopted cannot be determined in the absence of further information. Fairly obviously - by reasoning similar to that which proved the central intersection to represent an unstable solution - the particle will not pass into the upper operating state so long as its temperature is less than T_{crit}, nor will it drop down to the lower state so long as its surface temperature exceeds this value. T_{crit} is, of course, the temperature of the unstable intersection.

The possibility of two steady state conditions for the catalyst pellets means that ignition and extinction phenomena can be observed. This is shown diagrammatically in Figure 35. We imagine a process which raises and lowers in cyclic fashion the bulk temperature of the gas surrounding the pellet (whilst the bulk

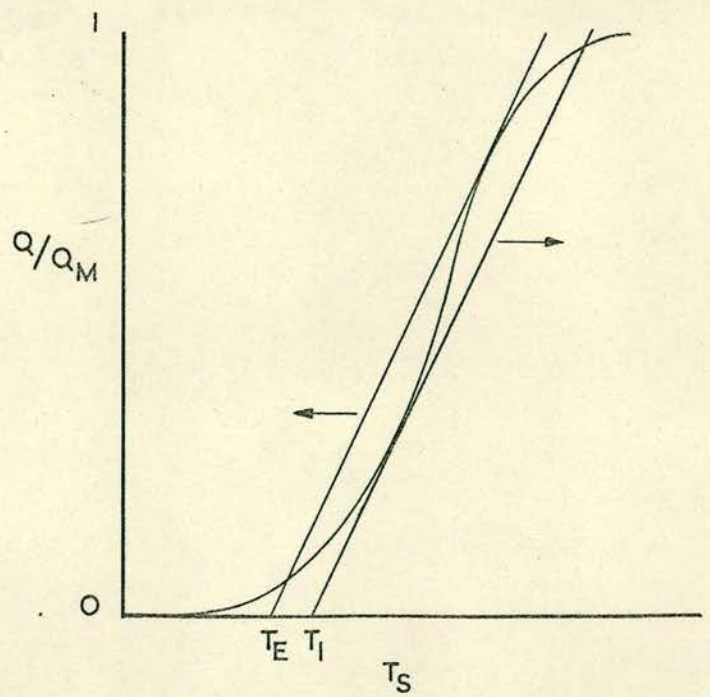

Figure 35

partial pressure of reactant and the mass and heat transfer coefficients are maintained constant). Since the S curve is determined by the surface temperature of the pellet its position on the diagram is unaltered throughout. On the other hand the heat removal line intersects the abscissa at the bulk gas temperature; hence the line is displaced to the right when this temperature is raised and to the left when it is lowered. If we suppose the process to begin with the line passing through the origin then the catalyst pellet is initially in the low reaction state. As the temperature rises the particle remains in this low state until the critical point when the line cuts the abscissa at T_I. Beyond this point only a single intersection of line and S curve occurs - and this is the upper reaction condition. Hence T_I is the ignition temperature above which the catalyst pellets jump to the upper state.

If the bulk gas temperature is now lowered the particle remains in the upper state until eventually - when the heat removal line cuts the abscissa at T_E - only the lower intersection occurs. The particle then returns to the lower operating state, and T_E is the extinction temperature. Clearly the degree of hysteresis, i.e. the amount by which T_I exceeds T_E, depends on the relative slopes of the heat removal line and the central portion of the S curve.

We may now attempt a quantitative application of this theory to o-xylene oxidation, but we immediately encounter certain difficulties. In the first place the experimental observations refer to a catalyst packed reactor whereas the theory applies to a single catalyst pellet. We must avoid assuming that the extinction and ignition behaviour will be identical for these two situations: nevertheless some comparison is possible. It will be fairly safe to assume that the conversion in an unignited reactor is not much above 15% at the outlet - the largest measured conversion was 17.9%

- and hence not much above 8% at the point of maximum reactor temperature. It also seems very reasonable to suggest that the reaction will always ignite at (or very near to) the point of maximum temperature. Hence we should be able to deal with reactor ignition by applying the single pellet theory to the point of maximum temperature with the assumption that the bulk partial pressure of reactant at that point is equal to the initial value with an accuracy which is probably better than 10%. An examination of Figure 22 suggests that the ignition temperature for the reactor was approximately 415°C. (The jacket temperature was 387°C; the peak temperature just prior to ignition was about 28°C above the jacket temperature.) By analogy with the ignition temperature it is suggested that the extinction temperature for a packed reactor is the bulk temperature immediately upstream of the first ignited particle at the moment of extinction: this temperature should be substantially unaltered by the action of extinction (there will be a slight drop due to the cessation of heat backmixing), and should be the same as the maximum reaction temperature after extinction. An examination of Figure 27 suggests that the reaction extinction temperature is 405°C (T_j = 376°C; T_{max} after extinction = 29°C above T_j).

A more fundamental difficulty is the fact that the theory applies to a single reaction, whereas the experimental results refer to an unknown number of reactions with possibly temperature dependent selectivities. However, the results obtained with the reactor in the ignited condition indicate that at least at the higher temperatures the selectivities are not temperature dependent - the yield being remarkably constant at about 60%. The nature of the secondary products is not known, even at high temperatures, but the general conclusion drawn from the results of other workers is that they are largely carbon oxides (see Chapter 1). The

assumption is therefore made that at high temperatures 60% of the o-xylene reacts to phthalic anhydride and the remaining 40% is burned to a mixture of CO and CO_2. (At lower temperatures the relative rates of these reactions are assumed not to vary, but the reactor may no longer suffice to convert all of the o-xylene.) Now the measurements of oxygen content of the gas leaving the reactor (at high yield conditions) were very uniform in several different runs at 16.95% by volume. At this level, and with the assumptions just quoted, it can be shown (Appendix 7) that all of the CO and CO_2 product must, in fact, be carbon monoxide. Although this is hardly likely to be the case (there is probably a mixture of CO, CO_2 and less oxidized products) it provides a reasonable basis for calculating the mean heat of reaction: as a crude approximation we may reckon the heat of reaction to be proportional to the amount of oxygen consumed and independent of the nature of the products. The mean heat of reaction was estimated to be 359.3 Kcal/gm.mole o-xylene (Appendix 7).

Not only are we ignorant of the exact nature of the reactions occurring in the reactor, we also have no idea of the magnitudes of the rate constants. For the sake of consistency with earlier calculations we shall employ Froment's kinetic data, adding together the terms for phthalic anhydride production and the direct formation of carbon oxides (as was done in preparing Figure 3), but ignoring the further oxidation of phthalic anhydride.

Finally we need to obtain values for the parameters $K_g.a$ and $\frac{h}{K_g.P.C_p}$, which appear in equations (2) and (4) respectively. Using the correlations of Hougen[73] these were calculated to be (Appendix 8);

$$K_g.a = 1.43 \times 10^{-3} \text{ gm.mols/gm.sec.atm.}$$

$$\frac{h}{K_g.P.C_p} = 2.29$$

Note Added, 22.4.1971

Professor G.F. Froment has expressed doubts about the explanation of the phenomenon of ignition in terms of multiple steady states arising from transport limitation. He suggests the following two possible explanations:

(1) All catalysts have an operating range outside which they are ineffective. For example, the catalyst which he employs for o-xylene oxidation is ineffective below 330°C and gives results of poor reproducibility when close to that limit. It might be that the catalyst used here has a lower limit of about 415°C and the ignition phenomenon is a consequence of the sudden improvement in activity at that temperature.

(2) The ignition phenomenon may be viewed as a temperature runaway in the usual sense of the term.

I accept that these explanations are not unreasonable and I do not think that either can be completely disproved at the present time. However, I am not inclined to accept them as complete explanations for the ignition phenomena for the following reasons:

(1) Calculations show that a reasonable choice of parameters for the system would lead to multiple steady states, with an ignition temperature for the reactor at approximately the value observed experimentally. To escape the conclusion that transport phenomena are important it must be demonstrated that the choice of parameters was not reasonable and neither of Professor Froment's explanations does this.

(2) Yields of phthalic anhydride of up to 20% were achieved with maximum reactor temperatures below 415°C. (See Table 9). Hence the catalyst does show appreciable activity below the reactor ignition temperature.

(3) A temperature runaway in the usual sense of the term does not imply that these exists a forbidden operating region

Table 10 was prepared from the above data and the results are plotted as the stability diagram of Figure 36. Considering the uncertainties involved in evaluating the rate constant and the heat of reaction this diagram shows a remarkable concordance between the observed and calculated conditions for reaction ignition and extinction. The calculated extinction/ignition range is seen from the diagram to be 435-440°C (with very little hysteresis), compared with the values estimated from the experimental work of 405-415°C.

This result, it is suggested, places beyond question the applicability of the theory to the experimental findings. There are, however, a number of factors which are not satisfactorily accounted for by the treatment so far: the lack of reproducibility as regards temperature profiles and the jacket temperatures necessary for ignition/extinction, the colour change of the catalyst pellets, and, most stringly, the failure of the reactor to perform at temperatures in the 350-380°C range. Froment's kinetic data suggests that the reactor will ignite at 440°C: it ignites in practice at 415°C. Clearly the catalyst is more active than suggested by Froment's data. Why therefore, does the reactor not give good yields at 350-380°C when theory (again based on Froment's data) suggests high yields?

Another unsatisfactory aspect of the theory is its failure to account for the observed independence of the temperature profile on the bulk partial pressure of xylene during start-up (i.e. in the low reaction state). The rate of heat production is proportional to $K.p_S$, and according to the theory

$$p_S \approx p_B$$

in the low reaction state. Hence a cut of 50% in p_B should have a

intermediate between the non-runaway and the runaway conditions. Any intermediate temperature profile can be achieved (although parametric sensitivity may render this difficult in practice.) In the present study, however, there did undoubtedly appear to be a forbidden operating region such that temperature profiles with excess temperatures of 30-90^{o}C could not be achieved under steady state conditions. Moreover, the temperature profile in the reactor just before ignition had no appearance of being on the verge of temperature runaway - there was no point of inflexion.

Table 10 Data for the stability diagram of a single pellet for xylene oxidation

Temperature (°C)	Rate Constant - K (gm.mols/gm.sec.atm)	$K_g a/K$	Q_P/Q_M	Q_R/Q_M
380	2.45×10^{-5}	58.5	0.0168	0.000
420	8.15×10^{-5}	17.55	0.054	0.196
460	2.40×10^{-4}	5.96	0.1439	0.392
500	6.25×10^{-4}	2.29	0.304	0.588
540	1.50×10^{-3}	0.954	0.512	0.785
580	3.30×10^{-3}	0.433	0.698	0.980
600	4.75×10^{-3}	0.303	0.767	-
620	6.70×10^{-3}	0.214	0.823	-

$$Kg.a = 1.43 \times 10^{-3} \text{ gm.mols/gm.sec.atm.}$$

$$\frac{h}{Kg.P.Cp} = 2.29$$

$$\Delta T_{ad} = \frac{359.3 \times 0.00970}{7.45} = 468^{\circ}C$$

$$(T_S - T_B)_{max} = \frac{468}{2.29} = 204^{\circ}C$$

T_B has been taken as 380°C in calculating Q_R/Q_M.

There is a discrepancy between Table 10 and Figure 36. The last column of Table 10 represents the heat removal line which would pass through the origin of Figure 36.

FIGURE 36

STABILITY DIAGRAM FOR XYLENE OXIDATION

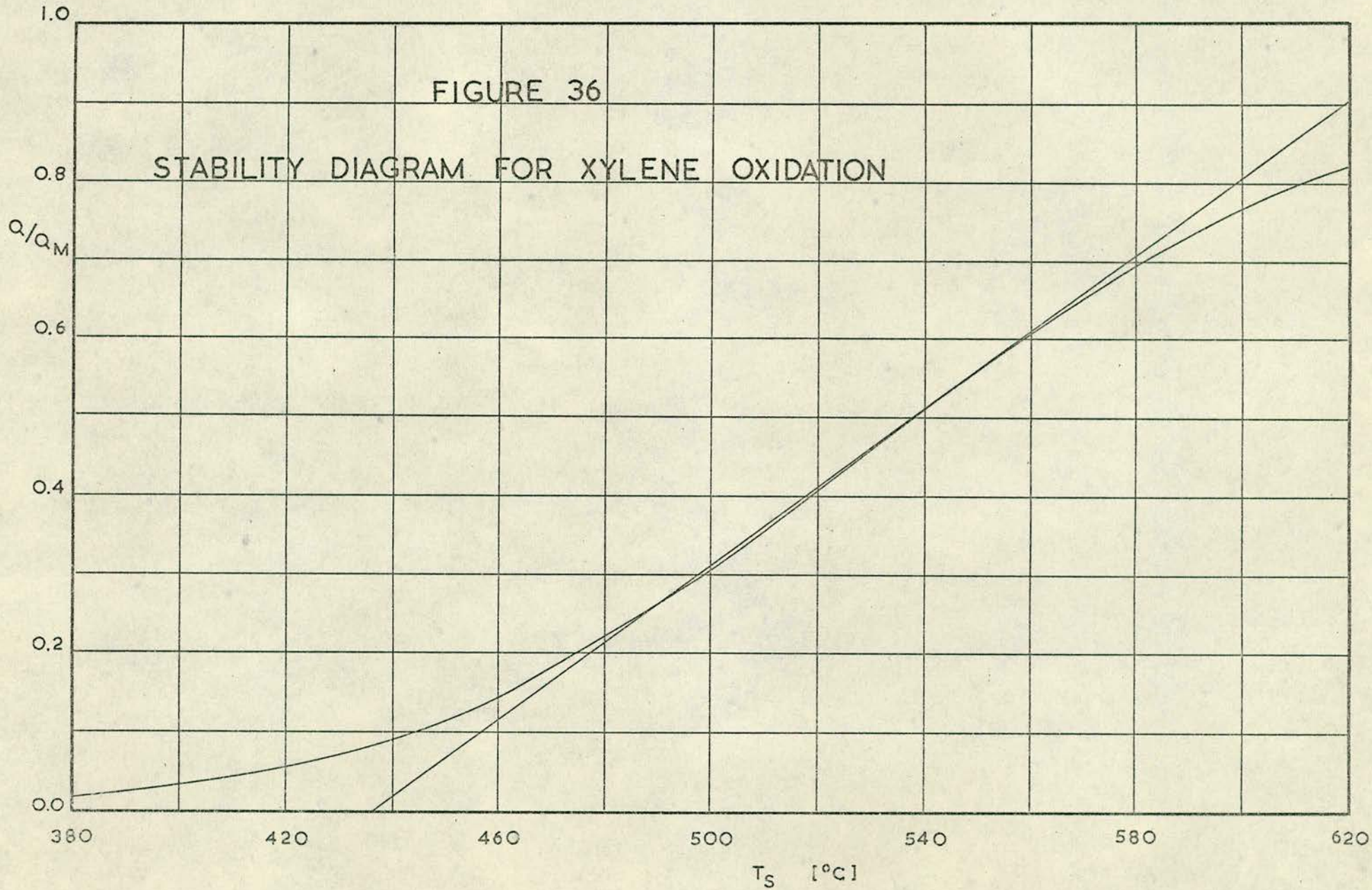

profound effect on the temperature profile.

Taking these four difficulties together there appears to be only one explanation which can account for them all. (It would be possible to explain the failure of the reactor to perform at low temperatures by suggesting that the simplified reaction scheme fails under these conditions, and that some reaction such as

Tolualdehyde ⟶ Phthalic anhydride

does not occur appreciably below about 380°C. There may well be some truth in this hypothesis, and it would be worthwhile investigating it in future work, but it fails to offer any explanation of the other difficulties). It is suggested that the theory fails to take account of the important changes taking place in the catalyst itself under the varying conditions of temperature and reactant concentration. These changes are, of course, the variations in the state of oxidation of the catalyst surface that have been shown to occur in much of the published literature (see Chapter 1). If we amplify the simple theory by allowing for a surface re-oxidation we can then account for

(1) Colour changes in the catalyst by varying oxidation states.

(2) Lack of reproducibility in the temperature profiles, etc. by the fact that the catalyst activity is now a variable quantity determined by the pre-history of the reactor.

(3) Failure to perform at low temperatures due to the fact that the catalyst is then largely in a reduced condition.

(4) Independence of the temperature profile on the bulk partial pressure of reactant in the low reaction state by the reduced condition of the catalyst - the re-oxidation of the catalyst being rate controlling

The suggested modification to the theory will now be presented.

Let

S = fraction of the potentially active catalyst surface in the oxidized state

K^* = rate constant for the re-oxidation of the catalyst surface (assumed 1st order)

N = number of oxygen molecules required to oxidize one hydrocarbon molecule

p_{O_2} = partial pressure of oxygen. Since oxygen is present in excess this will be assumed not to vary between the bulk gas and the catalyst surface.

With the other notation as earlier defined we have, under steady state conditions

$$K.p_S.S = K^*.p_{O_2}(1 - S)/N = K_g.a(p_B - p_S) \qquad (5)$$

therefore

$$S = \frac{K^*.p_{O_2}}{K^*.p_{O_2} + N.K.p_S} \qquad (5a)$$

therefore

$$K.p_S.S = \frac{K^*.p_{O_2}.K.p_S}{K^*.p_{O_2} + N.K.p_S}$$

$$= \frac{1}{\frac{1}{K.p_S} + \frac{N}{K^*.p_{O_2}}} = K_g.a(p_B - p_S) \qquad (6)$$

By a heat balance

$$K.p_S.S. - \Delta H = h.a(T_S - T_B) \qquad (7)$$

Combining (5) and (7)

$$-\Delta H = \frac{h.(T_S - T_B)}{K_g(p_B - p_S)}$$

or

$$p_B - p_S = \frac{h}{K_g. - \Delta H}.(T_S - T_B)$$

Substituting in equation (6) we obtain

$$\frac{1}{\dfrac{1}{K\left[p_B - \dfrac{h}{K_g.-\Delta H}(T_S - T_B)\right]} + \dfrac{N}{K^*.p_{O_2}}} = \frac{h.a(T_S - T_B)}{-\Delta H} \qquad (8)$$

Dividing through by $K_g.a.p_B$

$$\frac{1}{\dfrac{p_B}{R_1\left[p_B - \dfrac{h}{K_g.-\Delta H}(T_S - T_B)\right]} + \dfrac{p_B}{R_2.p_{O_2}}} = \frac{h}{K_g.P.C_p}.\frac{T_S - T_B}{\Delta T_{ad}}$$

where $R_1 = K/K_g.a$

$R_2 = K^*/K_g.a.N$

This may be finally simplified to

$$\frac{1}{\dfrac{1}{R_1(1 - J)} + \dfrac{p_B}{R_2.p_{O_2}}} = J \qquad (9)$$

where $J = \dfrac{h}{K_g.P.C_p}.\dfrac{T_S - T_B}{\Delta T_{ad}}$

The right hand side of (9) is identical with the heat removal line of equation (4). The left hand side corresponds to the heat production curve of equation (2) and reduces to it when $R_2 \rightarrow \infty$. Hence we may construct the stability diagram for a single particle by plotting the two sides of (9) as functions of T_S at given values of p_B and p_{O_2}.

This has been done in Figure 37 for the following set of data:

$K = 8.439 \times 10^4 \exp(-27,100/RT)$ gm.mols/gm.sec.atm.

$K^*/N = 3.972 \times 10^5 \exp(-33,200/RT)$ gm.mols/gm.sec.atm.

$K_g.a = 1.43 \times 10^{-3}$ gm.mols/gm.sec.atm.

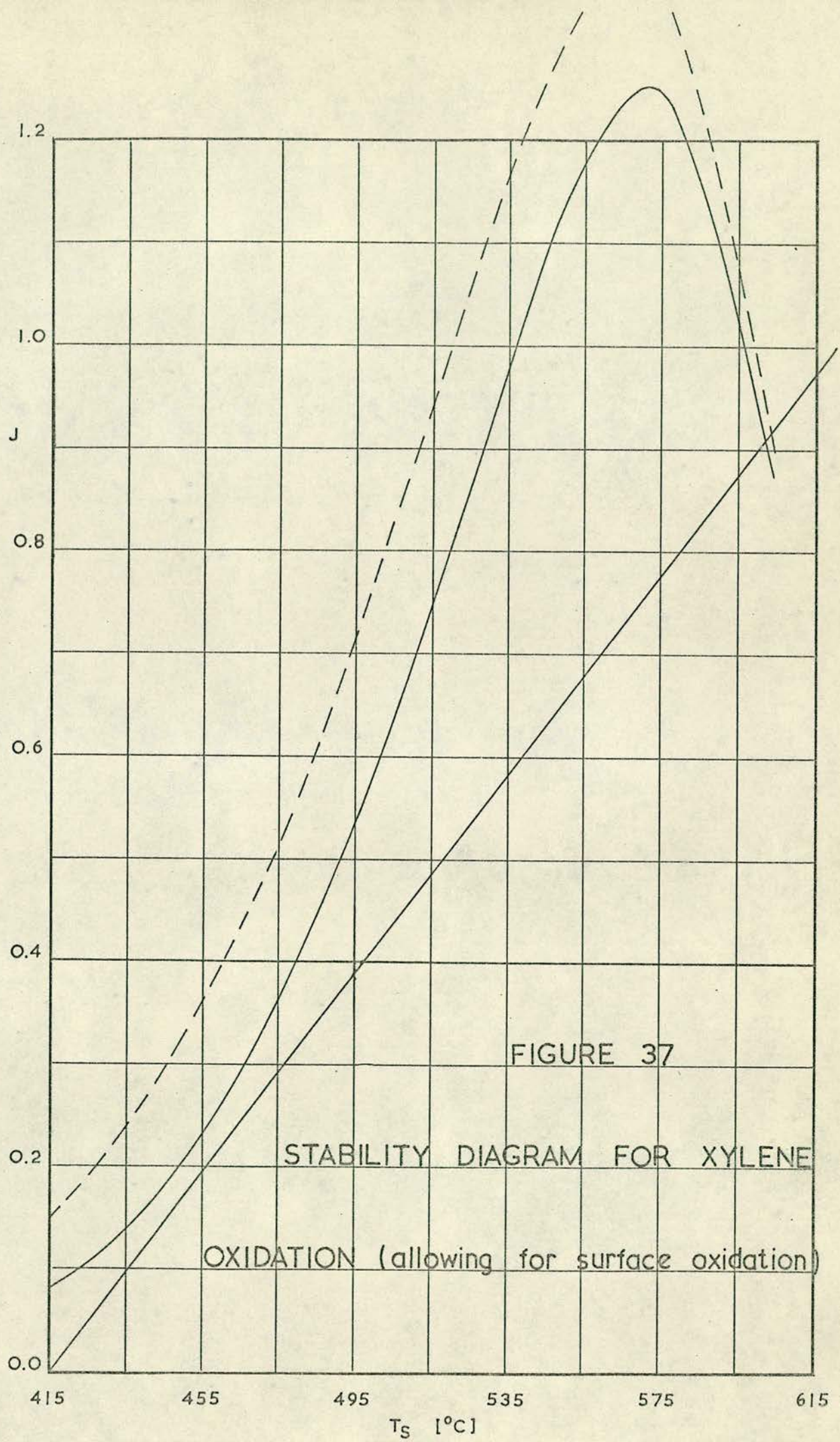

FIGURE 37

STABILITY DIAGRAM FOR XYLENE OXIDATION (allowing for surface oxidation)

$$\frac{h}{K_g.P.C_p} = 2.29$$

$$p_B = 0.0097$$

$$p_{O_2} = 0.200$$

The bulk gas partial pressures therefore correspond with those used experimentally at the reactor inlet before ignition. The value of K has been chosen so that the catalyst activity for o-xylene conversion is three times greater than in Froment's data. This choice (which is by no means unreasonable - see the spread of values in Figure 3) in conjunction with the arbitrarily selected value for K^*/N results in an ignition temperature of about 410°C (see Figure 37) in line with the experimental findings.

For the sake of comparison, the dotted curve in Figure 37 indicates the result obtained when $R_2 \longrightarrow \infty$, i.e. the surface is always fully oxidized. The ignition temperature is seen to be lower for this case, as one would expect, and the two curves merge at the right hand side of the scale when the rate is largely controlled by mass and heat transfer.

(It must be pointed out, incidentally, that the form of the function plotted in Figure 37 is not identical with that of Figure 36. This is best seen by considering the left hand side of equation 9 as $R_2 \longrightarrow \infty$. We have

$$\text{L.H.S.} \longrightarrow R_1(1 - J) \text{ as } R_2 \longrightarrow \infty$$

so that equation (9) reduces in this case to

$$R_1(1 - J) = J \qquad (10)$$

This could also be expressed in the form

$$\frac{1}{1 + 1/R_1} = J \qquad (11)$$

In Figure 37 we have plotted what is equivalent to the two sides of

equation (10)whereas in Figure 36 we have plotted the two sides of equation (11), which is the method usually adopted in the literature. This latter approach, however, is not suitable when surface re-oxidation is included.)

It is of interest to consider the effect of varying the bulk partial pressure of xylene at low temperatures. We may calculate the effect of a 50% increase in bulk partial pressure at a temperature of 380°C.

At 380°C: $K = 7.35 \times 10^{-5}$ gm.mols/gm.sec.atm.

$K^*/N = 3.15 \times 10^{-6}$ gm.mols/gm.sec.atm.

Now at low temperatures $p_S \approx p_B$ and hence from (5a)

$$S = \frac{(K^*/N).p_{O_2}}{(K^*/N).p_{O_2} + K.p_B}$$

$$= \frac{1}{1 + \frac{7.35 \times 10^{-5} \times 0.0097}{3.15 \times 10^{-6} \times 0.200}}$$

$$= \frac{1}{1 + \frac{7.13 \times 10^{-7}}{6.30 \times 10^{-7}}}$$

$$S = 0.470$$

Hence the rate of reaction, r_1, is given by

$$r_1 = 0.470.K.p_B$$

Now if the partial pressure is increased by 50% the new value of S is

$$S = \frac{1}{1 + (1.5 \times \frac{7.13}{6.30})} = 0.370$$

and the new rate of reaction becomes

$$r_2 = 0.370.K.(1.5p_B)$$

therefore

$$r_2/r_1 = \frac{0.370 \times 1.5}{0.470} = 1.18$$

Hence a 50 % increase in the partial pressure of xylene has caused only an 18% increase in reaction rate. This behaviour is similar to, but less pronounced than, the experimentally observed behaviour. It would seem from these calculations that a rather larger energy of activation for the re-oxidation reaction is called for, so that the surface is almost entirely reduced at 380°C under operating conditions. This would render the overall rate of reaction totally insensitive to changes in xylene partial pressure and (notwithstanding the threefold increase in catalytic activity above Froment's value) also give an overall rate of reaction at low temperatures which is very much less than that used in previous theoretical calculations based on Froment's kinetics.

The catalyst oxidation concept appears therefore to be a useful addition to the reaction model, although firm data for the rate of this process is lacking. The activation energy has been variously quoted as low as 23.6 K.cal/gm.mole[21] and as high as 45 K.cal/gm.mole[24]. As shown by Simard et al.[24], the activation energy will vary depending on which oxide form is involved. The selected value of 33.2 K.cal/mole used in preparing Figure 37 seemed a reasonable compromise. As far as the actual magnitude of K^*/N is concerned, Froment and Herten[21] give

$$K^*/N = 9.67 \times 10^{-6} \text{ gm.mols/gm.sec.atm. at } 402°C$$

compared with the value used here of

$$K^*/N = 7.3 \times 10^{-6} \text{ gm.mols/gm.sec.atm. at } 402°C$$

It may be noted that although Herten and Froment quote

a low value for the activation energy of re-oxidation, the value they give for the activation energy of xylene oxidation is even lower (E = 16.23 K.cal/gm.mole). The question of the relative magnitudes of these activation energies is quite important, since the catalyst behaviour would be quite different according as E^* is greater or less than E. If $E^* < E$ the reaction should go well at low temperatures but be limited by re-oxidation at high temperatures - a type of behaviour certainly not found in the present study. Juusola, Mann and Downie[23] do in fact report

$$E = 28{,}000 \text{ K.cal/mole}$$
$$E^* = 26{,}000 \text{ K.cal/mole}$$

but their experimental work was at abnormally low temperature with only tolueldehyde as major reaction product.

It would be of interest to compare the dynamic behaviour found with the xylene oxidation reactor with that observed in other studies. However, the only work known to the author is that of Wicke and Padberg[71] on carbon monoxide oxidation, but as this was carried out in a adiabatic reactor only a limited comparison is possible. The general observations made by Wicke and Padberg are confirmed by the present work: that is to say, ignition and extinction phenomena were observed in both cases. In their studies on the "long" catalyst bed (37 cm.) these authors found that on dropping the inlet temperature to an already ignited reactor the temperature step remained more or less stationary near the entrance over quite a large range but then moved sharply downstream. For example, they started with an inlet temperature of 153°C which was dropped to 128°C with virtually no effect on the position of the temperature step. At 118°C the profile detached itself from the entrance and moved downstream. The authors believed that it would

have adopted a stationary position at a greater distance from the entrance than the length of their catalyst bed. This behaviour is similar to that found here with xylene oxidation: on dropping the jacket temperature the peak remained fairly stationary at first but then moved sharply downstream. In this case, however, there was no doubt that this movement was the commencement of a total extinction of the reaction: the peak declined in magnitude and moved with ever increasing velocity. One might be inclined to doubt Padberg and Wicke's assertion that the peak would eventually have become stationary in a bed of sufficient length but for the fact that with even lower temperatures (down to 74°C) they were able to obtain stationary temperature steps at arbitrary positions in the catalyst bed - a fact which negates any suggestion of reaction extinction.

Hence the fact emerges that with adiabatic CO oxidation it was possible to achieve stable operation with the temperature step at a variety of places in the reactor; with xylene oxidation in a non-adiabatic reactor the peak was always close to the entrance under stable conditions. One would guess that this difference is due rather to the adiabatic as opposed to non-adiabatic operation rather than peculiarities of the reaction or catalyst. Presumably once the temperature peak in a non-adiabatic reactor moves beyond a certain point from the entrance the depletion of reactant and heat losses prior to that point become such that the upper operating state can no longer be attained.

Another difference between the present results and those of Padberg and Wicke is the occurrence of the "pseudo-steady state" induction period with o-xylene oxidation. No comparable phenomenon appears to have been noticed with CO oxidation. In this case the effect can probably be attributed to a slow inter-

action between rising temperature and the state of the catalyst surface. With a start-up at moderately low temperatures the catalyst will be initially reduced when the xylene feed is introduced to the reactor: with rising temperature the surface slowly re-oxidizes resulting in an ever increasing activity.

CHAPTER 6 CONCLUSIONS AND SUGGESTIONS FOR FURTHER WORK

1. It has been shown that a suitable policy of catalyst dilution is theoretically advantageous in the production of phthalic anhydride from o-xylene when the kinetics of the reaction are broadly as given by Froment[10] and transport processes are not rate determining. The experimental work failed to confirm this conclusion since the chosen catalyst had an activity such that the transfer of heat and mass between the bulk gas and the external surface assumed great importance.

   It would be of interest to investigate other catalysts for o-xylene oxidation (or possibly for quite different reaction schemes) to determine whether the theoretical advantages of dilution can be realised in practice.

2. The dynamic and steady state behaviour of the experimental reactor has been explained qualitatively by reference to the ideas of Wagner and Wicke (among others), according to which a catalyst pellet may exhibit more than a single steady state under given external conditions. This theory has been applied to a single catalyst particle and has been extended to include the surface re-oxidation concept of Mars and van Krevelen.

   It would be of interest to make precise measurements of the kinetic and transport parameters to replace the somewhat arbitrary values used in the development of the theory. The theory itself could be extended so as to develop a model of the fixed bed reactor, the dynamic and steady state behaviour of which could be compared with experimental observations.

   On the basis of the present theory the difference between the American and German types of catalyst might be explained by an increased rate of surface re-oxidation for

the latter type, so that it became active at a lower temperature. An experimental program might be initiated to check whether this is in fact so and also to find out whether the multiple steady state phenomena are ever encountered with German type catalysts. It may be that by virtue of the lower operating temperature the possibility of multiple states does not normally exist for these catalysts. (This is suggested by the calculations of Chapter 5 on the unmodified data of Froment, which showed an ignition temperature of 440°C - well above the normal operating range for a German catalyst.) One also wonders whether there is any real difference in the activities of the two basic types for hydrocarbon oxidation per se, or whether the difference is entirely in the rate of surface re-oxidation.

An alternative explanation for the difference between the two catalyst types in the 350-390°C range is to postulate that defect mobility in the bulk catalyst is necessary in order for the reaction to proceed, and that doping the catalyst with K_2SO_4 has the effect of lowering the Tamman temperature by 30-40°C. This suggestion is not, of course, included in the theory outlined in Chapter 5 but is worthy of further consideration.

3. The yield of phthalic anhydride obtained from the experimental reactor proved to be remarkably insensitive to conditions of temperature (above a certain critical level), flow rate and xylene concentration.

Further experimental work might be performed to determine how far reaction conditions may be altered without suffering a loss in yield. For example it might be possible

to substantially increase the reactor throughput. Also, if the yield is as independent of temperature as suggested here, it might be permissible to operate with reactors of two inch or even greater diameter. This would provide a great saving in the capital cost of the reactor.

Since the yield is temperature independent over a wide range there is a strong suggestion that the reaction can be represented as

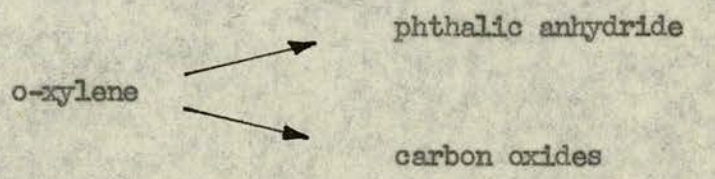

with similar or identical activation energies for the two reactions. One would therefore like to know what, if anything, will influence the selectivity of these two reactions. Is the state of oxidation of the surface the major factor? Is it simply a question of a steric effect, whereby the orientation of the o-xylene molecule striking the surface determines the nature of the reaction products? Are hydrocarbons (or hydrocarbon fragments) adsorbed more strongly on to a reduced surface than an oxidized surface, so that once adsorbed they may only escape after total oxidation?

4. In view of the obvious advantage of the fluid bed reactor (increased hydrocarbon:air ratio) it would be worth examining the implications of the present study for fluid bed operation. It is not difficult to imagine what might have gone wrong with previous attempts to operate a fluid bed reactor. One would probably attempt to start up with a low hydrocarbon concentration and a temperature about the same or slightly above the jacket temperature employed for fixed bed operation. Some reaction

would occur but at such low temperatures the catalyst would probably be reduced, especially if the hydrocarbon:air ratio were brought up to the desired operating level. As with the present work the reaction products would be under-oxidized and the conversion would be low. One might then try raising the reaction temperature, but because of the increased mass transfer coefficient the ignition temperature would be higher than for fixed bed operation. (This is readily seen by inspection of equations (2) and (4) in Chapter 5.) In consequence the reaction might either not ignite at all or alternatively the temperature achieved when ignition finally did occur might be excessively (and disastrously) high.

The above is, of course, purely speculative, but if one could establish the pattern of behaviour in the fluidized bed reactor this would be a major step towards operating such a reactor successfully.

APPENDIX 1 DERIVATION OF THE EQUATIONS BY WHICH THE YIELD AND SELECTIVITY FOR PHTHALIC ANHYDRIDE MAY BE CALCULATED FOR AN ISOTHERMAL REACTOR EMPLOYING FROMENT'S KINETIC DATA

Let

F' = total molar flow rate

N_A = mole fraction of o-xylene in feed

W = weight of catalyst

x = yield of phthalic anhydride

y = total conversion of o-xylene

The reaction scheme is

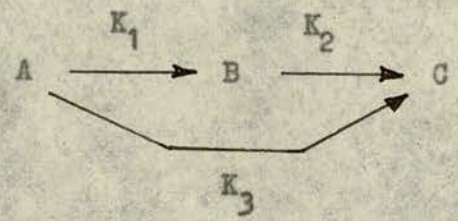

where the K's represent the 1st order rate constants and B represents phthalic anhydride.

For the disappearance of o-xylene we may write

$$F'.N_A.dy = (K_1 + K_3).N_A.P.(1 - y).dW$$

P represents the total pressure which we take to be 1 atmosphere.

Therefore

$$\int_0^y \frac{dy}{1 - y} = \int_0^W \frac{(K_1 + K_3).dW}{F'}$$

Therefore

$$1 - y = e^{\frac{-(K_1 + K_3)W}{F'}} = e^{-R.W} \qquad (1)$$

where

$$R = \frac{K_1 + K_3}{F'}$$

For the net rate of production of phthalic anhydride we have

$$F'.N_A.dx = N_A.\left[K_1(1 - y) - K_2.x\right] dW$$

$$= N_A.\left[K_1.e^{-R.W} - K_2.x\right] dW$$

Therefore

$$\frac{dx}{dW} + \frac{K_2}{F'}.x = \frac{K_1}{F'}.e^{-R.W}$$

This is a standard linear 1st order differential equation whose solution is

$$x.e^{P.W} = \frac{K_1}{F'.(P - R)}.e^{(P - R).W} + A$$

where

$P = K_2/F'$ and A is a constant of integration.

Now when $W = 0$, $x = 0$ and hence

$$0 = \frac{K_1}{F'(P - R)} + A$$

therefore

$$x.e^{P.W} = \frac{K_1}{F'.(P - R)}.\left[e^{(P - R).W} - 1\right]$$

which reduces to

$$x = \frac{K_1}{K_1 + K_3 - K_2}.\left[e^{-P.W} - e^{-R.W}\right] \qquad (2)$$

Equation (2) gives us the yield of phthalic anhydride for a given flow rate, F', and weight of catalyst, W, in terms of the known rates constants. The weight of catalyst required to maximize the yield, W_{max}, may be found by differentiating (2) with respect to W and equating to zero.

$$\frac{dx}{dW} = \frac{K_1}{K_1 + K_3 - K_2}.\left[-P.e^{-P.W} + R.e^{-R.W}\right]$$

which is zero if

$$P.e^{-P.W} = R.e^{-R.W}$$

or

$$e^{(R - P).W} = R/P$$

$$(R - P).W = \log_e(R/P)$$

therefore

$$W_{max} = \frac{F'}{K_1 + K_3 - K_2}.\log_e\left(\frac{K_1 + K_3}{K_2}\right) \qquad (3)$$

The value of the maximum possible yield, x_{max}, may be obtained by substituting equation (3) into (2).

$$x_{max} = \frac{K_1}{K_1 + K_3 - K_2}.\left[e^{-\frac{P.F'}{K_1 + K_3 - K_2}.\log_e\left(\frac{K_1 + K_3}{K_2}\right)} - e^{-\frac{R.F'}{K_1 + K_3 - K_2}.\log_e\left(\frac{K_1 + K_3}{K_2}\right)}\right]$$

therefore

$$x_{max}.e^{\frac{K_2}{K_1 + K_3 - K_2}.\log_e\left(\frac{K_1 + K_3}{K_2}\right)} = \frac{K_1}{K_1 + K_3 - K_2}\left[1 - e^{-\log_e\left(\frac{K_1 + K_3}{K_2}\right)}\right]$$

$$= \frac{K_1}{K_1 + K_3 - K_2}\left[1 - \frac{K_2}{K_1 + K_3}\right]$$

$$= \frac{K_1}{K_1 + K_3}$$

therefore

$$x_{max} = \frac{K_1}{K_1 + K_3}.e^{-\frac{K_2}{K_1 + K_3 - K_2}.\log_e\left(\frac{K_1 + K_3}{K_2}\right)}$$

$$x_{max} = \left(\frac{K_1}{K_1 + K_3}\right).\left(\frac{K_2}{K_1 + K_3}\right)^{\frac{K_2}{K_1 + K_3 - K_2}} \qquad (4)$$

The total conversion corresponding to x_{max} is given by combining equations (1) and (3):

$$y = 1 - e^{\frac{-K_1 + K_3}{K_1 + K_3 - K_2} \cdot \log_e \left(\frac{K_1 + K_3}{K_2}\right)}$$

$$y = 1 - \left(\frac{K_2}{K_1 + K_3}\right)^{\frac{K_1 + K_3}{K_1 + K_3 - K_2}} \qquad (5)$$

Hence the selectivity at maximum conversion for phthalic anhydride is

$$\frac{x_{max}}{y} = \frac{x_{max}}{1 - \left(\frac{K_2}{K_1 + K_3}\right)^{\frac{K_1 + K_3}{K_1 + K_3 - K_2}}} \qquad (6)$$

Equations (3), (4) and (6) were used to calculate the results of Table 4.

APPENDIX 2 CATALYST DILUTION SCHEDULE TO ACHIEVE ISOTHERMAL OPERATION IN A TUBULAR REACTOR WHERE THE REACTIONS FOLLOW FROMENT'S SCHEME FOR XYLENE OXIDATION

We adopt the nomenclature of Appendix 1 but in addition let

Cp = mean molar specific heat of fluid

F = total molar flow per unit cross section area

h = overall heat transfer coefficient between fluid and jacket

R = tube radius

ρ_B = catalyst bulk density

ΔH_1, ΔH_3 = heats of reaction for steps 1 and 3

ΔT_1, ΔT_3 = adiabatic temperature rise for steps 1 and 3

u = fraction of xylene feed not reacted

z = distance along the reactor axis

R' = catalyst dilution

T, Tj = fluid and jacket temperatures

The suffix 0 indicates reactor exit conditions.

By heat balance on a differential element of reactor

$$\pi R^2.F.Cp.dT + 2\pi R.dz.h.(T - Tj) = \pi R^2.F.N_A\left[dx.-\Delta H_1 + (dy - dx).-\Delta H_3\right]$$

Therefore

$$\frac{dT}{dz} + \frac{2h(T - Tj)}{F.R.Cp} = \Delta T_1.\frac{dx}{dz} + \Delta T_3\left(\frac{dy}{dz} - \frac{dx}{dz}\right)$$

$$= \Delta T_1.\frac{dx}{dz} - \Delta T_3\left(\frac{du}{dz} + \frac{dx}{dz}\right)$$

The reactor will be isothermal if $\frac{dT}{dz} = 0$, i.e.

$$\frac{2h(T - Tj)}{F.R.Cp} = (\Delta T_1 - \Delta T_3).\frac{dx}{dz} - \Delta T_3.\frac{du}{dz} \qquad (1)$$

By mass balance

$$\pi R^2.F.N_A.dx = N_A\left[K_1(1 - y) - K_2x\right]\pi R^2.\rho_B.dz/R'$$

therefore

$$\frac{dx}{dz} = \frac{\rho_B}{F.R'}\left[K_1 u - K_2 x\right]$$

and similarly

$$\frac{du}{dz} = \frac{-\rho_B}{F.R'}(K_1 + K_3).u$$

so that equation (1) becomes

$$\frac{2h(T - Tj)}{R.Cp} = \frac{\rho_B}{R'}\left[(\Delta T_1 - \Delta T_3)(K_1 u - K_2 x) + \Delta T_3(K_1 + K_3)u\right]$$

or

$$R' = \frac{\rho_B.R.Cp}{2h(T - Tj)}\left[(\Delta T_1 - \Delta T_3).(K_1 u - K_2 x) + \Delta T_3(K_1 + K_3)u\right] \qquad (2)$$

and if the dilution is set to unity at the reactor exit then

$$R' = \frac{(\Delta T_1 - \Delta T_3).(K_1 u - K_2 x) + \Delta T_3(K_1 + K_3)u}{(\Delta T_1 - \Delta T_3).(K_1 u_o - K_2 x_o) + \Delta T_3(K_1 + K_3)u_o} \qquad (3)$$

Moreover the temperature difference between the reactant fluid and the jacket is given by (2) at exit conditions:

$$T - Tj = \frac{\rho_B.R.Cp}{2h}\left[(\Delta T_1 - \Delta T_3)(K_1 u_o - K_2 x_o) + \Delta T_3(K_1 + K_3)u_o\right] \qquad (4)$$

Since the reactor is isothermal a relation between u and z can be obtained. We have

$$\frac{du}{dz} = -\frac{\rho_B}{F.R'}.(K_1 + K_3).u$$

Hence from (3)

$$\frac{du}{dz} = -\frac{\rho_B(K_1 + K_3).}{F}\left[\frac{(\Delta T_1 - \Delta T_3)(K_1 u_o - K_2 x_o) + \Delta T_3(K_1 + K_3)u_o}{(\Delta T_1 - \Delta T_3)(K_1 - K_2.x/u) + \Delta T_3(K_1 + K_3)}\right]$$

But (from Appendix 1)

$$x/u = x/1 - y = \frac{K_1}{K_1 + K_3 - K_2}.\left[e^{-(P - R).W} - 1\right]$$

$$= \frac{K_1}{K_1 + K_3 - K_2}\left[u^{\frac{K_2 - (K_1 + K_3)}{K_1 + K_3}} - 1\right]$$

$$= f(u) \quad \text{(say)}$$

therefore

$$(\Delta T_1 - \Delta T_3)(K_1 u - K_2 \int f(u).du) + \Delta T_3(K_1 + K_3)u \Big|_1^{u_o}$$

$$= -\frac{\rho_B(K_1 + K_3)}{F}.\left[(\Delta T_1 - \Delta T_3)(K_1 u_o - K_2 x_o) + \Delta T_3(K_1 + K_3)u_o\right] Z_o$$

But

$$\int f(u).du = \frac{K_1}{K_1 + K_3 - K_2}\left[\frac{K_1 + K_3}{K_2}.u^{\frac{K_2}{K_1 + K_3}} - u\right]$$

Hence

$$Z_o = \frac{\Delta T_3(K_1 + K_3)(1 - u_o) + (\Delta T_3 - \Delta T_1)(K_1 u_o - \frac{K_1}{K_1 + K_3 - K_2}.}{\frac{\rho_B(K_1 + K_3)}{F}.\left[\Delta T_3(K_1 + K_3)u_o - (\Delta T_3 - \Delta T_1)\right.}$$

$$\left.\frac{(u_o^{\frac{K_2}{K_1 + K_3}}.(K_1 + K_3) - K_2 u_o))}{(K_1 u_o - \frac{K_2 K_1}{K_1 + K_3 - K_2}(u_o^{\frac{K_2}{K_1 + K_3}} - u_o))}\right] \qquad (5)$$

Equation (5) is given as equation (19) in Chapter 2. An additional factor N_B appears in the denominator of equation (19). This represents the mole fraction of oxygen in the reactor gases (which may be taken as constant for xylene oxidation). Equation (19) would be appropriate if the reaction is assumed first order with respect to both xylene and oxygen, whereas in the present derivation the dependence on oxygen has been ignored.

Equations (3) and (4) are given as equations (21) and (20) respectively in Chapter 2, with x given in terms of u throughout.

APPENDIX 3 CALCULATION OF PECLET NUMBERS FOR HEAT AND MASS TRANSFER PRODUCED BY THE THREE WAY MIXING PATTERN OF THE MATRIX MODEL

The matrix model simulates a packed bed with steady state flow of a fluid through the bed. It will be shown that the three way mixing equations of the model give rise to a Peclet number of 9.8.

The proof will be given in terms of the transport of matter but the result is equally applicable to heat transfer. To eliminate wall effects we consider a packed bed of infinite dimensions. Suppose that a continuous stream of some tracer material is injected into the bed at the origin of the co-ordinate system. The movement of the tracer through the bed downstream from the point of injection may then be described (using cylindrical polar co-ordinate) by

$$\frac{\partial C}{\partial z} = \frac{D_e}{u}\left(\frac{\partial^2 C}{\partial r^2} + \frac{1}{r}.\frac{\partial C}{\partial r}\right)$$

where

C = concentration of tracer

u = superficial fluid velocity $\left(\frac{\text{volumetric flow}}{\text{cross section area}}\right)$

D_e = bed effective diffusivity

The solution of this equation must satisfy the following boundary conditions

(1) $C \longrightarrow 0$ as $r \longrightarrow \infty$ (all z)

(2) $C \longrightarrow 0$ as $z \longrightarrow \infty$ (all r)

(3) $C = 0$ at $z = 0$ $(r \neq 0)$

A possible solution is

$$C = \frac{K_1}{z}.e^{-K_2 r^2/z}, \text{ where } K_1, K_2 \text{ are constants.}$$

By inspection this is seen to satisfy the three boundary conditions. Differentiating with respect to r and z we obtain

$$\frac{\partial C}{\partial r} = -\frac{2K_1K_2r}{z^2}.e^{-K_2r^2/z}$$

$$\frac{\partial^2 C}{\partial r^2} = \frac{4K_1K_2^2r^2}{z^3}.e^{-K_2r^2/z} - \frac{2K_1K_2}{z^2}.e^{-K_2r^2/z}$$

$$= \frac{2K_1K_2}{z^2}.e^{-K_2r^2/z^2}\left[\frac{2K_2r^2}{z} - 1\right]$$

$$\frac{\partial C}{\partial z} = -\frac{K_1}{z^2}.e^{-K_2r^2/z} + \frac{K_1}{z}.\frac{K_2r^2}{z^2}.e^{-K_2r^2/z^2}$$

$$= \frac{K_1}{z^2}.e^{-K_2r^2/z}\left[\frac{K_2r^2}{z} - 1\right]$$

Hence the proposed solution satisfies the differential equation if:

$$\frac{K_1}{z^2}.e^{-K_2r^2/z}\left[\frac{K_2r^2}{z} - 1\right] = \frac{D_e}{u}\left[\frac{2K_1K_2}{z^2}.e^{-K_2r^2/z}\left[\frac{2K_2r^2}{z} - 1\right] - \frac{2K_1K_2}{z^2}.e^{-K_2r^2/z}\right]$$

therefore

$$\frac{K_2r^2}{z} - 1 = \frac{D_eK_2}{u}\left[\frac{4K_2r^2}{z} - 2 - 2\right]$$

$$1 = \frac{4D_e.K_2}{u}$$

$$\underline{\underline{K_2 = \frac{u}{4.D_e}}} \qquad (1)$$

The solution therefore becomes

$$C = \frac{K_1}{z}.e^{-u.r^2/4.D_e.z}$$

The term K_2 is clearly a measure of the dispersion in the packed bed: we should therefore be able to relate it to the standard deviation of tracer material from its point of injection.

Let

σ_z = standard deviation of tracer material at a distance z in the axial direction from the point of injection

Then by definition

$$\sigma_z^2 = \frac{\int_0^\infty r^2 . 2\pi r . C . dr}{\int_0^\infty 2\pi r . C . dr}$$

$$\int_0^\infty 2\pi r . C . dr = \int_0^\infty 2\pi r . \frac{K_1}{z} . e^{-K_2 r^2/z} . dr$$

$$= \frac{\pi K_1}{K_2} \int_0^\infty \frac{2K_2 r}{z} . e^{-K_2 r^2/z} . dr$$

$$= \left[-\frac{\pi K_1}{K_2} . e^{-K_2 r^2/z} \right]_0^\infty$$

$$= \frac{\pi K_1}{K_2}$$

therefore

$$\sigma_z^2 = \frac{K_2}{\pi K_1} \int_0^\infty r^2 . 2\pi r . \frac{K_1}{z} . e^{-K_2 r^2/z} . dr$$

$$= \int_0^\infty r^2 . \frac{2K_2 r}{z} . e^{-K_2 r^2/z} . dr$$

$$= -\left[r^2 . e^{-K_2 r^2/z} \right]_0^\infty + \int_0^\infty e^{-K_2 r^2/z} . 2r . dr$$

$$= 0 + \frac{z}{K_2} \int_0^\infty \frac{2K_2 r}{z} . e^{-K_2 r^2/z} . dr$$

$$= \left[-\frac{z}{K_2} . e^{-K_2 r^2/z} \right]_0^{\infty}$$

$$= \frac{z}{K_2}$$

Substituting from (1)

$$\sigma_z^2 = \frac{4.D_e.z}{u} \qquad (2)$$

This may be expressed as

$$\sigma_z^2 = 4.d_e.\tau$$

which is the Einstein diffusion equation derived for the case of dispersion in a plane at right angles to the direction of flow. (The equation normally encountered

$$\sigma_z^2 = 2.D_e.\tau$$

is applicable to a one dimensional diffusion[78, 79]).

To proceed further we must derive an expression for σ_z from the mixing equations of the matrix model. The model assumes that the packed bed consists of uniform spherical particles, diameter d, arranged in the hcp packing mode. Mixing is accounted for by assuming that the fluid moves in discrete streams (as it were along a network of pipes) between the centres of touching particles in adjacent rows. All streams within the bed are of equal magnitude and there are three streams (having the same temperature and composition) leaving each particle: these form the input streams to the three touching particles in the next row. It can then readily be shown that the displacements suffered by a fluid stream in moving between adjacent particle centres are

Displacement at right angles to flow direction = $d/\sqrt{3}$

Displacement in the direction of flow = $d\sqrt{2/3}$

The accompanying diagram shows the fraction of the original stream

arriving at each individual particle after 1, 2 3 and 4 successive displacements.

1.

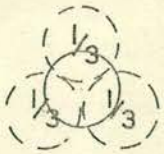

2.

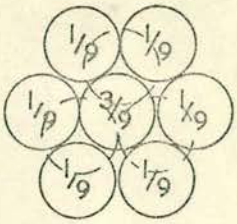

3.

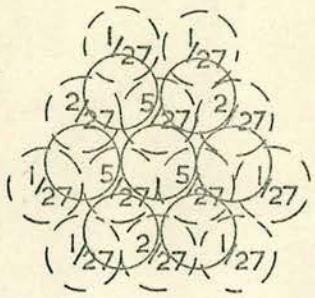

4.

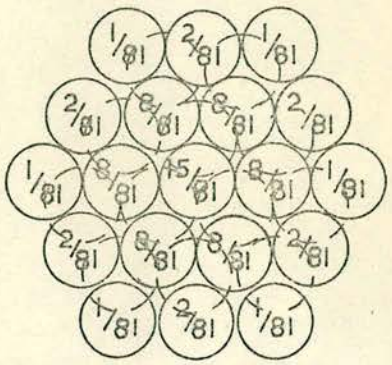

After a single encounter the standard deviation of the original stream material is σ_1 where

$$\sigma_1^2 = \frac{1.(d/\sqrt{3})^2 + 1.(d/\sqrt{3})^2 + 1.(d/\sqrt{3})^2}{3} = 1/3.d^2$$

After two encounters

$$\sigma_2^2 = \frac{6.(d)^2 + 3(0)^2}{9} = \frac{2}{3}.d^2$$

After three encounters

$$\sigma_3^2 = \frac{6.7/3.d^2 + 15(d/\sqrt{3})^2 + 6.4/3.d^2}{27} = \frac{3}{3}.d^2$$

After four encounters

$$\sigma_4^2 = \frac{15(0)^2 + 48(d)^2 + 6(2d)^2 + 36d^4}{81} = \frac{4}{3}.d^2$$

and clearly after n encounters

$$\sigma_n^2 = \frac{n}{3}.d^2 \qquad (3)$$

Combining equations (2) and (3)

$$\frac{4.D_e.z}{u} = \frac{n}{3}.d^2$$

But $z = n.d\sqrt{2/3}$

therefore $$\frac{u.d}{D_e} = Pe = 12\sqrt{2/3} = 9.8$$

APPENDIX 4 ERRORS ARISING FROM THE USE OF THE MATRIX MODEL

There are two principal sources of error in simulating the fixed bed reactor with the matrix model.

1. Hexagonal approximation to the circular cross section

The matrix model assumes a regular arrangement of spherical particles. Real reactors are packed irregularly and hence (even if we neglect wall effects) the voidage and bulk density of catalyst in the model cannot match those in the real reactor if the particle size and true densities agree. We must give some consideration to the wall effects, however, and as the diagram shows if we attempt to fit a hexagonal matrix of spherical particles into a tube of circular cross section we introduce regions of high voidage at the tube wall.

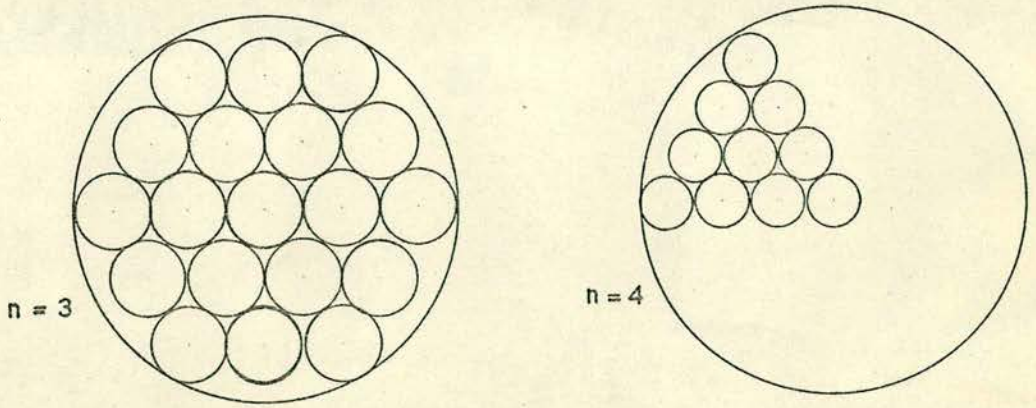

This situation reflects reality to some extent, but as the tube to particle diameter ratio increases the effect is exaggerated out of all proportion.

Let n = number of particles per side of the hexagonal matrix (counting both the end particles)

It may be seen from the diagrams that for $n \leq 4$ the tube diameter may reasonably be approximated by

$$D_t = 2(n - \tfrac{1}{2}).d$$

where

D_t = tube diameter

d = particle diameter

In the range $4 < n \leq 8$, however, a rather better fit is given by

$$D_t = 2(n - 1)d$$

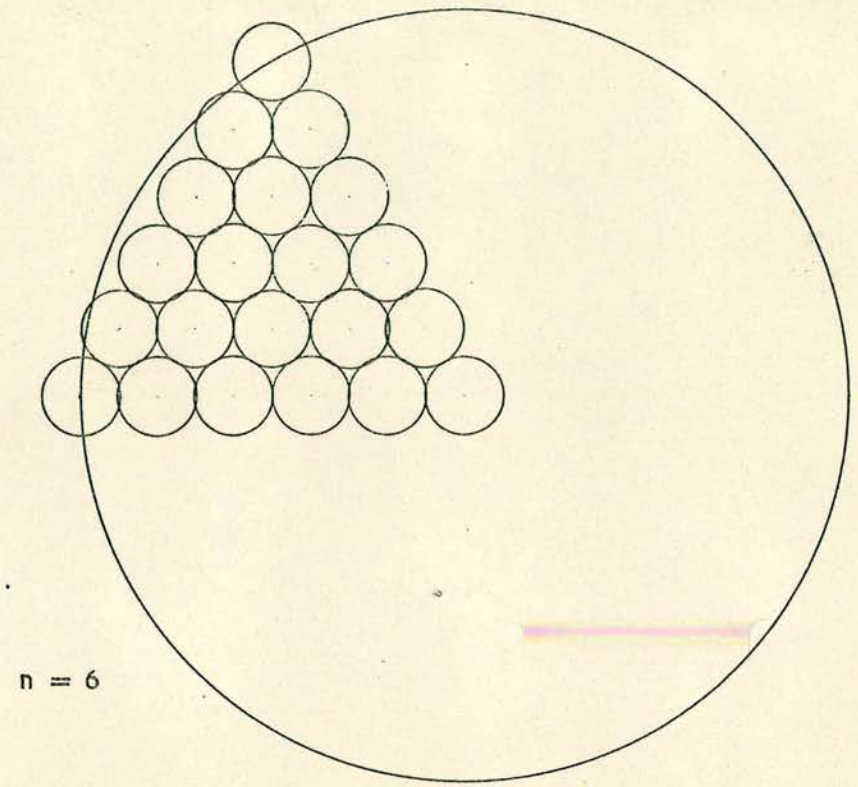

n = 6

If n is greater than about 8 the hexagonal matrix gives a very poor approximation to the circle. One could modify the hexagon by adding on particles at various points and so obtain quite a good fit, but this would be done at the expense of generality.

The number of particles, N_1, per layer of catalyst is given by

$$N_1 = 6\left[\frac{n(n + 1)}{2}\right] - 6(n - 1) - 5$$

$$N_1 = 3n^2 - 3n + 1$$

Alternate layers of catalyst will contain different numbers

of particles. If the second layer is supposed to lie wholly within the first (see diagram) then the number of particles in the second (non-

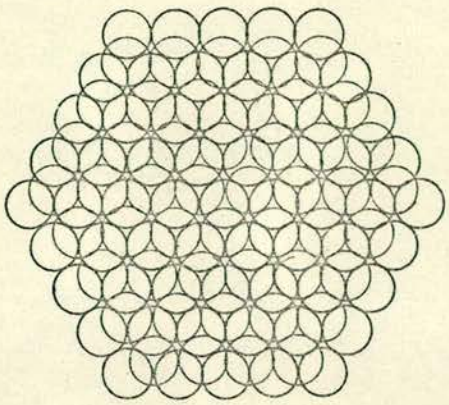

hexagonal) layer is given by

$$N_2 = 3(n - 1)^2$$

$$N_2 = 3n^2 - 6n + 3$$

The flow per particle must, of course, be the same in both rows; the total flow is also the same, and hence there are $(N_1 - N_2)$ bypass streams in row 2.

As mentioned already there will generally be a discrepancy between the true bulk density of catalyst in the real reactor and the apparent bulk density in the model. It is essential, however, that the model and the real reactor should agree as to the weight of catalyst in a given length - if this is so then the model will at least be correct under isothermal conditions. (We assume that the rate of reaction is given in terms of the weight of catalyst rather than, say, the surface area).

Let w = weight of a catalyst pellet in the model

R = reactor tube radius

ρ_B = true catalyst bulk density

L = reactor length

N = number of particles in length L in the model

Therefore

$$\pi R^2 . L . \rho_B = N . w$$

Now let L be the distance between the planes containing the particle centres in adjacent layers.

$$L = \sqrt{2/3}.d \qquad \text{(see Appendix 3)}$$

$$N = \frac{N_1 + N_2}{2} = \frac{3n^2 - 3n + 1 + 3n^2 - 6n + 3}{2}$$

$$= \frac{6n^2 - 9n + 4}{2}$$

and hence

$$w = \frac{2\pi R^2 . \sqrt{2/3}.d.\rho_B}{6n^2 - 9n + 4}$$

if $4 < n \leq 8$ (which is the range with which we are principally concerned) then

$$w = \frac{2\pi.(n-1)^2 d^2 . \sqrt{2/3}d.\rho_B}{6n^2 - 9n + 4}$$

$$w = \frac{1.633\pi.\rho_B (n-1)^2 d^3}{6n^2 - 9n + 4}$$

This equation is used in the computer programs of Appendix 5 to calculate the weight of a catalyst particle. In general the result will not agree with that obtained by multiplying the true particle volume by the true particle density. Hence it cannot be claimed that the matrix model is a cell model in which each cell incorporates the amount of catalyst contained in a single pellet.

2. Use of a triangular matrix

In the homogeneous model one may generally make the assumption of axial symmetry: this means that the integration of the differential equations has only to be performed so as to establish values of the dependent variables at a number of mesh points along a single radius of the reactor, thus greatly reducing the computation time. With

the matrix model no corresponding simplification is strictly permissible - since it is impossible to consider any row or column of particles in isolation from its neighbours. Nevertheless some simplification was attempted since it was clearly necessary to limit computation time as far as possible.

The hexagonal matrix may be subdivided into six equilateral triangles. The sides of these triangles are, in fact, radii of the tubular reactor which we are attempting to model, and hence if the reactor has axial symmetry there should be no net transfer of heat or

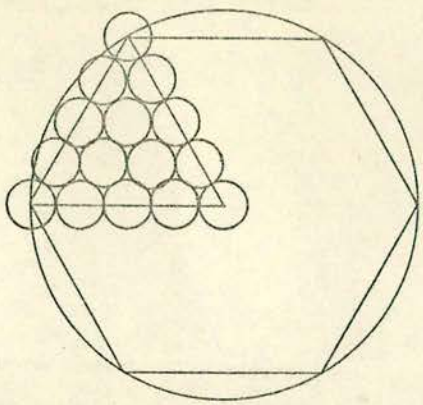

matter across these sides. Unfortunately these radii cut across the individual particles of the matrix, so that the actual triangular matrix of particles comprises rather more than one sixth of the hexagon. The particles which are situated on (or over) the boundaries will receive input streams from particles which are entirely outwith the triangular matrix. In estimating the magnitude of these input streams we inevitably introduce errors into the calculations. The method of estimating the inputs from outwith the matrix is shown below.

Let S = output temperature from a particle in row 1

$\bar{T}$ = input temperature to a particle in row 2

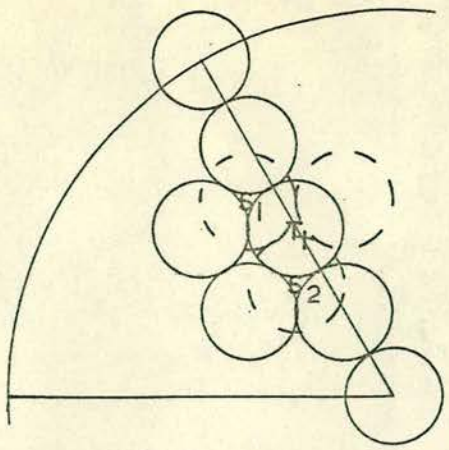

The particle with temperature T_1 has one input from S_1 and one from S_2. It also has an (unknown) input from across the boundary. We assume this to be the mean of S_1 and S_2 in magnitude.

Hence

$$T_1 = (S_1 + S_2 + \frac{S_1 + S_2}{2})/3$$

or

$$T_1 = \frac{S_1 + S_2}{2}$$

The error introduced by this procedure may be illustrated by the example below. Let a, b, c, etc. be the outputs from the first row in a bed where n = 3. f is from the central particle in the bed and a, b, d are from the wall particles. There is to be no transfer across the boundary wall and we suppose that the process within the bed

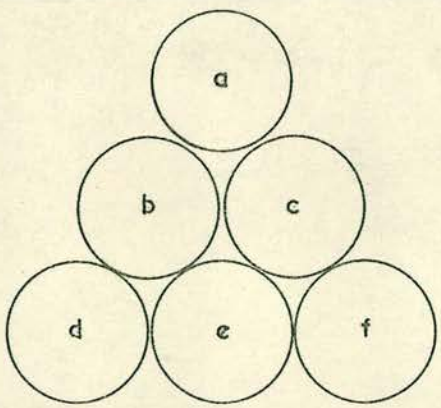

is simply one of mixing. The outputs from the second row are then

$$1/3(a + b + c)$$

$$1/3(b + d + e) \qquad 1/3(c + e + f)$$

- there being only three particles in this row

From the third row the outputs are:

$$1/3(2a + 1/3(a + b + c))$$

$$1/3(b + 1/3(a + b + c) + 1/3(b+d+e)) \qquad \tfrac{1}{2}(1/3(a + b + c) + 1/3(c + e + f))$$

$$1/3(2d + 1/3(b + d + e)) \qquad \tfrac{1}{2}(1/3(b + d + e) + 1/3(c + e + f)) \qquad 1/3(c + e + f)$$

which can be simplified to

$$1/9(7a + b + c)$$

$$1/9(5b + a + c + d + e) \qquad 1/6(a + b + 2c + e + f)$$

$$1/9(7d + e + f) \qquad 1/6(b + c + d + 2e + f) \qquad 1/3(c + e + f)$$

Since we are simulating a pure mixing process the mean output from row 3 should be identical with that from row 1. (In calculating the mean outputs we do not weigh all the particles equally. The central particle is common to all six triangles of the hexagon and it is given a weight of 1/6. The radial particles are common to two triangles and are given a weight of $\frac{1}{2}$: other particles are given a weight of unity. This procedure was followed in the computer programs given in Appendix 5).

The mean output from row 1 is therefore

$$\text{Output}_1 = \frac{3a + 6b + 3c + 3d + 3e + f}{19}$$

$$= \frac{54a + 108b + 54c + 54d + 54e + 18f}{342}$$

The mean output from row 3 is

$$\text{Output}_3 = \frac{1}{19}\left[\frac{21a + 3b + 3c}{9} + \frac{30b + 6a + 6c + 6d + 6e}{9}\right.$$

$$+ \frac{3a + 3b + 6c + 3e + 3f}{6} + \frac{21d + 3b + 3e}{9}$$

$$\left. + \frac{3b + 3c + 3d + 6e + 3f}{6} + \frac{c + e + f}{3}\right]$$

$$= \frac{63a + 90b + 51c + 63d + 51e + 24f}{342}$$

Hence the error introduced into the mean output from the third row by the approximating procedure is

$$\text{Error} = \frac{1}{342}\left[9a - 18b - 3c + 9d - 3e + 6f\right]$$

$$= \frac{1}{114}\left[3a - 6b + 3d\right] - \frac{1}{114}\left[c + e - 2f\right]$$

We note that the error is zero when a = b = c = d = e = f and increases as the gradients (of temperature or concentration) become more severe. We may also note that since a, b and d refer to the wall particles the numerical values of a, b and d should always be fairly close, and hence the first term in the expression for the error should always be small. Equally the values of c, e and f would normally be fairly close together and hence the second term should also be small.

As a numerical example we may consider the case

$a = d = 150^{\circ}$; $b = 200^{\circ}$; $c = e = 250^{\circ}$; $f = 300^{\circ}$

therefore

$$\text{Error} = \frac{450 - 1200 + 450}{114} - \frac{500 - 600}{114}$$

$$= \frac{-300 + 100}{114} = -1.75^{\circ}$$

An error of 1.75° in the mixed mean temperature after only two rows may seem excessive but in the example here we have chosen a very large temperature gradient and the matrix itself is of very small dimensions. In the results reported in this thesis the temperature difference between tube axis and tube wall was (at most) 60° and the matrix had five particles per side instead of three. (One would expect the error to vary roughly as $1/n^2$ - or probably to decrease even more rapidly as n increases because of the weighting procedure).

APPENDIX 5 COMPUTER PROGRAMS BASED ON THE MATRIX MODEL

The three programs referred to in Section 2.4.3 will be listed first: the routines which are common to some (or all) of these programs are listed at the end.

1. XYLOX

1.1 Nomenclature

B1,C1,T1	inputs (or outputs) of odd numbered rows in the matrix. B is the fraction converted to phthalic anhydride, C the fraction converted to carbon oxides, T the temperature.
B2, C2, T2	ditto, for even numbered rows.
SUM B, SUM C, SUM T	average (mixed mean) values of B1, C1, T1.
E1, E2, E3	activation energies.
H1, H3	heats of reaction
NAO, NO	mole fractions of o-xylene and oxygen in the feed mixture.
F	initially the molar flow per unit cross section later the molar flow per particle
CP	mean molar specific heat
J, G, L	defined in the program
Z	reduced reactor length (= True length/Particle diameter)
TW	tube wall temperature
d	particle diameter
K	wall heat transfer parameter (See Section 2.4.2)
ROW B	catalyst bulk density
n	number of particles per side of the triangular matrix
i, j	integers defining position within the matrix
k	integer defining the row number
y	an integer, varying with k, which defines the matrix size

1.2 Block diagram

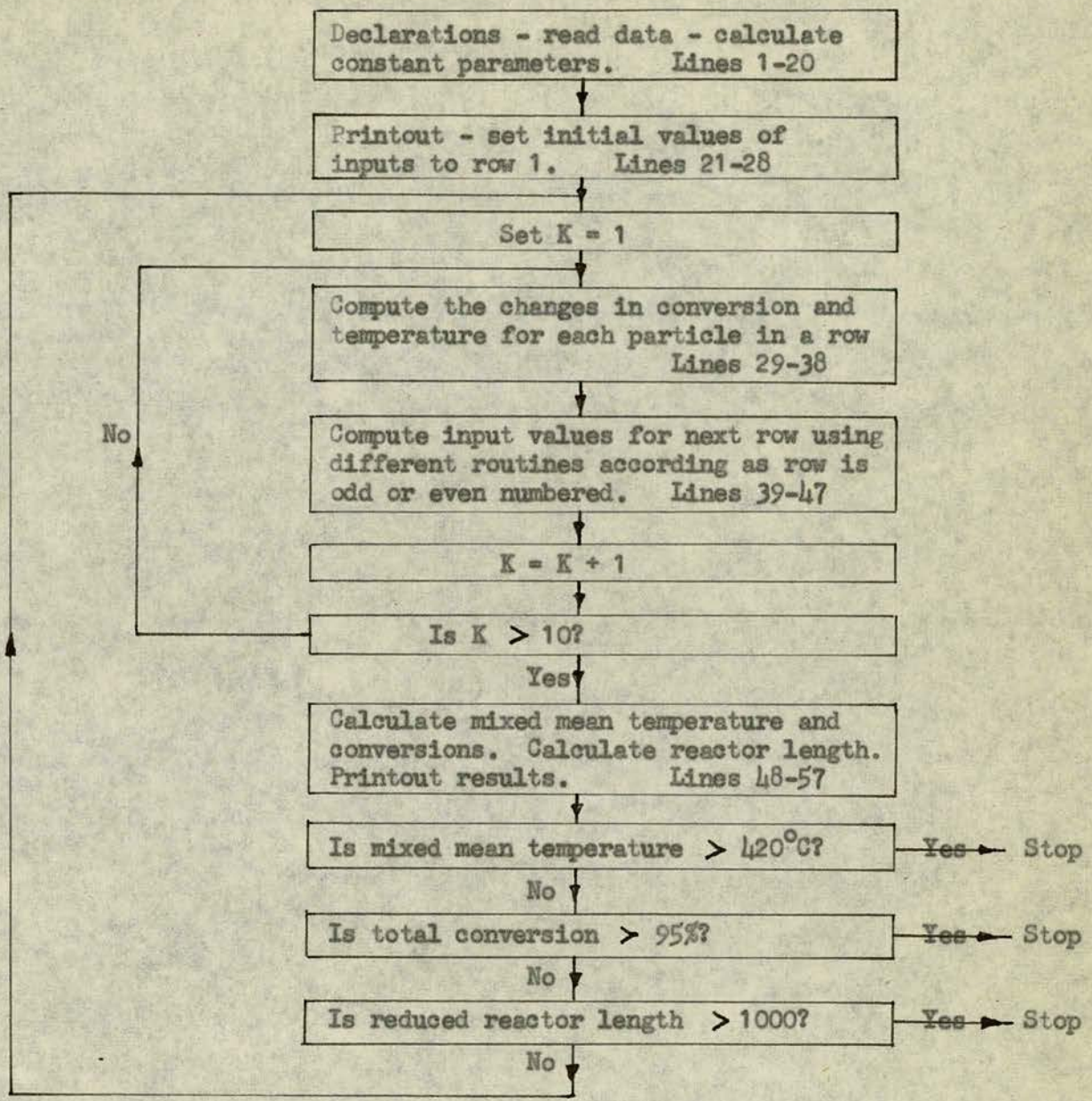

1.3 Program

```
1   begin
2   integer n
3   read(n)
4   begin
5   integer i,j,k,y
6   real E1,E2,E3,H1,H3,WT,NAO,NO,F,CP,J,G,L,Z,SUM B, SUM C, SUM T
7   real TW,d,K,ROW B
8   real array B1,C1,T1(1:n,1:n)
9    real array B2,C2,T2(1:n-1,1:n-1)
10  routine spec CONVERSION(real name B,C,T)
```

```
11  routine spec ENCOUNTER 1(real array name X1,X2)
12  routine spec ENCOUNTER 2(real array name X1,X2)
13  routine spec ENCOUNTER 3(real array name X1,X2)
14  routine spec AVERAGE(real array name X,real name SUM)
15  6:read(NAO,NO,B1(1,1),C1(1,1),T1(1,1),TW,d,E1,E2,E3,H1,H3)
16  read(F,CP,K,ROW B)
17  Z=0
18  J=NAO*NO ; F=F*π*(n-1)^2*d^2/(3*n^2-3*n+1)
19  G=F*NAO ; L=NAO/CP
20  WT=1.633*π*(n-1)^2*d↑3*ROW B/(6*n^2-9*n+4)
21  newline
22  print((TW-273),3,1)
23  cycle i=1,1,n
24  cycle j=1,1,n
25  if (i+j)>(n+1) then →1
26  B1(i,j)=B1(1,1) ; C1(i,j)=C1(1,1) ; T1(i,j)=T1(1,1)
27  1:repeat
28  repeat
29  5:cycle k=1,1,10
30  y=n
31  if frac pt(k/2)=0 then y=n-1
32  cycle i=1,1,y
33  cycle j=1,1,y
34  if(i+j)>(y+1) then →2
35  if y=n then CONVERSION(B1(i,j),C1(i,j),T1(i,j))
36  if y=n-1 then CONVERSION(B2(i,j),C2(i,j),T2(i,j))
37  2:repeat
38  repeat
39  if y=n-1 then →3
40  ENCOUNTER 1(B1,B2)
41  ENCOUNTER 1(C1,C2)
42  ENCOUNTER 1(T1,T2)
43  →4
44  3:ENCOUNTER 2(T1,T2)
45  ENCOUNTER 3(B1,B2)
46  ENCOUNTER 3(C1,C2)
47  4:repeat
48  AVERAGE(B1,SUM B)
49  AVERAGE(C1,SUM C)
50  AVERAGE(T1,SUM T)
51  Z=Z+8.165
```

```
52    newline
53    print(Z,3,1) ; spaces(2)
54    print(SUM B,1,3) ; spaces(2)
55    print(SUM C,1,3) ; spaces(2)
56    print((SUM T-273),3,1) ; spaces(2)
57    print (SUM B/(SUM B+SUM C),1,3)
58    if SUM T>693 then ->6
59    if (SUM B+SUM C)>0.95 then ->6
60    if Z>1000 then ->6
61    ->5
62    routine .....
          .
          .
          .
          .
```

2 XYLOX 2

2.1 Nomenclature

In addition to the list given in 1.1 the following symbols are used:

S	an integer, taking values between 1 and 10, which defines the section of the reactor under consideration
bias	an integer employed in the CATALYST SELECTION routine (see later) to ensure that particles were chosen to be active or inactive with the correct probability
test	an integer used in the catalyst dilution optimization procedure. If the temperature in a section of the bed exceeds the preset maximum the value of test is switched: this terminates the search
N1,N2	the numbers of active catalyst particles in odd and numbered rows
TT	the maximum permitted temperature at the reactor axis in an odd numbered row
x,x'	employed in the library random number generator
M	a counter
STOR B, STOR C, STOR T	arrays for storing the outputs from a section

	of the bed. Employed in the optimizing procedure
cat 1, cat 2	arrays for describing the catalytic state of the matrix. A value of zero indicates an inactive particle, a value of unity an active particle
Catcrite	an array giving the catalyst concentration in each section of the bed.

2.2 Block Diagram

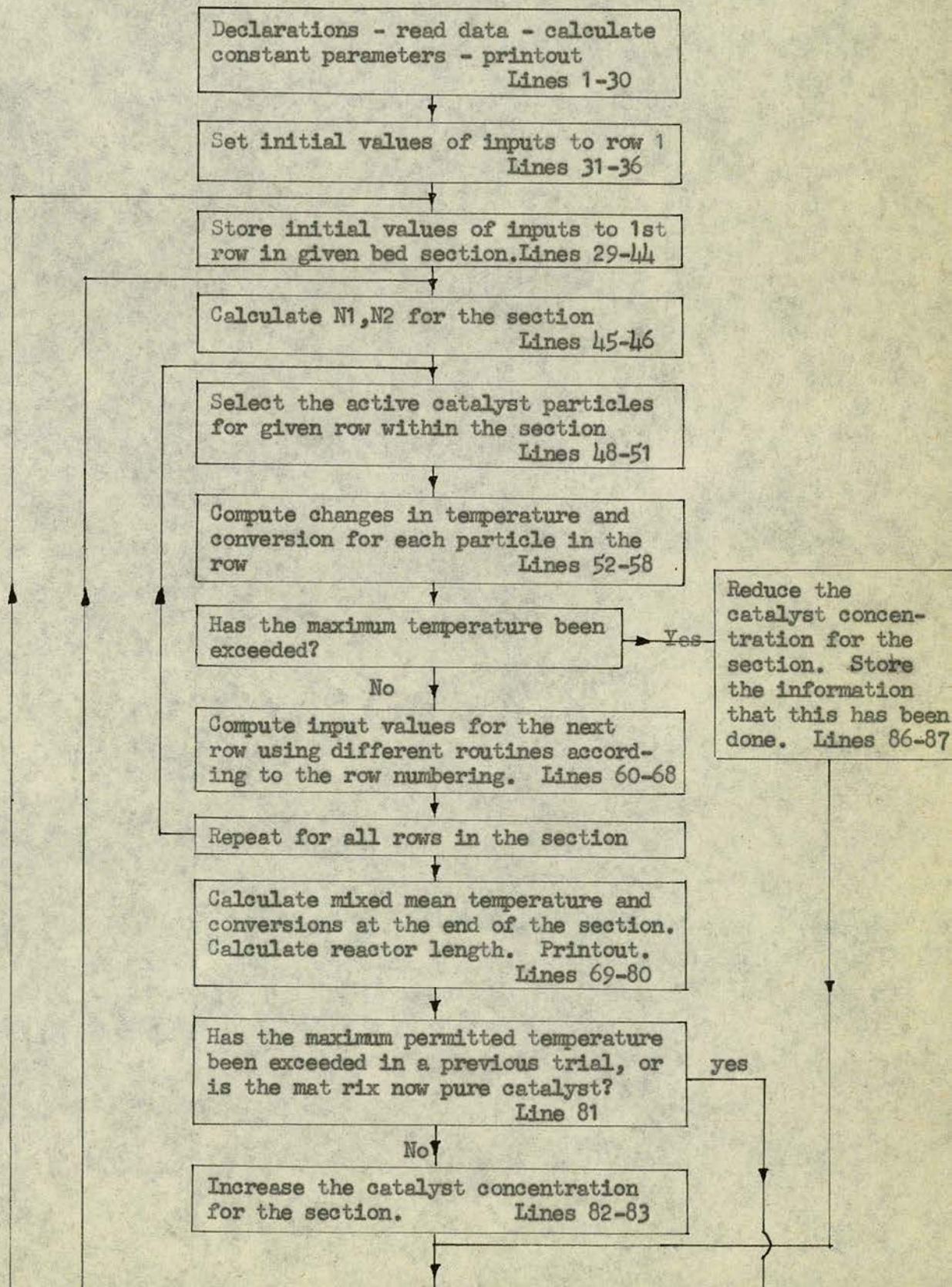

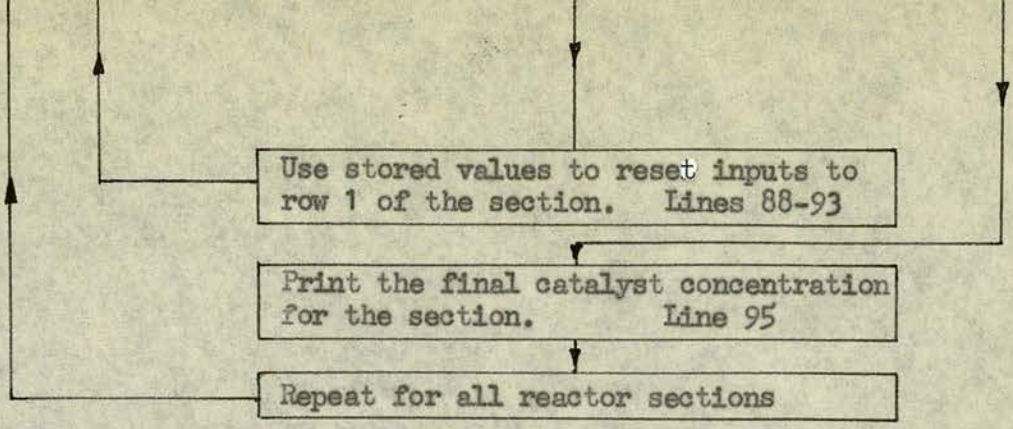

2.3 Program

```
1   begin
2   integer n
3   read(n)
4   begin
5   integer i,j,k,y,s,P,bias,test,N1,N2
6   real E1,E2,E3,H1,H3,WT,NAO,NO,F,CP,J,G,L,Z,SUM B,SUM C,SUM T
7   real TW,K,d,ROW B,TT,M,x,x'
8   real array B1,C1,T1,STOR B,STOR C,STOR T, cat1(1:n,1:n)
9   real array B2,C2,T2,cat2(1:n-1,1:n-1)
10  real array Catcrite(1:10)
11  real fn spec random k(real name x,integer n)
12  routine spec CONVERSION(real name B,C,T)
13  routine spec ENCOUNTER 1(real array name X1,X2)
14  routine spec ENCOUNTER 2(real array name X1,X2)
15  routine spec ENCOUNTER 3(real array name X1,X2)
16  routine spec AVERAGE(real array name X,real name SUM)
17  routine spec CATALYST SELECTION(integer name N,real array name cat)
18  read(NAO,NO,B1(1,1),C1(1,1),T1(1,1),TW,d,E1,E2,E3,H1,H3)
19  read(F,CP,K,ROW B,TT,x')
20  x=random k(x',0)
21  Z=0 ; P=0 ; bias=1
22  J=NAO*NO ; F=F*π*(n-1)^2*d^2/(3*n^2-3*n+1)
23  G=F*NAO ; L=NAO/CP
24  WT=1.633*π*(n-1)^2*d↑3*ROW B/(6*n^2-9*n+4)
25  newline
26  print((TW-273),3,1)
27  newline
28  cycle s=1,1,10
29  read(Catcrite(s))
30  repeat
31  cycle i=1,1,n
32  cycle j=1,1,n
```

```
33   if (i+j)>(n+1) then ->1
34   B1(i,j)=B1(1,1) ; C1(i,j)=C1(1,1) ; T1(i,j)=T1(1,1)
35   1:repeat
36   repeat
37   cycle s=1,1,10
38   test=0
39   cycle i=1,1,n
40   cycle j=1,1,n
41   if (i+j)>(n+1) then ->11
42   STOR B(i,j)=B1(i,j) ; STOR C(i,j)=C1(i,j) ; STOR T(i,j)=T1(i,j)
43   11:repeat
44   repeat
45   9:N1=int(Catcrite(s)*n*(n+1)/2)
46   N2=int(Catcrite(s)*n*(n-1)/2)
47   5:cycle k=1,1,124
48   y=n
49   if frac pt(k/2)=0 then y=n-1
50   if y=n then  CATALYST SELECTION(N1,cat1)
51   if y=n-1 then CATALYST SELECTION(N2,cat2)
52   cycle i=1,1,y
53   cycle j=1,1,y
54   if (i+j)>(y+1)then ->2
55   if y=n and cat1(i,j)=1 then CONVERSION(B1(i,j),C1(i,j),T1(i,j)
56   if y=n-1 and cat2(i,j)=1 then CONVERSION(B2(i,j),C2(i,j),T2(i,j))
57   2:repeat
58   repeat
59   if T1(1,n)>TT then ->10
60   if y=n-1 then ->3
61   ENCOUNTER 1(B1,B2)
62   ENCOUNTER 1(C1,C2)
63   ENCOUNTER 1(T1,T2)
64   ->4
65   3:ENCOUNTER 2(T1,T2)
66   ENCOUNTER 3(B1,B2)
67   ENCOUNTER 3(C1,C2)
68   4:repeat
69   AVERAGE(B1,SUM B)
70   AVERAGE(C1,SUM C)
71   AVERAGE(T1,SUM T)
72   Z=Z+101.2
```

```
73    newline
74    print(s,2,0) ; spaces(2)
75    print(Z,4,1) ; spaces(2)
76    print(SUM B,1,3) ; spaces(2)
77    print(SUM C,1,3) ; spaces(2)
78    print((SUM T-273),3,1) ; spaces(2)
79    print(SUM B/(SUM B+SUM C),1,3)
80    newline
81    if test=1 or Catcrite(s)=1 then ->8
82    Catcrite(s)=Catcrite(s)+0.050
83    if Catcrite(s)>1 then Catcrite(s)=1
84    Z=Z-101.2
85    ->13
86    10:Catcrite(s)=Catcrite(s)-0.020
87    test=1
88    13:cycle i=1,1,n
89    cycle j=1,1,n
90    if (i+j)>(n+1) then ->12
91    B1(i,j)=STOR B(i,j) ; C1(i,j)=STOR C(i,j) ; T1(i,j)=STOR T(i,j)
92    12:repeat
93    repeat
94    ->9
95    8:print(Catcrite(s),1,3)
96    newline
97    repeat
98    routine .....
          .
          .
          .
      end of program
```

3. Xylox 3

3.1 Nomenclature

See sections 1.1 and 2.1 of this Appendix.

3.2 Block diagram

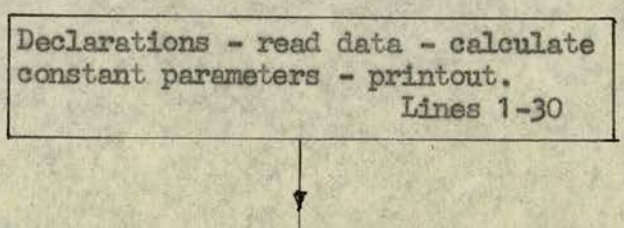

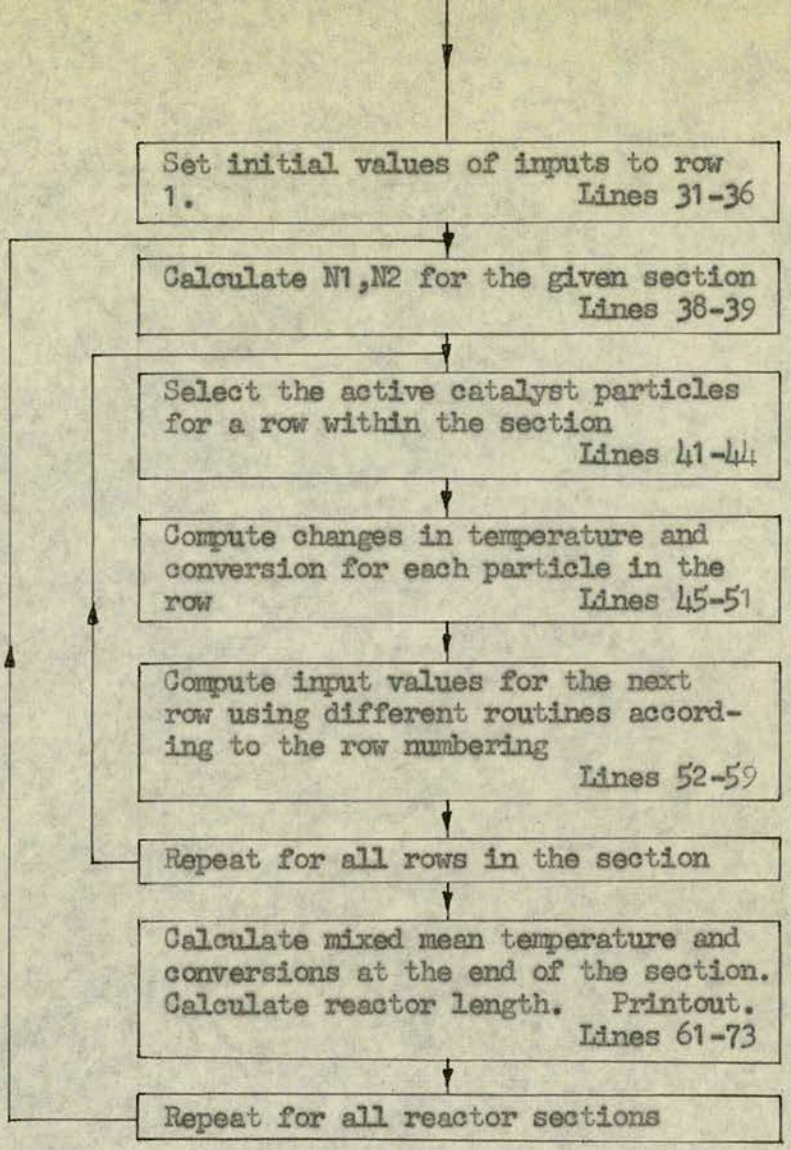

3.3 Program

```
1   begin
2   integer n
3   1:read(n)
4   begin
5   integer i,j,k,y,s,P,bias,N1,N2
6   real E1,E2,E3,H1,H3,WT,NAO,NO,F,CP,J,G,L,Z,SUM B,SUM C, SUM T
7   real TW,K,d,ROW B,M,x,x'
8   real array B1,C1,T1,cat1(1:n,1:n)
9   real array B2,C2,T2,cat2(1:n-1,1:n-1)
10  real array Catcrite(1:10)
11  real fn spec random k(real name x,integer n)
12  routine spec CONVERSION(real name B,C,T)
13  routine spec ENCOUNTER 1(real array name X1,X2)
14  routine spec ENCOUNTER 2(real array name X1,X2)
15  routine spec ENCOUNTER 3(real array name X1,X2)
16  routine spec AVERAGE(real array name X,real name SUM)
17  routine spec CATALYST SELECTION(integer name N,real array name cat)
18  read(NAO,NO,B1(1,1),C1(1,1),T1(1,1),TW,d,E1,E2,E3,H1,H3)
```

```
19    read(F,CP,K,ROW B,x')
20    x=random k(x',0)
21    Z=0 ; P=0 ; bias=1
22    J=NAO*NO :, F=F*π*(n-1)^2*d^2/(3*n^2-3*n+1)
23    G=F*NAO ; L=NAO/CP
24    WT=1.633*π*(n-1)^2*d+3*ROW B/(6*n^2-9*n+4)
25    newline
26    print((TW-273),3,1)
27    newline
28    cycle s=1,1,10
29    read(Catcrite(s))
30    repeat
31    cycle i=1,1,n
32    cycle j=1,1,n
33    if (i+j)>(n+1) then ->1
34    B1(i,j)=B1(1,1) ; C1(i,j)=C1(1,1) ; T1(i,j)=T1(1,1)
35    1:repeat
36    repeat
37    cycle s=1,1,10
38    9:N1=int(Catcrite(s)*n*(n+1)/2)
39    N2=int(Catcrite(s)*n*(n-1)/2)
40    5:cycle k=1,1,124
41    y=n
42    if frac pt(k/2)=0 then y=n-1
43    if y=n then CATALYST SELECTION(N1,cat1)
44    if y=n-1 then CATALYST SELECTION(N2,cat2)
45    cycle i=1,1,y
46    cycle j=1,1,y
47    if (i+j)>(y+1)then ->2
48    if y=n and cat1(i,j)=1 then CONVERSION(B1(i,j),C1(i,j),T1(i,j))
49    if y=n-1 and cat2(i,j)=1 then CONVERSION(B2(i,j),C2(i,j),T2(i,j))
50    2:repeat
51    repeat
52    if y=n-1 then ->3
53    ENCOUNTER 1(B1,B2)
54    ENCOUNTER 1(C1,C2)
55    ENCOUNTER 1(T1,T2)
56    ->4
57    3:ENCOUNTER 2(T1,T2)
58    ENCOUNTER 3(B1,B2)
```

```
59    ENCOUNTER 3(C1,C2)
60    4:repeat
61    AVERAGE(B1,SUM B)
62    AVERAGE(C1,SUM C)
63    AVERAGE(T1,SUM T)
64    Z=Z+101.25
65    newline
66    print(s,2,0)  ;  spaces(2)
67    print(Z,4,1)  ;  spaces(2)
68    print(SUM B,1,3)  ;  spaces(2)
69    print(SUM C,1,3)  ;  spaces(2)
70    print((SUM T-273),3,1)  ;  spaces(2)
71    print((T1(1,n)-273),3,1)  ;  spaces(2)
72    print(SUMB/(SUM B+SUM C),1,3)
73    newline
74    repeat
75    routine .....
          .
          .
          .
      end of program
```

4. List of Routines

4.1 Nomenclature

See sections 1.1, 2.1 and 3.1 of this Appendix. In addition the following symbols are used in routine CONVERSION.

DELB,DELC	changes in the fraction converted (to phthalic anhydride and carbon oxides) occurring across a single pellet
DELTGUESS,DELTCALC	guessed and calculated changes in temperature across a single pellet
DB,DC,DT	working values of B1,C1,T1 (or B2,C2,T2)
rB,rC	rates of reaction
K1,K2,K3	rate constants
I,H	internally defined

4.2 Programs

```
routine CONVERSION(real name B,C,T)
real DELB,DELC,DELTGUESS,DELTCALC,DB,DC,DT,rB,rC,I,H,K1,K2,K3
```

```
integer a
a=0 ; DELTGUESS=0.005
DB=B ; DC=C ; DT=T+DELTGUESS
4:K1=exp(-E1/(1.98*DT)+11.648)
K2=exp(-E2/(1.98*DT)+12.67)
K3=exp(-E3/(1.98*DT)+10.78)
2:H=1-(DB+DC)
I=K2*DB
rB=J*(K1*H-I)
rC=J*(I+K3*H)
DELB=WT*rB/G ; DELC=WT*rC/G
DB=B+DELB ; DC=C+DELC
if a=2 then ->1
a=a+1
->2
1:a=0
DELTCALC=L*(DELB*H1+DELC*H3)
if DELTCALC>DELTGUESS then ->3
DELTGUESS=2*DELTGUESS
DT=T+DELTGUESS
->4
3:if (DELTCALC-DELTGUESS)<0.001 then ->5
DELTGUESS=DELTCALC
DT=T+DELTGUESS
->4
5:B=B+DELB ; C=C+DELC ; T=T+DELTCALC
end
```

```
routine CATALYST SELECTION(integer name N,real array name cat)
cycle i=1,1,y
cycle j=1,1,y
if (i+j)>(y+1) then ->1
cat(i,j)=0
1:repeat
repeat
M=0
if N=0 then return
if N=y*(y+1)/2 then ->4
2:x=randomk(x',1)
i=int pt(10*x)
```

```
if i=0 then →2
6:x=random k(x',1)
j=int pt(10*x)
if j=0 then →6
if (i+j)>(y+1) then →2
if y=n-1 then → 3
bias=bias+1
if i=1 and j=n and frac pt(bias/6)≠0 then → 2
if (i=1 or (i+j)=(n+1)) and frac pt(bias/3)≠0 then →2
3:if cat(i,j)=1 then →2
cat(i,j)=1
M=M+1
if M<N then →2
return
4:cycle i=1,1,y
cycle j=1,1,y
if (i+j)>(y+1) then →5
cat(i,j)=1
5:repeat
repeat
end
```

```
routine AVERAGE(real array name X,real name SUM)
SUM=0
cycle j=1,1,n-1
SUM=SUM+3*X(1,j)
repeat
SUM=SUM+X(1,n)
cycle i=2,1,n-1
cycle j=1,1,n-2
if (i+j)>n then →1
SUM=SUM+6*X(i,j)
1:repeat
repeat
cycle i=2,1,n
j=n+1-i
SUM=SUM+3*X(i,j)
repeat
SUM=SUM/(3*n^2-3*n+1)
end
```

```
routine ENCOUNTER 1(real array name X1,X2)
cycle i=1,1,n
cycle j=1,1,n
if (i+j)>n then ->1
X2(i,j)=X1(i,j)+X1(i,j+1)+X1(i+1,j))/3
1 :repeat
repeat
end


routine ENCOUNTER 2(real array name X1,X2)
X1(1,1)=(X2(1,1)+2*(TW+(X1(1,1)-TW)*exp(-K/(F*CP))))/3
cycle j=2,1,n-1
X1(1,j)=(X2(1,j-1)+X2(1,j))/2
repeat
X1(1,n)=X2(1,n-1)
cycle i=2,1,n-1
X1(i,1)=(X2(i-1,1)+X2(i,1)+TW+(X1(i,1)-TW)*exp(-K/(F*CP)))/3
repeat
X1(n,1)=(X2(n-1,1)+2*(TW+(X1(n,1)-TW)*exp(-K/(F*CP))))/3
cycle i=2,1,n-1
j=n+1-i
X1(i,j)=(X2(i-1,j)+X2(i,j-1))/2
repeat
cycle i=2,1,n-2
cycle j=2,1,n-2
if (i+j)>n then ->1
X1(i,j)=(X2(i,j-1)+X2(i,j)+X2(i-1,j))/3
1 :repeat
repeat
end


routine ENCOUNTER 3(real array name X1,X2)
X1(1,1)=(2*X1(1,1)+X2(1,1))/3
cycle j=2,1,n-1
X1(1,j)=(X2(1,j-1)+X2(1,j))/2
repeat
X1(1,n)=X2(1,n-1)
cycle i=2,1,n-1
```

```
X1(i,1)=(X2(i-1,1)+X2(i,1)+X1(i,1))/3
repeat
X1(n,1)=(2*X1(n,1)+X2(n-1,1))/3
cycle i=2,1,n-1
j=n+1-i
X1(i,j)=(X2(i-1,j)+X2(i,j-1))/2
repeat
cycle i=2,1,n-2
cycle j=2,1,n-2
if (i+j)>n then ->1
X1(i,j)=(X2(i,j-1)+X2(i,j)+X2(i-1,j))/3
1 :repeat
repeat
end
```

Note routine CATALYST SELECTION utilizes the function "random k" which was provided by the Edinburgh University Computer Unit Library. The calls

```
x = random k(x',1)
```

generate a sequence of pseudo-random numbers rectangularly distributed in the range 0-1.

APPENDIX 6 AIR FLOW TO THE FLUIDIZED BED AND THE SHELL SIDE HEAT TRANSFER COEFFICIENT

For the greater part of the experimental work the rotameter setting was 6.0. Using the calibration chart for the rotameter, and applying a correction to allow for the fact the operating pressure was (approx.) 5 p.s.i.g., the flow to the fluidized bed was

$$\text{Flow} = 450 \times \sqrt{\frac{19.7}{14.7}} = 520 \text{ litres/minute}$$

$$= 18.4 \text{ c.f.m.}$$

The minimum fluidization velocity for the bed may be calculated from Leva's expression[74]:

$$G_{mf} = \frac{688 d^{1.82} (\rho_F (\rho_S - \rho_F))^{0.94}}{\mu^{0.88}}$$

where

G_{mf} = minimum fluidization velocity in lbs/ft^{2}hour

d = particle dia. (inches)

ρ_S = solids density (lbs/ft^3)

ρ_F = fluid density (lbs/ft^3)

μ = fluid viscosity (centipoise)

Taking values at 400°C

μ_{air} = 0.032 c.p.

ρ_F = 0.0327 lbs/ft^3

d = 0.119 mm = 0.00464 ins.

ρ_S = 165 lbs/ft^3

Hence

$$G_{mf} = \frac{688 \times 0.00464^{1.82} \times (0.0327 \times 165)^{0.94}}{0.032^{0.88}}$$

$$= \frac{688 \times 5.66 \times 10^{-5} \times 4.56}{4.84 \times 10^{-2}}$$

$$= 3.67 \text{ lbs/ft}^2\text{hr}$$

$$\equiv \frac{3.67 \times 1.77}{0.081 \times 60} = \underline{1.33 \text{ c.f.m.}} \text{ (at S.T.P.)}$$

Therefore

$$\frac{\text{Actual flow}}{\text{Minimum flow}} = \frac{G_f}{G_{mf}} = \frac{18.4}{1.33} = 13.8$$

Hence, using Fig. 4-16 in Ref. 74, the fluidization efficiency is found to be

$$\eta = 0.75$$

and using Fig. 4-17 the bed expansion ratio is

$$R = 1.35$$

Now

$$G_f = \frac{18.4 \times 60 \times 0.081 \times 4}{\pi \times 1.5^2} = 50.5 \text{ lbs/ft}^2\text{hr}$$

Therefore

$$\frac{G_f \cdot \eta}{\mu . R} = \frac{50.5 \times 0.75}{0.032 \times 1.35} = 875$$

Thermal conductivity of air at 400°C = 0.03 B.t.u./hr.ft°F

$$C_S \cdot \rho_S = 0.25 \times 165 = 41.3 \text{ B.t.u./ft}^3\,^\circ\text{F}$$

where C_S = solid specific heat.

Hence, from the nomograph on p.207 of Ref. 74

<u>Shell side heat transfer coefficient = 51 B.t.u./hr.ft^2 °F</u>

APPENDIX 7 CALCULATION OF THE RELATIVE AMOUNTS OF CO AND CO_2 FORMED IN THE REACTOR (AT HIGH YIELD CONDITIONS) AND HENCE OF THE OVERALL HEAT OF REACTION

The mole fraction of oxygen, N_B, is related to the conversion of o-xylene by

$$N_B = N_B^o - N.N_A.X$$

where

N_B^o = initial mole fraction of oxygen

N_A = initial mole fraction of xylene

N = average number of moles of oxygen reacting per mole of xylene

Now in a number of runs where a high yield of phthalic anhydride was obtained (e.g. Run 1-21) the value of N_B was

$$N_B = 0.1695$$

In this same run the value of N_A may be calculated as follows

Xylene input = 46.55 c.c.

$$= \frac{46.55 \times 0.881}{106.1} = 0.386 \text{ gm.mols.}$$

$$\text{Air input} = \frac{29.8 \times 30}{22.4} = 39.8 \text{ gm.mols.}$$

Therefore

$$N_A = \frac{0.386}{39.8} = 0.00970$$

and hence assuming that X = 1 (total conversion of o-xylene)

$$N = \frac{0.210 - 0.1695}{0.00970} = \underline{\underline{4.18}}$$

In this run the yield of phthalic anhydride was 59.7%, and yields in general averaged 60%. Assume that the remaining 40% was combusted to either CO or CO_2 and define

a = Conversion to CO_2

Therefore

$$N = (0.6 \times 3) + (a \times 10.5) + ((0.4 - a) \times 6.5)$$

$$4.18 - 1.8 - 2.6 = 4.0a$$

therefore

$$a = \frac{-0.22}{4} = -0.055$$

This result indicates that the consumption of oxygen is not even sufficient to give 40% conversion to CO and zero conversion to CO_2. Nevertheless, since $a \approx 0$ such an assumption will be in reasonable concordance with the experimental facts, and we shall adopt it for the purpose of calculating the overall (or effective) heat of reaction.

1. 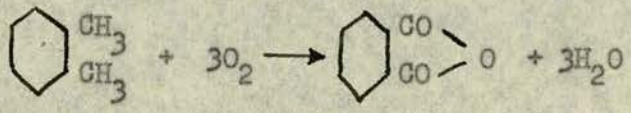

2. 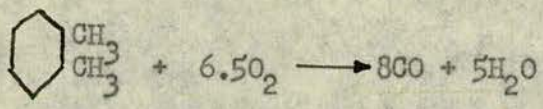

The heats of formation of the various components (at 1 atm., 25°C) are as follows[75]

Substance	Heats of formation - K cal/mole
H_2O - liquid	- 68.3174
H_2O - vapour	- 57.7979
CO_2	- 94.052
CO	- 26.416
o-xylene - vapour	4.540

Hence, for reaction 2 the heat of reaction is

$$\Delta H = (8 \times -26.416) + (5 \times -57.7979) - 4.540$$

$$= -211.328 - 288.9895 - 4.540$$

$$= \underline{-504.86 \text{ Kcal/mole}}$$

The heat for formation of phthalic anhydride is not quoted; however,

another source[76] gives the heat of combustion of solid phthalic anhydride to gaseous CO_2 and liquid H_2O at 20°C as

$$\Delta H = -783.4 \text{ Kcal/mole}$$

If we consider the following reaction scheme

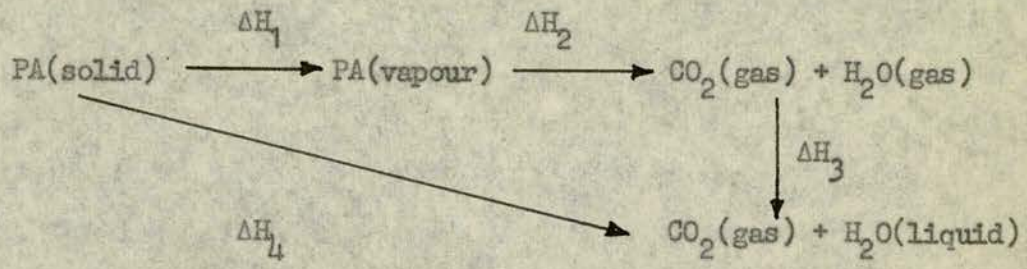

then by Hess's law

$$\Delta H_4 = \Delta H_1 + \Delta H_2 + \Delta H_3$$

Reference (76) also lists the heat of sublimation of phthalic anhydride (in the range 30-60°C) as 2.303 x R x 4632 cals/mole = +21.18 Kcal/mole

Also

$$\Delta H_3 = 2(-68.3174 - -57.7979)$$
$$= -21.039 \text{ Kcal/mole}$$

Therefore

$$\Delta H_2 = \Delta H_4 - \Delta H_1 - \Delta H_3$$
$$= -783.4 - 21.18 + 21.039$$
$$= -783.54 \text{ Kcal/mole}$$

Reference 75 gives the heat of combustion of gaseous o-xylene to gaseous CO_2 and H_2O as

$$\Delta H = -1045.94 \text{ Kcal/mole at } 25^\circ C.$$

Hence the heat of reaction of gaseous o-xylene to phthalic anhydride vapour and H_2O vapour is

$$\Delta H = -1045.94 - -783.54$$
$$= -262.4 \text{ K.cal/mole}$$

Finally if we assume 60% conversion to phthalic anhydride and 40% to CO in the experimental reactor, then the effective heat of reaction is

$$\Delta H = -((0.6 \times 262.4) + (0.4 \times 504.86))$$

$$\Delta H = -359.3 \text{ Kcal/gm.mole o-xylene reacted}$$

APPENDIX 8 HEAT AND MASS TRANSFER BETWEEN THE BULK GAS AND THE PELLET SURFACE

The correlations of Hougen et al[73] are

$$j_H = \frac{h}{C_p.G}.\left(\frac{C_p \mu}{k}\right)^{2/3} = 1.95\ \left(\frac{d.G}{\mu}\right)^{-0.51} \qquad Re_p < 350$$

$$j_D = \frac{k_G p_m}{G}.\left(\frac{\mu}{\rho.D}\right)^{2/3} = 1.82\ \left(\frac{d.G}{\mu}\right)^{-0.51} \qquad Re_p < 350$$

where p_m = partial pressure of non-diffusing component.

For the experimental conditions in the tubular reactor:

$d = 0.63$ cms.

μ(air, 400°C) = 0.0315 c.p.

$G \approx 29.7$ litres/minute

$$= 29.7 \times \frac{60}{22.4} \times \frac{4}{\pi \times 2.54^2}$$

$$= 15.7 \text{ gm.mols/cm}^2\text{hr}$$

therefore $$Re_p = \frac{0.63 \times (15.7 \times 29)}{0.0315 \times 0.01 \times 3600} = \frac{0.63 \times 456}{1.135} = 253$$

This lies within the range of application for the correlations.

Hence

$$\frac{j_H}{j_D} = \frac{h}{K_G C_{p_m}}.\frac{Pr^{2/3}}{Sc^{2/3}} = \frac{1.95}{1.82} = 1.071$$

Now the Prandtl number for air will be taken as 0.7 and the Schmidt number for o-xylene in air is 2.18 at 25°C[77]. It is well known that both these groups are to a great extent independent of temperature, and this assumption will be made here.

Therefore $$\left(\frac{Sc}{Pr}\right)^{2/3} = 3.11^{2/3} = 2.13$$

therefore

$$\frac{h}{k_G C_p p_m} = 2.29$$

(p_m may be taken as identical with the total pressure of the system in this particular case).

$$\text{Also } Re_p^{-0.51} = \frac{1}{253^{0.51}} = \frac{1}{16.9} = 0.0592$$

Hence

$$\frac{k_G p_m}{G} . 2.18^{2/3} = 1.82 \times 0.0592 = 0.1078$$

Therefore

$$k_G = \frac{0.1078 \times 15.7}{3600 \times 1 \times 1.68} = 2.80 \times 10^{-4} \text{ gm.mols/cm}^2\text{.sec.atm.}$$

(taking p_m = 1 atmosphere)

Let a = external surface area of catalyst per unit mass

therefore

$$a = \frac{4\pi r^2}{4/3\pi r^3 . \rho} = \frac{6}{\rho . d}$$

$$\rho = 1.87 \text{ gms/c.c.}$$

therefore

$$a = \frac{6}{1.87 \times 0.63} = 5.10 \text{ cm}^2/\text{gm}$$

Hence

$$k_G . a = 5.10 \times 2.80 \times 10^{-4}$$

$$k_G . a = 1.43 \times 10^{-3} \text{ gm.mols/gm.sec.ats.}$$

NOMENCLATURE

A	pre-experimental factor in the Arrhenius expression
A	$R.h_w/Ke$
a	external surface area per unit mass of catalyst ($cm^2/gm.$)
Cp	mean molar specific heat (cals/gm.mol.^oC)
D_T	reactor tube diameter (cms.)
d	catalyst pellet diameter (cms.)
E	activation energy in the Arrhenius expression (cals/gm.mol.)
F	total molar flow per unit cross sectional area (gm.mols/cm^2.sec
ΔH	heat ofreaction (cals/gm.mol.)
h	overall heat transfer coefficient between tubular reactor and tube wall
h	heat transfer coefficient for the gas film at the surface of a catalyst pellet
h_w	inside wall heat transfer coefficient for a tubular reactor
J	$\frac{h}{Kg.P.Cp} \cdot \frac{T_S - T_B}{\Delta T_{ad}}$
K, K_1, K_2, K_3	rateconstants
K	wall heat transfer parameter defined on p.41
K^*	rate constant for the re-oxidation of the catalyst surface
K_g	mass transfer coefficient for the reacting component in the gas film at the surface of a catalyst pellet
Ke	effective thermal conductivity for the catalyst bed
MA	maleic anhydride
N	average number of molecules of oxygen consumed when one molecule of hydrocarbon reacts
N	$2U/R.Cp.K.\rho_B.P$
N_A	mole fraction of o-xylene in the reactor feed
N_B	mole fraction of oxygen in the reactor feed
n	number of particles per side of the triangular matrix in the matrix model
OMBA	o-methyl benzyl alcohol

P	total pressure (atmospheres)
PA	phthalic anhydride
p_1, p_2	partial pressures of hydrocarbon and oxygen resp. (atmospheres)
p_B	partial pressure of reactant (o-xylene) in the bulk gas (atmospheres)
p_{o_2}	partial pressure of oxygen (atmospheres)
p_s	partial pressure of reactant (o-xylene) at the catalyst pellet surface (atmospheres)
Q_M	maximum rate of heat production per unit mass by a catalyst pellet
Q_P	rate of heat production per unit mass by a catalyst pellet
Q_R	rate of heat removal per unit mass from a catalyst pellet
R	tube radius
R'	catalyst dilution (see p.33)
$\bar{R}'$	mean catalyst dilution
R_G	gas constant
R_1	K/Kg.a
R_2	K^*/Kg.a
Re_p	Reynold's number based on particle diameter
r, r_1, r_2	rates ofreaction
S	fraction of the potentially active surface which is in the oxidized state
S	$\Delta T_{ad}.E/R_G.T_j^2$
T	reaction (reactor) temperature
T_B	bulk gas temperature
T_j	temperature of the reactor jacket
T_s	temperature of the catalyst pellet surface
T_w	reactor tube wall temperature
T_I	ignition temperature for a catalyst pellet
T_E	extinction temperature for a catalyst pellet

TA	tolualdehyde
$\Delta T_{ad}, \Delta T_1, \Delta T_3$	adiabatic temperature rises
U	overall heat transfer coefficient between the reactor and the jacketing fluid
U	fraction of o-xylene not reacted
U_o	fraction of o-xylene not reacted at the reactor exit
X	xylene
X	fractional conversion of reactant
X_o	Fractional conversion of reactant at the reactor exit
W	weight of catalyst
Z	distance along the reactor axis
Z_o	reactor length
β_1	first root of the equation $xJ_1(x) = AJ_o(x)$
ρ_B	bulk density of the catalyst

REFERENCES

1. R.A. Duckworth. Chemical and Process Engineering 50, 69-81, Jan. 1969.

2. H. Furkert and G. Helms. Chemical and Process Engineering 50, 74-77, Sept. 1969.

3. D.J. Leach. Large Plants Survey. (Supplement to European Chemical News), 66-71, Sept. 26 1969.

4. J.P. Allen. Ibid, 23-24.

5. P.H. Pinchbeck and H. Markham. "The Fluidized-Bed Process for the Manufacture of Phthalic Anhydride". Joint I. Chem. E., VTG/VDI meeting, Brighton, April 26th 1968.

6. C. Wickham-Jones. Large Plants Survey. (Supplement to European Chemical News), 10-12, Sept. 26 1969.

7. P. Ellwood. Chemical Engineering 76, 80-82, June 2 1969.

8. N.R.D.C. Report (unpublished).

9. Private communication from Professor G.F. Froment, June 13 1968.

10. G.F. Froment. Ind. Eng. Chem. 59(2), 18-27, 1967.

11. Private communication from Professor G.F. Froment, Sept. 29 1967.

12. Kirk-Othmer Encyclopaedia of Chemical Technology, Volume 15, 2nd edition, pp.448-454 (Interscience Publishers, 1968).

13. Chemical and Process Engineering 46, 138-139, 1965.

14. Chemical Engineering 76, 54-58, July 14 1969.

15. Kirk-Othmer Encyclopaedia of Chemical Technology, Volume 15, 1st edition, p.188 (Interscience Publishers, 1956).

16. Dangerous Properties of Industrial Materials. N.I. Sax. 2nd edition, p.1330 (Reinhold, 1963).

17. U.S. Patent 2,574,511. William G. Toland to California Research Corporation. Nov. 13 1951.

18. E. Costa Novella and A. Escardino Benlloch. Anales de la Real Sociedad Espanola de Fisica y Quimica 58B, 783-790, 1962.

19. Ibid 58B, 791-802, 1962.

20. Ibid 59B, 669-680, 1963.

21. J. Herten and G.F. Froment. Ind. Eng. Chem. - Process Design and Development 7(4), 516-526, Oct. 1968.

22. R.F. Mann and J. Downie. Canad. J. Chem. Eng. 46, 71-72, 1968.

23. J.A. Juusola, R.F. Mann and J. Downie. J. Catalysis 17, 106-113, 1970.

24. G.L. Simard, J.F. Steger, R.J. Arnott and L.A. Siegel. Ind. Eng. Chem. 47(7), 1424-1430, July 1955.

25. G.L. Simard. Unpublished research reported by J.K. Dixon and J.E. Longfield in "Catalysis" Volume VII, editor P.H. Emmett (Reinhold, 1960).

26. S.K. Bhattacharyya and I.B. Gulati. Ind. Eng. Chem. 50, 1719-26, 1958.

27. S.K. Bhattacharyya and R. Krishnamurthy. J. App. Chem. (London) 13(12), 547-552, 1963.

28. F. Bernardini and M. Ramacci. La Chimica e L'Industria 48(1), 9-17, 1966.

29. The Chemistry of Petroleum Hydrocarbons. I.E. Levine, Volume 3, pp. 1-7 (Reinhold, 1955).

30. T. Vrbaski and W.K. Matthews. J. Phys. Chem. 69(2), 457-466, 1965.

31. R. Landau and R.W. Simon. Chemistry & Industry 40, 70-75, Jan. 13, 1962.

32. M.F. Hughes and R.T. Adams. J. Phys. Chem. 64, 781, 1960.

33. J.H. Burgoyne. Proc. Roy. Soc. (London) 161A, 48-67, 1937.

34. F.J. Wright. J. Phys. Chem. 64, 1944-1950, 1960.

35. F.J. Wright. J. Phys. Chem. 66, 2023-2028, 1962.

36. C.N. Satterfield and J. Loftus. Ind. Eng. Chem. - Process Design and Development 4(1), 102-105, 1965.

37. L.N. Denisova and E.T. Denisov. Kinet. Katal. 10(6), 1244-1248, 1969. (Chemical Abstracts 72, 66159 b).

38. J.M. Weiss, C.R. Downs and R.M. Burns. Ind. Eng. Chem. 15, 965-967, 1923.

39. C.E. Sensiman. Ind. Eng. Chem. 15, 521-524, 1923.

40. E.B. Maxted. J. Soc. Chem. Ind. 47, 101T-105T, 1928.

41. P. Mars and D.W. van Krevelen. Special supplement to Chemical Engineering Science 3, 41-59, 1954.

42. H. Clark and D.J. Berets. Advances in Catalysis 9, 204-214, 1957.

43. L.A. Kasatkina, G.K. Boreskov, Z.L. Krylova and V.V. Popovskii. Izvest. Vysshikh Zavednii Khim i Khim Teknol 1, 1958. (Chemical Abstracts 52, 15208, 1958).

44. V. Roiter. Kinetika i Kataliz 1, 63, 1960.

45. K.A. Shelstad, J. Downie and W.F. Graydon. Canad. J. Chem. Eng. 38, 102-107, 1960.

46. J. Downie, K.A. Shelstad and W.F. Graydon. Canad. J. Chem. Eng. 39, 201-204, 1961.

47. R. Hayashi, R.R. Hudgins and W.F. Graydon. Canad. J. Chem. Eng. 41, 220-225, 1963.

48. I.S. Jaswal, R.F. Mann, J.A. Juusola and J. Downie. Canad. J. Chem. Eng. 47, 284-287, 1969.

49. J.A. Allen. Chemistry and Industry 41, 1225-1229, July 27 1963.

50. T. Vrbaski. J. Phys. Chem. 69(9), 3092-3097, 1965.

51. T. Vrbaski and W.K. Matthews. J. Catalysis 5, 125-134, 1966.

52. Concepts in Catalysis. E.K. Rideal, p.96 (Academic Press, 1968).

53. O. Bilous and N.R. Amundson. Chem. Eng. Sci. 5, 81-92, 115-126, 1956.

54. O. Bilous and N.R. Amundson. A.I.Ch.E. Journal 2, 117, 1956.

55. C.H. Barkelew. Chem. Eng. Prog. Symposium Series No. 25 55, 37-46, 1959.

56. C.M. van den Bleek, K. van der Wiele and P.J. van den Berg. Chem. Eng. Sci. 24, 681-694, 1969.

57. British Patent 610,007. Spolek pro Chemickou a Hutni Vyrobu. Application date: June 27 1941.

58. British Patent 978,520. The Distillers Co. Ltd., 1964.

59. Private communication.

60. B.S. Gilliatt. "Some catalytic oxidation reactions in the presence of ammonia". Ph.D. Thesis, University of Edinburgh, June 1967.

61. P.H. Calderbank, A.D. Caldwell and G. Ross. 4th European Symposium on Chemical Reaction Engineering, 2nd session, 4th paper.

62. A.D. Caldwell and P.H. Calderbank. Brit. Chem. Eng. 14(9), 1199-1201, Sept. 1969.

63. H.A. Deans and L. Lapidus. A.I.Ch.E. Journal 6, 656-663, 663-668, 1960.

64. J. Valstar. "A study of the fixed bed reactor with application to the synthesis of vinyl acetate". Ph.D. Thesis, Delft 1969.

64*. M. Leva, M. Weintraub, M. Grummer and E.L. Clark. Ind. Eng. Chem. 40, 747-752, 1948.

65. Chemical Reaction Analysis. E.E. Petersen, pp.222-223 (Prentice-Hall, 1965).

66. A.D. Caldwell. Chem. Eng. Sci. 23, 393-395, 1968.

67. Chemical Reaction Analysis. E.E. Petersen, pp.203-213 (Prentice-Hall, 1965).

68. C. Wagner. Chemische Technik 18, 28, 1945.

69. E. Wicke. Chem-Ing-Tech. 29, 305-311, 1957.

70. E. Wicke. Zeitschrift fur Elektrochemie 65, 267-275, 1961.

71. G. Padberg and E. Wicke. Chem. Eng. Sci. 22, 1035-1051, 1967.

72. Chemical Reaction Analysis. E.E. Petersen, pp.140-144 (Prentice-Hall, 1965).

73. Chemical Engineering Kinetics. J.M. Smith. 1st edition, pp.309, 390 (McGraw-Hill, 1956).

74. Fluidization. M. Leva. (McGraw-Hill, 1959).

75. Chemical Engineers Handbook. J.H. Perry. 4th edition, 3-134 (McGraw-Hill, 1963).

76. Handbook of Chemistry and Physics. 48th edition. (The Chemical Rubber Co., 1967).

77. Chemical Engineering. J.M. Coulson and J.F. Richardson. Volume I, Sixth impression, p.239 (Pergamon Press, 1960).

78. T. Baron. Chem. Eng. Prog. 48, 118, 1952.

79. Chemical Reaction Analysis. E.E. Petersen, pp.220-221 (Prentice-Hall, 1965).